Faculty of Science and Engineering
Department of Mathematics and Statistics

Analysis and Modelling of Implied Market Parameters

Hin Lin Yee

This thesis is presented for the Degree of
Doctor of Philosophy
of
Curtin University

December 2015

Declaration

To the best of my knowledge and belief this thesis contains no material previously published by any other person except where due acknowledgement has been made.

This thesis contains no material which has been accepted for the award of any other degree or diploma in any university.

Signature: .....

Date: 2/12/2015.

Analysis and modelling of implied market parameters

by

Lin Yee Hin

Submitted to the Department of Mathematics & Statistics

on December 2015, in fulfilment of the

requirements for the Degree of Doctor of Philosophy

The central theme of this dissertation is the extraction of market information from the cross-sectional data of the European vanilla call option prices and the zero coupon bond prices, the representation of this information in the form of implied contingent claim pricing model parameters, and the application of these implied model parameters to the analysis and forecast of financial state variables. Each of the three core chapters addresses a separate but related research question that can be cast within the mathematical framework of contingent claim pricing model calibration. While Chapters 2 and 3 address the issue of implied volatility calibration in the context of discount rate uncertainty with respect to European vanilla call option prices, Chapter 4 addresses the issue of using short rate model parameters calibration with respect to zero coupon bond prices for short rate forecast within a multi-curve yield curve modelling framework.

Chapter 2 of this dissertation presents a strategy for the sensitivity analysis of implied volatility calibration with respect to discount rate uncertainty. We cast this calibration problem as seeking the approximate solution to an under-defined system of non-linear equations that map a set of option prices to their respective implied volatility and discount rate. Our empirical analysis based on a set of historical S&P500 index European vanilla call option prices demonstrates that even a narrow range of discount rate uncertainty may lead to a noticeable range of implied volatility calibration uncertainty. It highlights the potential impact of discount rate uncertainty on implied volatility uncertainty, pointing to the mediation that an accurate specification of the discount rate is crucial for accurate and reliable implied volatility calibration.

The fact that the market participants' aggregate choice of discount rate reflected by the option prices is an unobservable financial state variable provides impetus for the development of a strategy to jointly infer the implied discount rates and implied volatilities from a set of European vanilla call option prices. This forms the central research question addressed in Chapter 3. We cast this calibration problem as seeking the approximate solution to an over-defined system of non-linear equations that map a set of option prices to their respective implied volatility and discount rate. Due to the non-convexity of the loss metric with respect to the implied discount rates and implied volatilities, we use the

Zhang-Sanderson algorithm, a stochastic-based multi-point direct-search optimization algorithm, to attain global convergence. We also propose a simple approach to construct an empirical range of calibration uncertainty interval for the implied discount rates and implied volatilities. Precision analysis of our proposed strategy based on synthetic test data set demonstrates reasonable level of accuracy and convergence profile. Empirical analysis using our proposed strategy based on samples of historical S&P500 index European vanilla call options data reveals an interesting empirical observation that for option prices sampled from 2004 to 2007, the implied discount rates appear to be comparable to or slightly lower than the contemporaneously quoted Libor rates but for option prices sampled from 2008 to 2013, the implied discount rates appear to be higher than the contemporaneously quoted Libor rates. Additionally, the spreads between the implied discount rates and the contemporaneously quoted Overnight Indexed Swap rates are comparable to the credit default swap spreads of US firms with an average Moody's and S&P ratings that range between BBB and BB.

An additional contribution of the work presented in Chapter 2 is the demonstration of the extent of computational acceleration that can be achieved by executing the computationally intensive yet highly scalable Zhang-Sanderson algorithm across a grid computing hardware framework. The speed of this computational framework and the accuracy of our proposed strategy serves as a basis for the research problem addressed in Chapter 4.

Chapter 4 of this dissertation readdress the problem of short rate forecast. Instead of doing so based on the classical interest rate modelling paradigm of assuming the existence of a single yield curve that spans the entire tenor range, our approach is motivated by the multi-curve approach for yield curve modelling. We partition the yield curve into as many non-overlapping tenor intervals as possible, and model each tenor interval using a separate single-factor Cox-Ingersoll-Ross (CIR) short rate model. Each non-overlapping triplet from a cross-sectional set of zero coupon bond prices arranged in ascending tenors that correspond to the non-overlapping tenor intervals is mapped to three CIR model parameters, formulating a system of well-defined non-linear equations. The sets of implied CIR model parameters for various tenor intervals are inferred from the corresponding triplet as approximate solution to this system of well-defined non-linear equations. Numerically, it is solved using the Zhang-Sanderson algorithm across a grid computing hardware framework. These sets of inferred CIR model parameters are then used to forecast future short rate at horizons comparable to the corresponding tenor ranges. We perform empirical analysis of our proposed model calibration and short rate forecast strategy by extract the market participants' aggregate expectation of future short rate from samples of historical

US STRIPS prices and use this information to forecast the effective Federal Funds rate. For this data set, our proposed one-factor CIR model implemented in a multi-curve framework appears to perform better than the random walk at forecast horizons between 0.8 to 1.6 years, a considerably difficult forecast benchmark for the affine term structure models to beat. Additionally, the forecast performance of the one-factor CIR model implemented in the multi-curve framework is better than that implemented in the classical single-curve framework. It appears that the improvement in forecast performance of the one-factor CIR model is due to its implementation in the multi-curve framework.

List of keywords:

1. **Keywords for Chapter 2**:

   implied volatility, risk-free rate, sensitivity analysis, under-defined system, nonlinear equations.

2. **Keywords for Chapter 3**:

   implied volatility, risk-free rate, over-defined system, nonlinear equations, differential evolution, Zhang-Sanderson algorithm.

3. **Keywords for Chapter 4**:

   short rate forecast, multi-curve modelling, Cox-Ingersoll-Ross process, nonlinear equations, differential evolution, Zhang-Sanderson algorithm.

Australian and New Zealand Standard Research Classifications (ANZSRC)

ANZSRC code: 010205, Financial Mathematics, 100%.

Fields of Research (FoR) Classification

FoR code: 010205, Financial Mathematics, 100%.

Publications and presentations during candidature

I. Peer-review papers:

1. Hin, L.-Y. and Dokuchaev, N. (2014) "On the Implied Volatility Layers Under the Future Risk-Free Rate Uncertainty," *International Journal of Financial Markets and Derivatives*, 3(4), 392–408.

   This paper is derived from the work presented in Chapter 2 of this thesis.

2. Hin, L.-Y. and Dokuchaev, N. (2015) "Computation of the Implied Discount Rate and Volatility for an over-defined System using Stochastic Optimization," *IMA Journal Of Management Mathematics*, in press. DOI:10.1093/imaman/dpv007

   This paper is derived from the work presented in Chapter 3 of this thesis.

3. Hin, L.-Y. and Dokuchaev, N. (2015) "Short Rate Forecasting based on the Inference from the CIR Model for Multiple Yield Curve Dynamics," *Annals of Financial Economics*, accepted.

   This paper is derived from the work presented in Chapter 4 of this thesis.

II. Conference presentations:

1. Hin, L.-Y. and Dokuchaev, N. (2014) "An Analysis of Volatility Spread via the Risk-Free Rate Proxy." Presented at the Fourth Institute for Mathematical Statistics - Finance, Probability and Statistics Workshop (IMS-FPS 2014), Sydney, 3rd July 2014.

   This presentation is derived from the work presented in Chapter 3 of this thesis.

2. Hin, L.-Y. and Dokuchaev, N. (2014) "Analysis of Implied Volatilities and Discount Rates via under-defined and over-defined Systems of Equations." Presented at the 6th Australasian Actuarial Education and Research Symposium, Perth, 9th December 2014.

   This presentation is derived from the work presented in Chapter 2 and Chapter 3 of this thesis.

Acknowledgements

I am grateful to my supervisor Associate Professor Nikolai Dokuchaev for his kind and precious advice, encouragement, guidance and relentless support at all times, in addition to his financial support through his 2012-2015 Australian Research Council (ARC) grant of Australia DP120100928.

I am grateful to Professor Yong Hong Wu, the Chairperson of my Thesis Committee. He is always ready to help.

I gratefully acknowledge the financial support of the 2013 Curtin International Postgraduate Scholarship (CIPRS), and Department of Mathematics and Statistics - ARC Discovery Grant Scholarship.

I gratefully acknowledge Curtin University for the Support for Conference Attendance pertaining to my attendance to the Fourth Institute for Mathematical Statistics - Finance, Probability and Statistics Workshop (IMS-FPS 2014), Sydney, July 3rd - 5th 2014.

I gratefully acknowledge the Department of Mathematics & Statistics, Curtin University for the Support for Conference Attendance pertaining to my attendance to the 6th Australasian Actuarial Education and Research Symposium, Perth, Dec. 8th - 9th 2014.

The provision of ICT support and computing resources by Curtin IT Services is gratefully acknowledged. Curtin Information Technology Services (CITS) provides Information and Communication Technology systems and services in support of Curtin's teaching, learning, research and administrative activities.

The provision of computing resources from the NeCTAR Research Cloud is gratefully acknowledged. NeCTAR is an Australian Government project conducted as part of the Super Science initiative and financed by the Education Investment Fund.

The provision of access to the data from the Thomson Reuters Tick History (TRTH) supplied by the Securities Industry Research Centre of Asia-Pacific (SIRCA) is gratefully acknowledged.

Contents

List of Figures

List of Tables

Chapter 1

Introduction

Prices of contingent claims contain information on the market participants' aggregate view on certain financial state variables. Depending on the context of application, the time series data or the cross-sectional data of the contingent claim prices may be used to infer these financial state variables from the respective contingent claim prices for various applications, including econometric analysis, risk management, and pricing of other contingent claims.

The extraction of market information from the cross-sectional data of contingent claim prices constitute a large collection of strategies collectively referred to as the model calibration strategies. This approach is regarded as an inverse problem where the known prices are mapped to some unknown parameters. Typically, one makes an assumption on the stochastic process that may be used to model the dynamic evolution of the underlying asset price of the contingent claim, specify a relevant asset pricing formula, and then choose a set of values for the corresponding set of model parameters and relevant financial state variables involved in the model in order to match the model price to the observed price as closely as possible (see, among many others, Detlefsen and Härdle, 2007a; Deryabin, 2012; Madan, 2015, and the reference therein).

From this perspective, we may construct systems of equations with model prices on one sides, and market prices on the other in order to map a given set of contingent claim market prices to a set of implied financial state variables that we would like to infer and a set of unknown model parameters that we would like to recover. The precise characteristics of the model parameters and the financial state variables that one may infer from the prices depends on the contingent claim pricing model we choose to use as a mapping tool. Since it is not possible, in general, to match model price to market price perfectly, we can

only infer the unknown parameters as approximate solution to these systems of equations. If the number of equations is less than the number of unknown parameters, the system is regarded to as being under-defined. If the number of equations is equals to or larger than the number of unknown parameters, the system is referred to as being well-defined and over-defined respectively. We utilize this approach of parameter inference from market prices as approximate solutions to systems of equations to address the research problems considered in Chapters 2, 3 and 4 of this dissertation.

The central theme of this dissertation is the extraction of market information from the cross-sectional data of the European vanilla call option prices and the zero coupon bond prices, the representation of this information in the form of implied contingent claim pricing model parameters, and the application of these implied model parameters to the analysis and forecast of financial state variables.

Chapter 2 of this dissertation considers the problem of inferring financial state variables from market price of option contracts as approximate solutions to under-defined systems of nonlinear equations to present an empirical analysis of how the uncertainty of discount rates may lead to the inference uncertainty of implied volatilities from a set of option prices. In this chapter, we model the asset price dynamics using the log-normal process, and use the Black-Scholes (Black and Scholes, 1973) option pricing formula as a mapping tool to map the day-close bid-ask mid-quote market prices of a set of exchange-traded European vanilla call option contracts to the corresponding implied volatilities and the discount rates. The discount rate uncertainty in this under-defined system of equations leads to uncertainty in the inference of implied volatility. We then quantify the range of implied volatility inference uncertainty based on a set of historical option prices under different plausible scenarios of the future discount rate uncertainty.

Chapter 3 of this dissertation considers the problem of inferring financial state variables from market price of option contracts as approximate solutions to over-defined systems of nonlinear equations in order to infer the market consensus on the discount rates and the implied volatilities simultaneously from a set of option prices. The purpose is to formulate a strategy to circumvent the need to make *a priori* assumption of the discount rates when inferring the implied volatilities from a set of option prices. Similar to Chapter 2, we model the asset price dynamics using the log-normal process, and use the Black-Scholes option pricing formula as a mapping tool to construct the systems of nonlinear equations. We make an additional assumption that there is some stability in the implied volatility and the discount rate for an option contract within a short time span. This assumption facilitates our construction of over-defined systems of nonlinear equations to

map the day-close bid-ask mid-quote market prices of a set of exchange-traded European vanilla call option contracts observed on two consecutive trading days to the corresponding implied volatilities and the discount rates. We then infer the implied discount rates and the implied volatilities by seeking an approximate solution to this system of equations via differential evolution, a computationally intensive stochastic-based multi-point direct-search optimization technique, implemented on a grid-based high performance computing platform.

Chapter 4 of this dissertation considers the problem of inferring model parameters of a zero coupon bond pricing formula from market price of zero coupon bonds as approximate solutions to well-defined systems of nonlinear equations and perform forecast of financial state variable based on these inferred model parameters. The purpose is to explore whether, given a stochastic process to model the short rate process, the short rate forecast algorithm formulated within a recently proposed multiple yield curve framework improves the short rate forecast performance beyond the short rate forecast algorithm formulated within the classical single yield curve framework. We model the short rate process using the one-factor Cox-Ingersoll-Ross (CIR, Cox, Ingersoll and Ross, 1985) process. Instead of working within the classical asset pricing paradigm that assumes the existence of a unique yield curve to forecast interest rates and to discount cash flows, we do so within the multi-curve framework where the interest rates spanning different tenors are modelled using different yield curves, and are assumed to be associated with different short rate processes. We organize the cross-sectional set of zero coupon bonds into multiple triplets arranged in ascending order of tenor, and, assuming that each triplet that corresponds to a different segment of the yield curve is associated with a different short rate process, we model each of these short rate processes using a separate one-factor CIR process. In doing so, we attempt to capture the salient features of different segments of the interest rate term structure in order to extract the information on the market participants' aggregate view of the future short rate at various forecast horizons from the triplets with comparable tenors, and represent this information as different sets of implied CIR model parameters that correspond to these tenor specific short rate processes. Using these implied CIR model parameters, we derive an algorithm to predict the future short rate.

In Section 1.1, we survey the extant literature on the motivation and the challenges encountered by practitioners in the financial industry in extracting market information on financial state variables, such as the implied volatility, from the market price of option contracts. It is intended to provide an overview of the background for the problems considered in Chapters 2 and 3. Building on the survey in this section, we detail the in-depth

literature review specific to the motivation of study for Chapters 2 and 3 in Section 2.1 and Section 3.2 respectively. Therein, we showcase their contribution of Chapters 2 and 3 within the vast field of inverse problems in finance.

In Section 1.2, we survey the extant literature on interest rate term structure modelling, the challenges faced by practitioners in interest rate model calibration, and the recent development of multi-curve interest rate modelling framework. Building on the survey in this section, we detail, the in-depth literature review specific to the motivation of study for Chapter 4 in Section 4.2. Therein, we highlight the contribution of Chapter 4 to the literature of interest rate modelling and forecasting.

1.1 Inferring market information from option prices by fitting the implied volatility surface

In 1973, the Chicago Board Options Exchange (CBOE) was founded and became the first platform for trading listed options. In the same year, Black and Scholes (1973) proposed a framework for the valuation of European vanilla option contracts. Assuming that the underlying asset price process follows a log-normal stochastic process, they proposed the celebrated Black-Scholes option pricing formula that maps six parameters, namely the spot underlying asset price, the contract strike price, the time to maturity of the option contract, the dividend rate, the short term interest rate, and the implied volatility, i.e., the volatility of the underlying asset for the remaining lifespan of the option contract, to a theoretical net present value of the option contract. The first five parameters are regarded as known quantities; the last is not.

In the spirit that the option price contain information of the market participants' aggregate expectation of the underlying asset volatility for the remaining lifespan of the option contract, financial economist and financial industry practitioners alike have tried to infer the implied volatility from the option prices. The notion of implied volatility as a value that matches the Black-Scholes model price to the market price as closely as possible is first introduced by Latané and Rendleman (1976b); an errata to this paper was subsequently published by (Latané and Rendleman, 1976a).

From the econometric perspective, one may utilize the implied volatility inferred from the option price to provide forecast of the future realized volatility of the underlying asset for the remaining lifespan of the option contract. The literature in this area is voluminous,

including, among many others, Christensen and Prabhala (1998), Canina and Figlewski (1993a), Poon and Granger (2003a), and Busch, Christensen and Nielsen (2011).

From the arbitrage-free pricing perspective, one may utilize the implied volatilities inferred from a cross-sectional set of option prices via the Black-Scholes option pricing formula, along with the values of other input parameters, to infer the prices of more complex contingent claims that have the same underlying asset but are not exchange traded, i.e., traded "over-the-counter" (OTC), and European vanilla option with strike-expiry pair that are OTC traded. This is to ensures that the same set of modelling assumptions of asset price dynamics is applied to all exchange traded and OTC traded contingent claims with the same underlying asset. In do so, the asset price dynamics assumptions and parameter values used as input to price the OTC contingent claims can recover, at least to a close approximation, the exchanged traded European vanilla options, thereby abrogating the possibility of constructing an arbitrage position that exploits the pricing difference between these exchange traded and OTC traded contingent claims. This practice of consistent pricing of exchange traded and OTC contingent claims is not confined to the Black-Scholes pricing framework. A wide range of models that are more sophisticated than the Black-Scholes model can be calibrated with this approach (see, among many others, Perignon and Villa, 2003; Taylor, Yadav and Zhang, 2010; Gatheral, 2006; Benko, Fengler, Härdle and Kopa, 2007; Fengler, 2012; Fabozzi, Leccadito and Tunaru, 2014; Madan, 2015).

1.1.1 Volatility smile: The impetus for more flexible asset pricing models

A crucial assumption of the Black-Scholes option pricing formula is that the implied volatility is assumed to be constant. This assumption is not met in reality. Before the Oct. 19th 1987 stock market crash, the relationship between the implied volatility and the strike price for otherwise identical options from samples of S&P500 index option prices is close to a horizontal line. However, the relationship between the implied volatility and the strike price or the time to maturity for option prices sampled at dates subsequent to the 1987 crash are found to be markedly non-horizontal, and non-linear (see, among many others, Rubinstein, 1994; Fengler, 2012). They exhibit a set of features not previously observed from option prices sampled prior to 1987 (see, among many others, Derman and Kani, 1994; Dupire, 1994; Cont, 2001; Cont, da Fonseca and Durrleman, 2002; Rebonato, 2004; Cont and Tankov, 2004; Carr and Madan, 2005; Klebaner, Le and Lipster, 2006; da Fonseca and Grasselli, 2011; Fengler, 2012). The non-linear relationship between the

implied volatility and the strike price, referred to as "volatility smile", is more pronounced for options with shorter time to maturity. The contingent claims for different asset classes exhibit different features of volatility smile; for example, the smile is negatively skewed for equity and index options, while the smile exhibits less skewed for foreign exchange options. The option contracts with shorter time to maturity exhibit larger extent of fluctuation of the smile across time. The term structure of implied volatility is typically upward sloping in calm times, while in times of market turmoil it is downward sloping with the short dated options having higher levels of implied volatilities then the longer dated ones. Additionally, the volatility smile and the volatility term structure fluctuates with time.

These empirical findings that demonstrate non-negligible violation of the constant volatility assumption of the Black-Scholes option pricing formula fuelled active research in several directions. Various generalization of the constant volatility log-normal process assumed in the Black-Scholes option pricing formula have been made to better capture salient features of the volatility smile and the implied volatility term structure.

1.1.2 Deterministic volatility models

Relaxing the constant volatility assumption, Dupire (1994) proposed the local volatility model in which a more flexible log-normal process is used to model the underlying asset price process. The volatility coefficient of this log-normal process is assumed to be a deterministic function of the spot time and the spot underlying asset price. Based on this assumption, the notion of local volatility is introduced, where the square of the local volatility, i.e., the local variance, is a conditional expectation of the square of the instantaneous volatility, i.e., the instantaneous variance. Within the local volatility model framework, the local volatility can be expressed in terms of the Black-Scholes implied volatility via the Dupire's formula and the Black-Scholes option pricing formula (see, e.g., Gatheral, 2006). In a broader sense, the implied volatility can be regarded as the market participants' estimate of expected average volatility of the underlying asset for the remaining lifespan of the option contract (see, e.g., Fengler, 2005).

The local volatility model can be implemented via the Dupire's formula (Dupire, 1994) or via the implied trinomial tree Derman, Kani and Chriss (1996). However, direct implementation of the Dupire's formula to calibrate the local volatility model encounters numerical instability issues for option contracts that are far out of the money (OTM), i.e., where the spot underlying asset price is much lower than the strike price. Unlike the implied binomial tree which is well-defined, the implied trinomial tree proposed by Derman,

Kani and Chriss (1996) is under-defined, having five unknown parameters at each node, i.e., three subsequent asset prices and two transition probabilities, requiring one to *a priori* fix the state space of the asset price evolution and to reduce the construction of the implied tree in order to infer the transition probabilities by forward induction.

Various numerical strategies have been proposed in the extant literature to address the inverse problem of mapping a cross-sectional set of European vanilla option prices to the local, i.e., instantaneous, volatilities. Due to the finite number of option prices available for the calibration of the entire local volatility surface, many numerical strategies utilize interpolation techniques, such as B-splines (de Boor, 2001), in the numerical solution of the partial differential equation pertaining to this calibration problem (see, e.g., Andersen and Brotherton-Ratcliffe, 1997; Ben Hamida and Cont, 2005; Turinici, 2014; Skindilias and Lo, 2015).

Andersen and Brotherton-Ratcliffe (1997) proposed a framework that accommodates the implicit and semi-implicit Crank-Nicholson finite-difference schemes that provides an accurate fit to the entire volatility smile, offers excellent convergence properties, and flexible in terms of price- and time-space partitioning, and report empirical implementation of their proposed technique on S&P500 index European vanilla call options data. In fact, we use a portion of the data analysed in this paper to construct the synthetic test data sets used in our numerical experiment reported in Section 3.5.

An alternative approach to this inverse problem in option pricing is to use only the market option prices to calibrate the local volatility model without the use of extrapolation and interpolation techniques (see, e.g., Avellaneda, Friedman, Holmes and Samperi, 1997; Lagnado and Osher, 1997; Samperi, 2002). While this approach has its merits, it is much slower than the method used in Andersen and Brotherton-Ratcliffe (1997) as large-scale nonlinear optimization is typically necessary.

The approach proposed by Lagnado and Osher (1997) utilize regularization techniques to recast this ill-posed inverse problem into a well-posed problem that delivers stable solutions. The smoothness of the inferred local volatility surface is controlled by the non-negative regularization parameter and the functional form of the regularization term. In comparison, the approach that utilize interpolation schemes such as B-splines offers more control over the smoothing and modelling of the local volatility surface. In the case of B-splines, for example, one can fine tune the knot sequence and the order of B-spline to achieve better match of the local volatility surface to the target option prices.

With the notable exception of the work by Andersen and Brotherton-Ratcliffe (1997)

and Ben Hamida and Cont (2005), a large body of literature that address the inverse problem of local volatility model calibration involves an *a priori* specified regularization term. A wide range of functional forms have been used in extant literature, including Tikhonov, i.e., ridge, regularization (see, e.g., Tikhonov, 1943; Neubauer, 1989; Engl, Kunisch and Neubauer, 1989; Crépey, 2003; Egger and Engl, 2005; Hein, 2005), and the first and second order finite difference roughness penalty regularization (see, e.g., Eilers and Marx, 1996). How may one determine the optimal regularization functional form in the finite sample context is an open research question.

One must also specify *a priori* the magnitude of the regularization parameter. Whether generalized cross-validation (see, e.g., Kohn, Ansley and Tharm, 1991), Kullback-Leibler distance based model selection criteria (see, e.g., Akaike, 1973; Schwarz, 1978; Hurvich, Simonoff and Tsai, 1998), or L-curve based model selection criteria (see, e.g., Smith and Bowers, 1993; Hansen and O'Leary, 1993; Farquharson and Oldenburg, 2000; Hansen, 2000) is a more appropriate regularization parameter selection strategy in this context is yet an open research question.

A notable contribution of Ben Hamida and Cont (2005) is the proposal of a local volatility model calibration strategy that utilize B-spline interpolation techniques to provide control over the smoothness while circumventing the need to use regularization to provide a stable solution. This is achieved by implementing the global minimization of the objective function using evolutionary optimization techniques, a family of stochastic-based multi-point direct-search optimization algorithms designed to search for the global minimum when the objective function is non-convex with respect to the parameters of interest. Chapters 3 and 4 of this dissertation leverage on the contribution of Ben Hamida and Cont (2005) in this respect, utilizing the Zhang-Sanderson's differential evolution algorithm (Zhang and Sanderson, 2009) to facilitate attainment of global minimum in the model calibration strategies implemented therein to address the respective research questions.

More precisely, Chapters 2, 3 and 4 of this dissertation address different but related econometric issues that are closely related to the inverse problem of model calibration of option and zero coupon bond prices as approximate solutions to systems of nonlinear equations. From a numerical point of view, the problem of seeking approximate solutions to systems of nonlinear equations can be recast into a optimization problem where the objective function is a metric measuring the discrepancy between the left hand side and the right side of the system of equations (see, e.g., Hensen and Walster, 1993; Karr, Weck and Freeman, 1998; Yamamura and Suda, 2007; Yin, Qi and Xiao, 2010). Due to the

fact that the objective function may not be convex with respect to the unknown variables in question, the use of non-gradient-dependent optimization strategies prevents trapping in the local minima. We adopt the Zhang-Sanderson's differential evolution algorithm (Zhang and Sanderson, 2009) to implement the numerical solutions carried out in Chapters 3 and 4 due to the adaptive nature of this algorithm that ensures convergence towards global minimum (Hu, Xiong, Su and Zhang, 2013). As such, the numerical strategies implemented to address the problems considered in this dissertation sit in the same strand of literature as Ben Hamida and Cont (2005).

Besides the afore-mentioned literature, various other attempts have also been reported in the modelling of the volatility smile based on deterministic volatility models. Rodrigo and Mamon (2008b) considered a deterministic volatility model where the implied volatility is assumed to be a function of time to maturity only, and showed that the problem of recovering this time-dependent parameters can be formulated as an inverse Stieltjes moment problem, while Xi, Rodrigo and Mamon (2011) considered a similar approach for an asset price process where the drift and volatility coefficients of the asset price process are subjected to regime-switching. Rodrigo and Mamon (2008a) derived a semi-explicit solution of the Dupire's equation which involved functions that satisfy a first-order nonlinear system of PDEs. However, this system has no closed-form solution in general, except the restrictive case when the local volatility is assumed to depend only on the time to maturity. That said, the numerical experiments reported in Rodrigo and Mamon (2008a) only considered the special case of constant local volatility, leaving the performance of this approach under more realistic local volatility scenarios an open question. Typically, the curvature of the local volatility surface is greater than that of the corresponding implied volatility surface (see, e.g., Derman, Kani and Zou, 1996); as depicted in, for example, Figure 3.1 of Fengler (2005), Figure 6 of Ben Hamida and Cont (2005), and Figures 2 & 4 of Feil, Kucherenko and Shah (2009).

Brigo and Mercurio (2001), and Brigo and Mercurio (2002b) proposed to choose *a priori* a particular parametric risk neutral distribution that depends on several, possibly time-dependent, parameters and then use such parameters for the volatility calibration. One may construct such parametric risk neutral transition probability distribution functions based on the probability density functions of some stochastic processes with known densities that have been subjected to location shift transformation, such as log-normal processes (see, e.g., Rubinstein, 1983). Alternatively, one may construct parametric risk neutral transition probability distribution functions based on mixtures of known, basic probability density functions. Both construct leads to analytical formulas for European

options, facilitating rapid calibration of the pricing model to market data and the rapid computation of Greeks.

Although smile consistent models such as the local volatility model can provide an excellent fit to a given set of cross-sectional option prices, there are some short-comings. Among them is that the local volatility model predicts an unrealistic flat future smile; the longer the forecast horizon, the flatter the predicted implied volatility and local volatility surfaces. Therefore, even it can be calibrated perfectly to current option prices, it not suitable for pricing contingent claims in the likes of forward starting options and cliquet options that require a model that can offer a realistic future smile prediction.

1.1.3 Stochastic volatility models

Moving beyond the deterministic volatility models, research activities into the development of modelling strategies aimed at capturing the salient features of the asset price processes and its return distribution while providing an excellent fit to a given set of cross-sectional option prices. The empirical asset return distribution characteristics such as the high peaked, leptokurtic state-price density of the cross-sectional asset return distribution (see, among many others, Jackwerth and Rubinstein, 1996; Bakshi, Cao and Chen, 1997; Aït-Sahalia and Lo, 1998; Jackwerth, 1999; Aït-Sahalia and Duarte, 2003; Fengler and Hin, 2015b), and the volatility clustering in the asset return time series (see, among many others, Cont, 2001; Cont and Tankov, 2004; Gatheral, 2006) motivates the development of stochastic volatility models. Since the high central peaked and leptokurtic features of the state-price density can be modelled using mixtures of distributions with difference variances, and that the volatility clustering feature implies that volatility itself is auto-correlated, both features may be captured by modelling the asset price and the volatility coefficient in the asset price process as two stochastic processes that may be correlated.

Hull and White (1987), Scott (1987), and Stein and Stein (1991) are among the earliest work to consider the problem of option pricing in the presence of stochastic volatility. Hull and White (1987) obtained the important theoretical result that the price of a European vanilla option contract can be obtained by integrating Black-Scholes prices over the distribution of volatilities, Scott (1987) considered option pricing in the context of stochastic volatility while taking into account the effect of volatility risk premium, while Stein and Stein (1991) derived a closed-form option pricing formula for a stochastic volatility model wherein the volatility is modelled with an arithmetic Ornstein-Uhlenbeck, i.e., first order auto-regressive, process.

Typically, in a stochastic volatility modelling framework, both the price and the instantaneous volatility dynamics for the underlying asset pertaining to the contingent claim modelled as correlated stochastic processes, and the model parameters are usually assumed to be time-homogeneous. While the asset price dynamics in these stochastic are usually modelled as log-normal processes, the instantaneous volatility process is modelled using different stochastic processes, giving rise to a wide range of stochastic volatility models. We cite a few examples. Heston (1993) model the instantaneous volatility process using the Cox-Ingersoll-Ross process (Cox et al., 1985) to ensure non-negative instantaneous volatility, and assume that the asset and instantaneous volatility processes are imperfectly correlated. Heston and Nandi (2000) proposed a stochastic volatility model which is special case of that proposed by Heston (1993) by specifying the asset price process and the instantaneous volatility process to be perfectly negatively correlated. However, the transition density of the Heston-Nandi model is unrealistic as the right tail of the density is overly platykurtic. Lewis (2000) suggest that the 3/2 model may be used to model the instantaneous volatility process in order to mimic the not uncommon scenario where the option price is not a martingale, merely local martingale. Carr and Sun (2007) takes a different approach. Instead of modelling the unobservable instantaneous volatility process of an underlying asset, they propose to model the dynamics of some process which is a known function of option prices, such as the variance swap price process. Unlike the aforementioned stochastic volatility models, their framework circumvents the need to make *a priori* specification of the market price of volatility risk. Hagan, Kumar, Lesniewski and Woodward (2002) instead proposed the so-called SABR model that allows the market price and the market risks to be obtained immediately from BlackâĂŹs formula and matches the implied volatility curves observed in the market well.

Among the plethora of stochastic volatility models in the extant literature, the Heston model (Heston, 1993) is the most widely researched and widely used in academia and industry alike. Gatheral (2006), among others, pointed out that such popularity is in part due to its availability of closed-form pricing formula and numerical algorithms that facilitates fast and accurate computation of option prices, a crucial feature in the calibration of the model so that it may be used for consistent pricing of OTC contingent claims with the same underlying asset.

Heston (1993) modelled the asset price as a log-normal process, and modelled the variance process, i.e., the square of the volatility coefficient in the asset price log-normal process, as a Cox-Ingersoll-Ross process (Cox et al., 1985). This construct guarantees that the variance process will be non-negative. The transition density of asset price process

modelled by the Henton's model, obtained as a solution to the valuation partial differential equation which can be solved as a Riccati equation (see, e.g., Bakshi and Madan, 2000; Duffie, Pan. and Singleton, 2000; Gatheral, 2006), is a mixture of a log-normal density from the asset price process, and a non-central chi-squared density from the variance process. However, the corresponding probability density function is not available in closed-form, and must be represented as a characteristic function. In order to obtain a European vanilla option price using the Heston's option pricing formula, numerical evaluation of the inverse Fourier transform is necessary.

That said, the practical implementation of the numerical integration for the inverse Fourier transform evaluation is faced with three numerical issues. Firstly, the integrand is undefined at the origin, rendering it necessary to perform the numerical integration at a point very close to zero, and to avoid inaccuracies due to the removal of the origin, the integrand must not be too steep at this point. Secondly, the integrand may contain discontinuities. Albrecher, Mayer, Schoutens and Tistaert (2007) pointed out that while the representation of the integrand in Heston (1993) and Kahl and Jäckel (2005) are affected by this numerical instability issue, an alternative representation of the same integrand used by Schoutens and Simons (2004) and Gatheral (2006) is not. Thirdly, for option contracts with short maturity, the integrand may oscillate widely and may be very steep near the origin, requiring the use of a wide range for numerical integration and fine grid for integral to address these issues respectively.

Direct numerical evaluation can be performed along the lines of Mikhailov and Nögel (2003) and Attari (2004). In particular, the numerical strategy proposed by Attari (2004) reduces the two numerical integrations needed to compute option prices using Fourier inversion into a single numerical integration and reduces the number of characteristic function evaluations needed to obtain a given level of accuracy.

Carr and Madan (1999) address the European vanilla option pricing problem by Fourier inversion on the characteristic function of the option pricing formula instead of performing Fourier inversion on the characteristic function of the probability distribution function and the use of an *a priori* chosen dampening factor, thereby ensuring that the integrand is numerically stable around the origin. It utilize fast Fourier transform to obtain the option prices simultaneously computes the values of options for the set of strikes, thereby accelerating the computation speed by circumventing the need to perform one or two numerical integration per option price. Building on the work of Carr and Madan (1999), Lee (2004) proposed a strategy to determine the range of admissible values of the dampening factor within which an *a priori* chosen dampening factor may be chosen, and an approach to

select the damping factor with a minimization procedure. Lord and Kahl (2007) proposed a strategy to determine the optimal dampening factor on the basis that the optimal dampening factor is one that reduces the total variation of the integrand over the integration domain.

Chourdakis (2005) adapt the strategy proposed by Carr and Madan (1999) to a fractional fast Fourier transform framework which makes more efficient use of the information in the characteristic functions in question. The numerical experiments reported therein deminstrated up to forty-five fold computational time acceleration compared to the FFT strategy proposed by Carr and Madan (1999) without substantial losses in the accuracy of the results.

While Carr and Madan (1999) first construct the expression for the Fourier transform of the scaled option price, and then perform inverse fast Fourier transform on this expression to obtain a set of option prices at desired strike prices, Heston (1993), Kahl and Jäckel (2005) & Attari (2004), among many others, perform inverse fast Fourier transform on the characteristic function to obtain probabilities of the option contract being in the money at expiry in order to obtain the option price. Lewis (2000) instead proposed a strategy to obtain the option price by inverse transform of the product between the Fourier transform of the terminal payoff function and the characteristic function.

The inverse problem of Heston model calibration aims to search for a set of model parameters that match a given set of option prices as closely as possible. This is usually done by minimizing an objective function that measure the discrepancy between the given set of option prices and their corresponding model prices in a setting where the number of option prices exceed the number of model parameters. From a numerical perspective, this is equivalent to seeking approximate solutions to systems of over-defined nonlinear equations via optimization, a research focus considered in Chapter 3 of this dissertation.

However, the choice of model-market price discrepancy is a delicate one. Various discrepancy measures have been considered in extant literature, including price discrepancy measures in the L_1 and L_2 metrics, with or without uniform weights (see, among many others, Berestycki, Busca and Florent, 2002; 2004; Christoffersen and Jacobs, 2004; Detlefsen and Härdle, 2007a; da Fonseca and Grasselli, 2011; Levendorskii and Xie, 2012; Boyarchenko and Levendorskii, 2014). Although it is well known that these different specifications of price discrepancy measures give rise to different sets of calibrated model parameters that, when used to infer prices of exotic options, they result in prices that vary significantly. That said, there is as yet no consensus on the best choice of price discrepancy measure.

In general, the objective function, i.e., price discrepancy measure, is non-convex with respect to the model parameters. This poses challenges to the implementation of optimization procedures used to minimize the price discrepancy measure as one must avoid gradient-dependent starting-value dependent algorithms that may be trapped in the local minima and thus fail to locate the set of model parameters that correspond to the global minimum. This provided impetus for the application of non-gradient-dependent multi-point direct-search algorithms that are capable of locate global minimum in this context. The family of stochastic-based optimization procedures collectively referred to as differential evolution (see, e.g., Price, Storn and Lampinen, 2005) is gaining popularity in the area of option pricing model calibration due to its capability to locate global minimum within a pre-defined parameter space independent of starting value, and its ease in implementing the algorithm across parallel computational threads in a scalable manner such that significant computational acceleration can be achieved without sacrificing precision (see, among others, Vollrath and Wendland, 2009; Gilli and Schumann, 2011).

1.1.4 Models with jump

Although stochastic volatility models predict more realistic future volatility smile compared to the local volatility model, and provide a reasonable match to the empirically observed gentle implied volatility smile for longer-dated options, they do not provide a good fit to the steep implied volatility smile empirically observed for shorter-dated options. Put differently, the transition density inferred from market prices of option chain for short-dated equity and index options is more negatively skewed and leptokurtic with a long and fat left tail than their transition density of the longer-dated counterparts. This motivates the search for sources of uncertainties beyond volatility uncertainty to contribute towards the mixture distribution of the model transition density to better match the empirically inferred transition density. It was found that by adding jumps as an additional random variable to the Wiener process used in the constant volatility, local deterministic volatility, and stochastic volatility models, steep volatility skew can be generated and this skew decays rapidly beyond a certain time to maturity (see, e.g., Gatheral, 2006). Bakshi et al. (1997) carried out an extensive empirical analysis to compare the performance of deterministic and stochastic volatility models with or without jumps in fitting in-sample and out-of-sample option prices, and found that incorporating stochastic volatility and jumps is important for option pricing and internal consistency.

The idea of using Wiener process to model small movements of asset price, and using

random jumps of uncertain sizes, that can be modelled as Poisson processes, to model infrequent large movements of asst prices leads naturally to the use of jump-diffusion Lévy processes to model asset prices. A second approach is to model all price movements as jumps of different sizes; small price movements that are modelled in the jump-diffusion framework using Wiener process is now modelled here as jumps of small magnitudes, while large price movements that are modelled in the jump-diffusion framework using independent Poisson process is now modelled here as jumps of large magnitudes. More precisely, the jump-diffusion model jumps as infrequent random events with random magnitudes, while the second approach, referred to as the infinite activity models, model the price process with infinite number of jumps in every interval. Each of the two approaches have their merits and drawbacks. The jump-diffusion models are easier to simulate compared to the infinite activity models that may require Brownian subordination and other numerical techniques to enhance tractability (see, among others, Rubenthaler and Wiktorsson, 2003a;b).

From among the models proposed in the jump-diffusion strand of literature, Merton (1976) models jumps in the log-price process as Gaussian random variables, and Kou (2002) models the distribution of jumps in the log-price process as an asymmetric exponential distribution. Examples from among the models belonging to the infinite activity Lévy processes include the Brownian subordination Lévy processes proposed by Madan and Seneta (1990), and the "CGMY" model (Carr, Geman, Madan and Yor, 2004) which belongs to a class of tempered stable processes which are represented as time changed Wiener process.

Bates (1996) & Bates (2000) proposed a stochastic volatility model with jumps in the underlying asset only. This model may be viewed upon as a generalization of the Heston's stochastic volatility model by added random jumps with uncertain jump size to the underlying asset price process. Duffie et al. (2000) proposed a general framework that encompass, as special cases, the Heston's model Heston (1993) and the Bate's model Bates (1996) that are widely used to model asset price dynamics in option pricing, and the Gaussian and squared-root models of Vasicek (1977) and Cox et al. (1985) that are widely used to model short rate dynamics in fixed income contingent claim valuation.

While the probability density function for some of the aforementioned models classes are available in closed-form, e.g., the Variance Gamma model (Madan and Seneta, 1990), the probability density function for most of the models involving Lévy processes are not available in closed form, but are instead express in terms of the corresponding characteristic functions, e.g., Kou's model (Kou, 2002). In fact, all tempered stable process models,

e.g., the "CGMY" model (Carr et al., 2004), do not have probability density functions available in closed form.

Barring a few exceptions, the model calibration strategy for models with jumps, with or without stochastic volatility, in general require numerical solution to the partial integro-differential equations of the option price (see, e.g., d'Halluin, Forsyth and Vetzal, 2005; Carr and Mayo, 2007) or the numerical Fourier inversion to obtain the model price from a set of model parameters, similar to the calibration of stochastic volatility models discussed in Section 1.1.3 above.

Andersen and Andreasen (2000) proposed a finite difference scheme for use to calibrate the jump-diffusion models to the market price via an alternating direction implicit scheme to solve the forward partial integro-differential equation pertaining to the models. Carr and Mayo (2007) proposed a strategy to calibrate jump-diffusion models by iterative solution of the discretized partial integro-differential equation that has the advantage of being able to reduce computation time by accelerating the numerical evaluation of the presence of the non-local, integral terms in the partial integro-differential equation. Itkin and Carr (2012) develop a new approach on how to transform the PIDE into a class of so-called pseudo-parabolic equations. Although the numerical complexity of their solution is higher than that of the fast Fourier transform, their proposed algorithm provides the second order approximation in both space and time, and does not require re-interpolation of the fast Fourier transform results to the finite difference mesh grid which was previously used to find the solution for the diffusion part of the original partial integro-differential equation.

Belomestny and Reiß (2006), Belomestny and Schoenmakers (2011), and Söhl and Trabs (2012), among others, proposed strategies to calibrate exponential Lévy models by explicit inversion of the option price formula in the spectral domain, followed by the use of a cut-off scheme for high frequencies that act as a regularisation device.

In a sequel paper to Lewis (2000), Lewis (2001) extended this approach, using the Parseval's identity to obtain option prices for general jump-diffusion and other exponential Lévy processes. Ardia, Boudt, Carl, Mullen and Peterson (2010) demonstrated the potential role of differential evolution, a global optimization procedure that has seen application in local volatility model calibration (Ben Hamida and Cont, 2005), and stochastic volatility models calibration (Vollrath and Wendland, 2009; Gilli and Schumann, 2011), in calibration of a time-homogeneous jump-diffusion model.

1.1.5 Relaxing the assumption of known discount rate in model calibration

In the process of contingent claim pricing model calibration, it is a common practice to assume that the discount rate is known *a priori*, and, based on this assumption, choose a set of unobservable financial state variables and model parameters that best match the model prices to the corresponding cross-sectional set of market prices. In reality, market participants may choose different discount rates depending on, among other factors, their respective liquidity and credit risks. Additionally, they may have different expectation of the underlying asset volatility for the remaining lifespan of the contingent claim. As such, it is not unreasonable to conjecture that the prices at which the market participants are willing to trade a financial instrument may reflect an aggregation of this information on investor preferences.

Motivated by this prospect, a major stand of econometric literature evolved in the direction of investigating the information content of the implied volatility and its role in predicting future realized volatility (see, among many others, Christensen and Prabhala, 1998; Poon and Granger, 2003b; Jiang and Tian, 2005; Busch et al., 2011). The extant literature in this area share a common assumption: the discount rate is assumed to be known. On a separate theme, the literature on option pricing model calibration, including but not limited to the aforementioned constant volatility, local volatility and stochastic volatility models with or without jumps, also rely on the assumption that the discount rate is assumed to be known, or at least can be modelled adequately in the context of stochastic discount rate (see, e.g., Jiang and Van Der Sluis, 1999; Rindell, 1995; Scott, 1997; Medvedev and Scaillet, 2007; Nowak and Romaniuk, 2010; SenGupta, 2013; Zhang and Wang, 2013; Ahlip and Rutkowski, 2013a;b). The caveat is that if the assumed discount rate differs from the market participants' aggregate choice of discount rate, the inferred implied volatility will not be an accurate reflection of the market participants' aggregate expectation of the underlying asset volatility for the remaining lifespan of the option contracts. Furthermore, since the model parameters inferred from the aforementioned non-constant volatility option pricing models based on different choices of discount rate may be different, the practice of making *a priori* assumption on the discount rate may introduce model calibration risk.

Following this line of thought, we analyse the sensitivity of implied volatility calibration with respect to discount rate uncertainty. We use the Black-Scholes option pricing model as our mapping tool because, besides the unobservable implied volatility and the

uncertainty in discount rate, the other parameters can be observed directly from the market, relieving the need to account for the unobservable model parameters that are present in more sophisticated model. This form the basis of Chapter 2 of this dissertation.

Extending this idea further, we regard the market participants' aggregate choice discount rate as an unobservable financial state variable since each market participant will know their own choice of discount rate, but is unlikely to have accurate information on the choice of discount rate for all other market participants trading the same option contracts at the same time. Along with the unobservable implied volatility, they form two unobservable financial state variables that may be inferred from option prices. We use the Black-Scholes option pricing formula to construct an over-defined system of non-linear equations, and infer these two variables as approximate solution to this system of equations using the differential evolution to ensure that the global minimum is reached. This form the basis of Chapter 3 of this dissertation.

1.2 Inferring market information from bond prices by fitting the yield curve

While the option contracts are arguably some of the most actively traded financial instruments in the equity sphere, the zero coupon bonds are some of the most liquid instruments traded in the fixed-income market. Notwithstanding their apparent differences, there is an intricate link between these two classes of contingent claims (see, among many others, Cairns, 2004; Brigo and Mercurio, 2006). The net present value of an option contract is the expected discounted payoff. If it pays one dollar at terminal time only, the net present value of the option equivalent to that of a zero coupon bond paying one dollar at maturity. If it delivers a fixed cash flow at fixed, pre-defined dates, and pays a terminal cash flow, then it is replicates a coupon-bearing bond. In fact, the portfolio replication argument Black and Scholes (1973) invoked to derive the celebrated Black-Scholes option pricing formula is to use cash and zero coupon bonds to replicate a European vanilla option contract.

While the majority of the option pricing literature focus primarily on modelling the asset price dynamics and assume deterministic discount rate for ease of exposition, the primary focus of the interest rate modelling is to capture the stochastic nature of the interest rate dynamics observed in the market. While one of the main objectives of asset price dynamics, such as the models discussed in Sections 1.1.1 to 1.1.4, is to develop a

working model that can adequately simulate realistic features of implied volatility surface at some forecast horizon for applications such as interpolation of OTC traded equity or index linked option prices and exotic contingent claims valuation, one of the main objectives of interest rate dynamics modelling is to develop a working model that can adequately simulate realistic features of the yield curve, i.e., the term structure of interest rates, at some forecast horizon so that cash flows of interest rate linked contingent claims can be determined and discounted in a coherent pricing framework.

1.2.1 Short rate models

The short rate approach of yield curve modelling requires *a priori* specification of a stochastic process to describe the short rate process that span the tenor axis, and then recover, from the corresponding integrated short rate process, the yield to maturity corresponding to the respective tenors.

Ho and Lee (1986) proposed to model the short rate as a martingale process with constant volatility coefficient. However, this model has serious drawbacks. For example, it implies an unrealistic feature of long-dated forward rates being less volatile than short-dated ones, and it allows negative spot and forward rates, and is deemed unrealistic. These shortcomings precludes the use of this model for most, if not all, pricing applications.

The Vasicek model (Vasicek, 1977), a mean reverting Gaussian short rate model, assumed that the short rate follows a one-factor Ornstein-Uhlenbeck process. However, it does not guarantee non-negativity of short rate. Additionally, if we assume the Vasicek model parameters to be time-homogeneous, then the forward rate volatility implied by this model is an exponentially decay function. In order to better capture the salient features of interest rate term structure, such as the humped-shaped forward rate volatility structure that the time homogeneous Vasicek model cannot model, one must relax the time-homogeneity assumption to allow for time varying model parameters (see, e.g., Hull and White, 1994a;b).

In the Cox-Ingersoll-Ross model (CIR, Cox et al., 1985), the instantaneous short rate process is modelled with a squared-root process, thereby guaranteeing non-negativity of the short rate, and preserve the mean-reverting property of the short rate. Hull and White (1990) proposed an extension of the CIR model by relaxing the time-homogeneous model parameter constraints so that they may be modelled as time-dependent model parameters. For certain choices of model parameters, the CIR model reduce to a special case of the generalized constant elasticity of variance model commonly used to model stock prices

(see, e.g., Guo, 2008).

Duffie and Kan (1996) introduced the affine term structure framework to model the short rate as an affine function of a Markov system of latent state variables where these state variables may follow Gaussian or squared-root diffusion. Under this modelling construct, closed-form zero coupon bond pricing formulae are available, facilitating the calibration of these models for contingent claim pricing pricing and econometric analysis. In fact, many short rate models are special cases that can be nested within this modelling framework.

The Gaussian short rate models, including the Ho-Lee model and the Vasicek model, and squared-root models, such as the CIR model, are among the many special cases encompassed by this class of affine term structure models. Dai and Singleton (2000) expounded on the work of Duffie and Kan (1996) to provide a complete characterization of the admissible and identified affine term structure models according to the most general known sufficient conditions for admissibility. In fact, the affine term structure model may be viewed as a multi-factor Markov parametrization of the Heath, Jarrow and Morton (1992) model.

Motivated by the fact that the model construct considered in Duffie and Kan (1996) as well as Dai and Singleton (2000) involve latent state variables, Collin-Dufresne, Goldstein and Jones (2008) proposed an alternative characterization of the affine term structure model in terms of the level, slope and curvature of the yield curve as the three state variables in the affine term structure model construct. That said, the state variables proposed in Collin-Dufresne et al. (2008) are still not directly observable as the practical implementation of the affine term structure model representation requires extrapolation of the yield curve to zero maturity. While there are many efficient numerical algorithms that can be used for this purpose, the no-arbitrage constraints of the yield curve requires the use of shape preserving extrapolation algorithms in the likes of Laurini and Moura (2010) and Fengler and Hin (2015a) to provide arbitrage free zero maturity extrapolation of the yield curve.

Black and Karasinski (1991) address the issue of possible negative short rate in the interest rate model by proposing to model the short rate dynamics using an exponential Ornstein-Uhlenbeck process with time-dependent coefficients. However, similar to a discrete version of this model proposed by Black, Derman and Toy (1990), it is not analytically tractable, rendering model calibration to market data time consuming.

The calibration of short rate models is typically performed by choosing a set of model

parameter values that map the zero coupon bond prices to the set of cross-sectional zero coupon bond market prices as closely as possible. From a numerical perspective, it is equivalent to seeking approximate solution to a system of nonlinear equations constructed by mapping the market prices of zero coupon bonds to short rate model parameters via the corresponding zero coupon bond pricing formula. Similar to model calibration for equity option pricing models discussed in Section 1.1.3 above, the choice of discrepancy gauge that measure the discrepancy between a given cross-sectional set of zero coupon bond prices and their corresponding model prices may affect the values of inferred model parameters. Additionally, in view of the non-convex relationship between the objective function and the model parameters to be inferred, the use of a gradient independent multi-point direct search optimization algorithm in the likes of differential evolution that has been used in the option pricing model calibration (see, e.g., Ben Hamida and Cont, 2005; Vollrath and Wendland, 2009; Ardia et al., 2010; Gilli and Schumann, 2011) in this context facilitates efficient numerical search for a set of model parameters. Due to the computationally intensive nature of model calibration procedures, especially one that involves optimization algorithms in the likes of differential evolution, the availability of closed-form zero coupon bond pricing formulae helps to shorten the computational time considerably. This practical consideration that is one of the main reason for the popularity of affine term structure models among academic researchers and banking and financial practitioners.

Rodrigo and Mamon (2014) proposed an alternative approach to the calibration of the Vasicek and CIR models by constructing a system of well defined nonlinear equations using finite integral transform to map the zero coupon bond prices to the model parameters as a solution to this system of equation. In order to construct the system of equations, this approach requires the evaluation of a numerical integral of the weighted sum of log bond price across the entire continuum of tenor. In reality, since only a discrete number of zero coupon bond prices are quoted at any instance in the market, numerical algorithms need to be used to interpolate the zero coupon prices along the tenor grid in order to evaluate the said numerical integral. Whether spline-based smoothing and interpolation algorithms that observe the no-arbitrage constraints, such the the algorithms proposed by Hagan and West (2006), and Fengler and Hin (2015a), may be useful in help providing an arbitrage-free input of interpolated bond prices for numerical evaluation of this integral is an interesting open research question.

1.2.2 Multi-factor models and the interest rate volatility smile

The one-factor short rate models are not flexible enough to capture the salient features of the yield curve dynamics, thereby impairing the econometric analysis of short rate forecast and the pricing of path-dependent exotic contingent claims. This inadequacy prompted research in several different direction.

One-factor short rate models, in the likes of those discussed in Section 1.2.1, are extended to multi-factor versions of their counterparts. In fact, the affine term structure modelling framework proposed by Duffie and Kan (1996), Dai and Singleton (2000), and Collin-Dufresne et al. (2008), among others, readily accommodate multi-factor short rate modelling paradigm.

Litterman and Scheinkman (1991) and Jungbacker, Koopman and van der Wel (2014), among others, performed principal component analysis on a time series of interest rate term structure data to model the level, slope and curvature of the yield curve. Modelling in this framework requires the calibration of the model to a time series of interest rate term structure data, hence pertain to analysis under the physical measure, in contrast to the models that calibrate to a cross-sectional data of interest rate term structure that pertain to analysis under the risk-neutral measure. Audrino, Barone-Adesi and Mira (2005), among others, reported empirical evidence that the factor loadings are unstable through time for daily data of interest rate term structure.

Nelson and Siegel (1987), Diebold and Li (2006), and Diebold, Li and Yue (2008), among others, model the yield curve using a parametric function which can be viewed as a level shifted Laguerre function that can be calibrated to a cross-sectional set of interest rate term structure data, and is flexible enough to model the up-sloping, down-sloping and humped-shaped yield curve caricatures. Diebold and Li (2006) provided an elegant exposition showing that the Nelson-Siegel exponential components framework can be formulated in terms of a factor model.

While the short rate models imposes stochastic structure on the evolution of the instantaneous short rate curve, and describe the evolution of the yield curve in terms of a small set of Markovian state variables, the Heath-Harrow-Morton (HJM) framework (Heath et al., 1992) imposes stochastic structure on the evolution of the forward rate curve instead. In an important departure from the short rate modelling approach, the HJM framework extends the Ho and Lee (1986) approach of modelling the evolution of the entire yield curve in a discrete time binomial tree setting to a continuous time setting. In contrast to the short rate models, the HJM framework does not require making prior assumption

on the parametric form of the market price of risk. Instead, one derives, from the HJM construct, a no arbitrage constraint that expresses the drift of the stochastic structure of the instantaneous forward curve in terms of the volatilities across different tenors of the forward rates so that contingent claims can be valued independently of the market price of risk. In fact, virtually any exogenous term structure interest rate model can be derived as special cases of the HJM model. However, only a restricted class of volatilities can be used to construct Markovian short rate processes in this framework, while, in general, the HJM model is non-Markovian.

Despite the generality of the HJM framework, the sheer dimensionality of the model is computationally prohibitive for its direct application. Directly calibration of the HJM model poses serious numerical issues. Formally, it requires an infinite number of bond prices available to characterise the entire continuum of the forward rate curve; in reality, the number of bond prices is finite. The HJM require modelling of the instantaneous forward rate, a quantity that is not directly observable in the market.

Based on the HJM framework, Brace, Gatarek and Musiela (1997), Jamshidian (1997), and Miltersen, Sandmann and Sondermann (1997) proposed a more tractable special case of the HJM model by formulating it in terms of non-overlapping set of simply compounded market-quoted forward rates, such as the Libor forward rates. Admittedly, despite widely known as the Libor Market Model (LMM), it can be applied to model the term structure other than the Libor term structure. The model calibration procedure for the LMM is more involved than the short rate models. While the short rate models are calibrated by choosing a set of model parameters that match a set of market prices of zero coupon bonds to the corresponding theoretical model prices, the calibration of LMM require calibration of the volatilities of each piecewise continuous segment of the market quoted forward rate, and the instantaneous correlation among the Wiener processes driving each segment of the forward rate curve. It is an area of active research where a multitude of calibration strategies have been proposed to take into account information from the caplet and swaption market as appropriate for the context of application.

The usual practice (see, among many others, Brigo, Mercurio and Morini, 2005; Brigo and Mercurio, 2006; Brace, 2008) is to calibrate the instantaneous volatilities of each segment of forward rates in the LMM to the implied volatilities inferred from the tenor-matching caplet and swaption prices via numerical inversion of the Black's model in forward measure using yield curve bootstrapping techniques such as the cascade calibration algorithm (Brigo and Mercurio, 2002a). For the calibration of the instantaneous correlation matrix, one may use the correlation matrix obtained from historical time series term

structure data as an exogenous input. Brigo and Mercurio (2006) pointed out that this practice is applicable even in the risk-neutral measure calibration because the instantaneous correlation between driving Wiener processes in forward rate dynamics do not depend on the probability measure under which we specify the joint forward rate dynamics as only the drift depends on the measure. Alternatively, one may parametrize the instantaneous correlation structure, and infer the correlation model parameters from the market prices of caplets and swaptions the model is calibrated to (see, e.g., Rebonato, 1999; Morini and Webber, 2006).

The implied volatilities inferred from caplet prices via the Black's formula under the forward measure exhibit non-linearity across tenor, exhibiting volatility smile in the interest rate contingent claims (see, among many others, Jarrow, Li and Zhao, 2007). Similar to the development experienced in the modelling of the equity options implied volatility surface modelling, the basic LMM was extended by numerous researchers to better model the volatility smile in the interest rate market. Brigo and Mercurio (2002a) and Brace (2008), among others, proposed shifting the log-normal diffusion process of the forward rates to model the volatility smile. Henrard (2010) and Zhu and Qu (2016), among others, proposed the Libor local volatility model, for former calibrates the model using an approximation approach, while the latter calibrates by volatility stripping via a backward pricing partial differential equation under the spot measure. Jarrow et al. (2007) proposed a version of LMM with stochastic volatility and jump to model, while Leippold and Stromberg (2014) proposed a time-changed Lévy LIBOR market model; they calibrate their respective models to historical time series of interest rate term structure data, i.e., under the real world measure, via maximum log-likelihood estimation. Da Fonseca, Gnoatto and Grasselli (2013) proposed an alternative LMM framework that, by modelling ratio of bonds instead of directly modelling forward rates, provide a unified framework that can accommodate consistent valuation of caps, floors and swaptions simultaneously, a challenge in the LMM calibration literature due to the fact that the forward rate and the swap rate cannot both be log-normal at the same time.

1.2.3 Relaxing the assumption of single yield curve in modelling interest rate term structure

After the subprime mortgage crisis of 2007, financial market practitioners observed the empirical phenomenon from the interest rate market that the quoted interest rates that were once very close to each other, such as the overnight indexed swap (OIS) rate and deposit

rate with the same maturity or the swap rates with the same tenor but based on different floating-leg frequencies, started to diverge substantially, displaying non-negligible interest rate spreads (Mercurio, 2009). This immediately posed the problem of the consistent definition of a zero-coupon, i.e., yield, curve. In order to construct a working model for consistent pricing and discounting in the face of this new empirical phenomenon, financial market practitioners adopted an empirical approach of constructing as many curves as possible rate tenors so that future values of interest rates are projected through the associated forward (or projection) curves, whereas future cash flows are discounted by a possibly different discount curve. Mercurio (2009), Madan and Schoutens (2012), Moreni and Pallavicini (2014), and Baviera and Cassaro (2015) are among the first authors working in this direction to capture the salient features corresponding to different tenors using different yield curves. This approach is commonly referred to as the multi-curve approach, as opposed to the classical single-curve approach that models the entire interest rate term structure using a single yield curve.

Typically, the vast literature of interest rate forecast builds on the practice of using a single yield curve to model the entire interest rate term structure (see, among many others and references therein, Fisher, 1896; Culberston, 1957; Fama, 1976; Hein and Spudeck, 1988; Fama, 1990; Garfinkel and Thornton, 1995; Duffie and Kan, 1996; Aït-Sahalia, 1996a; Duffee, 2002; Diebold and Li, 2006; Collin-Dufresne et al., 2008; Audrino and Medeiros, 2011; Dewachter, Iania and Lyrio, 2014). It begs the question whether constructing predictors to forecast short rate in the multi-curve framework would improve the forecast performance.

In order to analyse the potential role of the multi-curve term structure modelling framework on interest rate forecasting, we may choose an interest rate model that has well understood forecast performance in the single-curve framework, and implement this interest rate model in the multi-curve framework for interest rate forecasting so that the interest rate forecast performance of the same model implemented in the two different frameworks, i.e., single-curve and multi-curve framework, may be compared.

It is well known that the single-factor CIR process does not perform well in forecasting future interest rate in the classical single-curve framework. We implement the single-factor CIR process in a multi-curve framework to extract the market participants' aggregate expectation of the future short rate at various available tenors from a cross-sectional set of zero coupon bond prices. More precisely, we utilize the single-factor CIR model zero coupon bond pricing formula as a mapping tool to map the market mid-quote prices of a triplet of zero coupon bonds to the three model parameters of a single-factor

CIR model in order to construct systems of well-defined non-linear equations. By seeking approximate solution to the systems of non-linear equations, we capture the information contained in the prices of the triplets of zero coupon bonds and represent them as the corresponding inferred CIR model parameters. We use the various sets of inferred CIR model parameters inferred from zero coupons of different tenors to construct predictors to forecast short rates at different tenors. We then compare its forecast performance against a predictor constructed based on the classical single-curve framework. Due to the non-convex relationship between the CIR model parameters and the objective function, we use the Zhang-Sanderson differential evolution algorithm Zhang and Sanderson (2009), an algorithm that has also been used in Chapter 3 of this dissertation, to ensure that global optimization is achieved in implementing the numerical algorithm to seek approximate solutions to the well-defined systems of equations. In this sense, the numerical strategies used in this context also follow the strand of model calibration literature for equity options in the likes of Ben Hamida and Cont (2005), Vollrath and Wendland (2009), Ardia et al. (2010), and Gilli and Schumann (2011), and that in interest rate model calibration in the likes of Gimeno and Nave (2009). This form the basis of Chapter 4 of this dissertation. Further in depth literature review pertaining to the precise construct of our proposed short rate prediction algorithm is further expounded in Section 4.2.

Admittedly, the long held notion that interest rates should be non-negative has been violated in recent times. In June 2014, the European Central Bank (ECB) set the first negative deposit rate; in March 2016, the ECB further reduced the deposit rate to -0.4%. In January 2016, Bank of Japan followed the ECB in adopting negative interest rates. This renders the investors in shorter-terms Japanese and German government bonds receive negative yield (Randow and Kennedy, 2016). That said, the interest rate dynamics that allow possibility of negative interest rates cannot be modelled by straight forward application of Gaussian short-rate models in the likes of the Ho Lee model. Instead, more sophisticated models in the likes of the arbitrage-free SABR model proposed by Hagan, Kumar and Lesniewski (2014) and the modified SABR model Antonov, Konikov and Spector (2015) need to be used in order to capture the salient features of the short rate transition density. The interest rate modelling that allow for negative rates is yet an unsettled research question, and more research results are expected to emerge to try to merge this empirical phenomenon into a coherent pricing framework. In the present dissertation, we restrict our consideration to non-negative interest rates for ease of exposition.

Chapter 2

Sensitivity analysis of implied volatility estimation with respect to future discount rate uncertainty

2.1 Introduction and motivation of study

Motivated by the fact that the market practitioners may choose their own discount rate in contingent claim pricing to reflect their own funding cost, and that the market participants' aggregate choice of discount rate reflected by a cross-sectional set of option prices is a financial parameter that cannot be observed directly, as discussed in Section 1.1.5, we presents an analysis of the implied volatility estimation uncertainty pertaining to a set of option prices due to the uncertainty of the future discount rate beyond the contemporaneous spot time. We approach this research question by first constructing an under-defined system of equations to map a cross-sectional set of option prices to their corresponding discount rates and implied volatilities. We then show that different choices of discount rates map the implied volatilities to different values.

In this chapter, we consider the probability space in the background under the risk-neutral probability measure, and use cross-sectional option prices for our empirical analysis. We merely use *ex post* interest rate uncertainty interval as an illustrative example for our empirical numerical analysis. This choice is not borne out of the real world probability measure. In fact, the interest rate uncertainty interval may be constructed via a variety of scenario generating strategies.

The implied volatility of the option contract is an important financial market parameter that is commonly used to predict the future realized volatility of the underlying asset for the remaining lifespan of the option contract. However, this parameter is not directly observable, and must be estimated from the option prices.

It is a common practice to estimate the implied volatility based on the option prices by inverting the Black-Scholes option pricing formula. In order to do so, we need to know the cumulative future discount rate. However, this parameter cannot be known with certainty. For the purpose of calculating the implied volatility, one usually specifies an observed interest rate as a proxy for the discount rate (see, e.g., Leibowitz, Sorensen, Arnott and Hanson, 1989; Adams and Booth, 1995; Brenner and Subrahmanyam, 1988; Jamshidian and Zhu, 1997; Cont, 2005; Li, 2005; Haug, 2006; Kanevski, Maignan, Pozdnoukhov and Timonin, 2008; Palandri, 2014). However, the contemporaneous discount rate does not necessary coincides with the future discount rate as there is always some uncertainty in the future evolution of the discount rate.

In this chapter, we investigate the effect of discount rate uncertainty on the estimation of implied volatility based on European vanilla call option prices. We use the option prices observed at one spot time, and use the discount rates observed at two different times, one at contemporaneous spot time, the other at some subsequent time, as a proxy to a plausible range of discount rate uncertainty that may take place as time evolve. The range between the discount rates observed at these two points in time is regarded as the range of future discount rate uncertainty across that period of time.

We consider the setting where both the implied volatilities and the discount rates are regarded as unknown parameters that need to be estimated from the observed option prices. The literature on the joint consideration of the implied volatility and the discount rate is vast (see, e.g., Avellaneda, Friedman, Holmes and Samperi, 1996; Cont and da Fonseca, 2002; Cont et al., 2002; Goncalves and Guidolin, 2004; Panigirtzoglou and Skiadopoulos, 2004; Dokuchaev, 2006; Fengler, Härdle and Mammen, 2007; Câmara, Krehbiel and Li, 2011; Homescu, 2011). The model considered in this chapter is a modification of the model proposed in Dokuchaev (2006). While the approach proposed in Dokuchaev (2006) requires the restrictive assumption that option contracts with different strike prices are mapped to the same implied volatility, this restriction is removed in the present setting. Some related bibliography can also be found in Butler and Schachter (1996), who suggested using a similar system for calculations of implied volatility distributions for the case of option prices obtained via the unbiased estimate of option price for random volatility.

We assume that option contracts with different strike and expiry characteristics are associated with different implied volatilities, while option contracts with the same time to maturity and expiry date are associated with the same discount rate. Based on these assumptions, we construct an under-defined system of nonlinear equations that maps a cross-sectional set of option prices to the corresponding implied volatilities and discount rates via the Black-Scholes option pricing formula where the uncertainty of the discount rate leads to the estimation uncertainty of the implied volatility. There exists a set of possible solutions for this under-defined system of equations. For a given plausible range of discount rate uncertainty, we calculate the corresponding range of estimation uncertainty of the implied volatility. We investigate the quantification of this range of implied volatility estimation uncertainty under different scenarios using samples of historical option prices. This investigation may be considered as a sensitivity analysis of the implied volatility with respect to discount rate uncertainty when the option price is held fixed.

We apply this sensitivity analysis strategy to a sample of historical prices of S&P500 European vanilla call option contracts. As a proxy to the plausible range of future discount rate uncertainty, we use the realized fluctuation in the London Interbank Offer Rate (Libor) time series beyond the spot time. For the time periods considered in this study, these fluctuations were small in absolute terms. Nonetheless, even such a narrow range of discount rate uncertainty leads to a noticeable range of implied volatility estimation uncertainty.

The rest of this chapter is organized as follows. In Section 2.2, we describe the extended Black-Scholes framework that accommodates the setting where the implied volatilities and the discount rates are regarded as unknown parameters. In Section 2.3, we analyse the relationship between the implied volatility and the discount rate for a given European vanilla call option price. In Section 2.4, we describe the construction of an under-defined system of nonlinear equations that maps a set of option prices to the corresponding implied volatilities and discount rates to facilitate our analysis of implied volatility estimation sensitivity with respect to discount rate uncertainty. In Section 2.5, we apply the proposed strategy to samples of historical S&P500 European vanilla call options data to analyse the implied volatility estimation sensitivity with respect to future discount rate uncertainty mimicked using different ranges of *ex post* Libor rate fluctuation. In Section 2.6, we apply the proposed strategy to samples of historical option prices to analyse the evolution of the range of implied volatility estimation uncertainty for option contracts with different strike and expiry characteristics. In Section 2.7, we discuss related matters.

2.2 The model framework

Let $(\Omega, \mathscr{F}, \mathbb{P})$ be a standard probability space where Ω is a set of elementary events, $\mathscr{F}$ is a complete sigma algebra of events, and $\mathbb{P}$ is a risk-neutral probability measure. Let $\mathscr{F}_t$ be a complete sigma algebra of events generated by the data observed at time t. Let the stochastic process of the price of a risky asset that evolve under the risk neutral probability measure be

$$S(T) = S(t) + S(t)\,\rho(t)\int_t^T ds + S(t)\,\sigma(t)\int_t^T dW(s)\,, \quad t < T, \tag{2.1}$$

where $W(s)$ is a standard Wiener process under the risk neutral probability measure,

$$\rho(t) \triangleq \frac{1}{T-t}\int_s^T \widetilde{\rho}(u)du\,, \quad \text{and} \quad \sigma(t) \triangleq \left(\frac{1}{T-t}\int_t^T \widetilde{\sigma}(u)^2 du\right)^{1/2}, \quad t < T, \tag{2.2}$$

where $\widetilde{\rho}(u)$ is the instantaneous, i.e., short, rate at time u under the risk-neutral measure that is related to the price of a risk free zero coupon bond $B(t,T)$ such that

$$B(t,T) = \exp\Big(-\int_t^T \widetilde{\rho}(u)du\Big)B(T,T)\,,$$

and where $\widetilde{\sigma}(u)$ is the instantaneous volatility, and $S(0) > 0$ is a given deterministic constant. We assume that $S(t)$, $\widetilde{\rho}(t)$, and $\widetilde{\sigma}(t)$ are adapted to the filtration $\mathscr{F}_t$, and does not depend on $\{W(\tilde{s}) - W(t)\}_{t<\tilde{s}}$, and we consider the probability measure associated with $\mathscr{F}_t$ to be the risk-neutral probability measure.

Let $K > 0$ be the strike price of a European vanilla call option contract with terminal payoff function $(S(T)-K)^+ = \max(0, S(T)-K)$, let $\sigma(t)$ and $\rho(t)$ be non-random at time t, let $0 < t < T$ be fixed, and let $C_{BS}(t, T, S(t), \sigma(t), \rho(t), K)$ be the price of a European vanilla call option contract evaluated using the Black-Scholes option pricing formula assuming the dividend rate is zero such that

$$\begin{aligned}
C_{BS}(t,T,S(t),\sigma(t),\rho(t),K) &= S(t)\mathscr{N}(d_+(t,T,S(t),\sigma(t),\rho(t),K)) \\
&\quad - Ke^{-\rho(t)\tau}\mathscr{N}(d_-(t,T,S(t),\sigma(t),\rho(t),K))\,, \qquad (2.3)\\
d_+(t,T,S(t),\sigma(t),\rho(t),K) &= \left[\log(S(t)/K) + \rho(t)\tau\right]/(\sigma(t)\sqrt{\tau}) + (\sigma(t)\sqrt{\tau})/2\,,\\
d_-(t,T,S(t),\sigma(t),\rho(t),K) &= d_+(t,T,S(t),\sigma(t),\rho(t),K) - \sigma(t)\sqrt{\tau}\,,
\end{aligned}$$

where $\tau = T - t$, and where $\mathscr{N}(d) \triangleq \frac{1}{\sqrt{2\pi}}\int_{-\infty}^{d} e^{-x^2/2}dx$. In the classical Black-Scholes

framework, $\rho(t)$ is assumed to be known, while $\sigma(t)$ is the only unknown parameter to be estimated. In our current model setting, we relax this assumption and regard both $\sigma(t)$ and $\rho(t)$ as unknown model parameters.

2.3 The relationship between implied volatility and discount rate for a given European vanilla call option price

Let the dynamics of an asset price follow the stochastic process (2.1). We consider the payoff function of a European vanilla call option struck at K. We apply the Tanaka-Meyer formula, see Tanaka (1963), Meyer (1976), and Theorem 3.6.22 and page 220 of Karatzas and Shreve (2005), on $(S(t)-K)^+$ to obtain

$$\begin{aligned}(S(T)-K)^+ &= 8\,(S(t)-K)^+ + \int_t^T \mathbf{1}_{S(s)>K}\, dS(s) + \frac{1}{2}L_t^K \\ &= (S(t)-K)^+ + \int_t^T \mathbf{1}_{S(s)>K}\,\widetilde{\rho}(s)ds + \int_t^T \mathbf{1}_{S(s)>K}\,\widetilde{\sigma}(s)dW(s) + \frac{1}{2}L_t^K\ , \quad (2.4)\end{aligned}$$

where $\mathbf{1}_{S(s)>K}$ is an indicator function of the set $S(s)>K$,

$$\begin{aligned}L_t^K &\stackrel{\Delta}{=} \lim_{n\uparrow\infty}\int_t^T n\mathbf{1}_{S(s)\,\in\,\left(K,K+\frac{1}{n}\right)}\, d\langle S\rangle_s \\ &= \int_t^T \delta(S(s)-K)\,\widetilde{\sigma}(s)^2 ds\ ,\end{aligned}$$

where $\mathbf{1}_{S(s)\,\in\,\left(K,K+\frac{1}{n}\right)}$ is an indicator function of the set $S(s) \in \left(K, K+\frac{1}{n}\right)$, $\langle S\rangle_s$ is the quadratic variation process of S, i.e.,

$$\langle S\rangle_s \stackrel{\Delta}{=} \int_0^s \widetilde{\sigma}(u)^2 du\ , \qquad 0\le u\le s,$$

and $\delta(S(s)-K)$ is the Dirac's delta function centred at K. Taking expectation on both sides of (2.4) with respect to $S(s), t<T, s\in[t,T]$, conditional on the filtration $\mathscr{F}_t$, we obtain

$$\begin{aligned}\mathbf{E}\left[(S(T)-K)^+ \,\middle|\, \mathscr{F}_t\right] = {} & (S(t)-K)^+ + \mathbf{E}\left[\int_t^T \mathbf{1}_{S(s)>K}\,\widetilde{\rho}(s)ds \,\middle|\, \mathscr{F}_t\right] \\ & + \frac{1}{2}\mathbf{E}\left[\int_t^T \delta(S(s)-K)\,\widetilde{\sigma}(s)^2 ds \,\middle|\, \mathscr{F}_t\right]. \quad (2.5)\end{aligned}$$

From (2.5), other things being equal, larger values of $\widetilde{\sigma}(s)$ will result in larger values of $\mathbf{E}\left[\int_t^T \delta(S(s)-K)\,\widetilde{\sigma}(s)^2 ds \;\middle|\; \mathscr{F}_t\right]$, leading to larger values of $\mathbf{E}\left[(S(T)-K)^+ \;\middle|\; \mathscr{F}_t\right]$, and vice versa.

If $\mathbf{E}\left[(S(T)-K)^+ \;\middle|\; \mathscr{F}_t\right]$ is a given, fixed quantity, larger values of $\widetilde{\sigma}(s)$ that lead to larger values of the expected local time at level K, i.e., $\mathbf{E}\left[\int_t^T \delta(S_s-K)\widetilde{\sigma}(s)^2 ds \;\middle|\; \mathscr{F}_t\right]$, are associated with smaller values of $\widetilde{\rho}(s)$ that lead to smaller values of $\mathbf{E}\left[\int_t^T \mathbf{1}_{S(s)>K}\widetilde{\rho}(s) ds \;\middle|\; \mathscr{F}_t\right]$. Multiplying (2.5) on both sides with a deterministic discount factor $e^{-\rho(t)\tau}$, this association still holds, implying that this association holds for the net present value of a European vanilla call option contract $e^{-\rho(t)\tau}\mathbf{E}\left[(S(T)-K)^+ \;\middle|\; \mathscr{F}_t\right]$.

From (2.2), we see that larger values of $\widetilde{\sigma}(s)$ are associated with larger values of $\sigma(t)$, while smaller values of $\widetilde{\rho}(s)$ are associated with smaller values of $\rho(t)$. It follows that for a given, fixed net present value of a European vanilla call option contract $e^{-\rho(t)\tau}\mathbf{E}\left[(S(T)-K)^+ \;\middle|\; \mathscr{F}_t\right]$, if we specify a larger value for $\rho(t)$ while estimating $\sigma(t)$ from the given, fixed option price $e^{-\rho(t)\tau}\mathbf{E}\left[(S(T)-K)^+ \;\middle|\; \mathscr{F}_t\right]$, it will result in a smaller estimate of $\sigma(t)$.

2.4 Sensitivity analysis of implied volatility estimation with respect to discount rate uncertainty based on an under-defined system of nonlinear equations

Let $C(t,T_j,K_{j.\ell}), j=1,\ldots,m, \ell=1,\ldots,n_j$, be the prices of $\sum_{j=1}^m n_j$ European vanilla call option contracts written on the same underlying asset observed at time t with times to maturity $\left\{\tau_j\right\}_{j=1}^m$, $\tau_j = T_j - t$, and struck at $\left\{K_{j,\ell}\right\}_{j=1,\ldots,m,\ell=1,\ldots,n_i}$ respectively. By mapping $C(t,T_j,K_{j.\ell})$ to their corresponding theoretical prices evaluated using the Black-Scholes option pricing formula, we construct a system of nonlinear equations

$$C_{BS}(t,T_j,S(t),\sigma_{imp,j,\ell}(t),\rho_j(t),K_{j,\ell}) = C(t,T_j,K_{j,\ell})\,, \quad j=1,\ldots,m,\ell=1,\ldots,n_j, \quad (2.6)$$

where $\sigma_{imp,j,\ell}(t)$ is the Black-Scholes model-based implied volatility corresponding to $C(t,T_j,K_{j,\ell})$, $\rho_j(t)$ is the discount rate for tenor τ_j at time t, and where $S(t)$ is the spot price of the underlying asset at time t. By regarding $\left\{\rho_j(t)\right\}_{j=1}^m$ as unknown parameters, (2.6) becomes an under-defined system of equations where the solution of $\sum_{j=1}^m n_j$ equations necessitates finding solutions for $m+\sum_{j=1}^m n_j$ unknown parameters, namely

$\left\{\sigma_{imp,j,\ell}(t)\right\}_{j=1,\ldots,m,\ell=1,\ldots,n_j}$ and $\left\{\rho_j(t)\right\}_{j=1}^{m}$. Under this construction, uncertainty of the discount rate leads to estimation uncertainty of the implied volatility.

We suggest to use (2.6) as a convenient working model to quantify the estimation uncertainty of implied volatility based on some pre-defined interval $[\rho_{min}, \rho_{max}]$ that mimic plausible fluctuation of discount rate with respect to two instances in time, one at spot time t, the other at some later time $t', t < t'$. Let $\rho_{min} = \min\left(\rho_j(t), \rho_j(t')\right)$, and $\rho_{max} = \max\left(\rho_j(t), \rho_j(t')\right)$, where $\rho_j(t)$ and $\rho_j(t')$ are the discount rates for tenor τ_j at times t and t' respectively. Specifically, we have chosen to construct $\rho_j(t)$ by interpolating at tenor τ_j from the yield curve historical data of a reference rate quoted at time t, and construct $\rho_j(t')$ by interpolating also at tenor τ_j from the yield curve historical data of the same reference rate quoted at time t'. For our current context, we do not construct $\rho_j(t')$ by interpolating at tenor $\tau_j - (t' - t)$ from the yield curve historical data quoted at time t'. Our simple construction of ρ_{min} and ρ_{min} is aimed at capturing the vertical shift of the yield curve in consideration, i.e., the change in constant maturity rate at a horizon τ_j, instead of taking into account the more complicated joint dynamics of the rolldown yield change from tenor τ_j to tenor $\tau_j - (t' - t)$ and the change in constant maturity rate at a horizon $\tau_j - (t' - t)$. Granted, different strategies may be used to construct ρ_{min} and ρ_{max} depending on the context of application.

For example, in *ex-post* study of future discount rate uncertainty, the discount rates at the corresponding instances, $\rho_j(t_1)$ and $\rho_j(t_2)$, $t_1 < t_2$, from the relevant historical interest rates may be used to construct ρ_{min} and ρ_{max}. Additionally, in portfolio scenario simulation (see, e.g., Jamshidian and Zhu, 1997), the current discount rate $\rho_j(t_{\text{spot}})$, and a simulated future discount rate $\rho_j(t_{\text{future}})$ may also be used to construct ρ_{min} and ρ_{max} to facilitate quantification of the corresponding implied volatility uncertainty for risk management purposes. Furthermore, in rare event simulation for stress-testing, one may use the current discount rate $\rho_j(t_{\text{spot}})$ and a simulated future discount rate that mimics wide fluctuation in discount rate comparable to those observed in catastrophic financial events to construct ρ_{min} and ρ_{max}.

2.5 Numerical analysis using cross-sectional S&P500 call options data

We use future London Interbank Offer Rate (Libor) uncertainty, in an *ex post* manner, to mimic plausible future discount rate uncertainty. We construct the intervals of the discount

rate uncertainty using the historical Libor time series downloaded from the Economic Research Division, Federal Reserve Bank of St. Louis. The Libor time series depicted in Figures 1 and 2 showcase two different time frames that display contrasting trends of Libor rates during different market conditions. Figure 1 depicts wide fluctuation of interest rates that can take place during market turmoil, while Figure 2 depicts narrow fluctuation typical of stable market conditions. For our empirical analysis, we consider future discount rate uncertainty mimicked using Libor rates quoted during stable market conditions. At the time when this analysis was carried out, 2009 to 2013 was the most recent time interval within which daily fluctuations of the Libor rates were small. We have chosen May 2011 as a subinterval in the middle of this wider time interval for our empirical analysis. In this section, we use the day-close prices of the S&P500 index European vanilla call option contracts traded at the Chicago Board Options Exchange (CBOE) on May 5th 2011, obtained from Market Data Express LLC., to analyse the impact of a given, small interval of discount rate uncertainty on the interval of the implied volatility estimation uncertainty for option contracts with different strike prices and times to maturity.

We obtain the proxy for the discount rates that are used in Sections 2.5 and 2.6 by first fitting smoothing spline curves to the Libor rates where the smoothing parameters are estimated using generalized cross-validation, and then interpolate the discount rate proxies from the spline curves at the respective tenors that correspond to the times to maturity of the option contracts considered. In order to do so, we use the smoothing spline modelling algorithm implemented as the in-build function `smooth.spline()` for the `R` computing environment (R Core Team, 2012). This suffice for our current purpose of constructing plausible discount rate uncertainty intervals to analyse implied volatility estimation uncertainty in our simple empirical examples. However, in order to construct arbitrage-free discount rate term structures for other purposes such as to perform coherent pricing and hedging of contingent claims, and to provide input to econometric models, more sophisticated techniques may be required instead (see, e.g., Marangio, Bernaschi and Ramponi, 2002; Ramponi, 2002; Hagan and West, 2006; Chiu, Fang, Lavery, Lin and Wang, 2008; Laurini and Moura, 2010; Fengler and Hin, 2015a).

Table 1 depicts the interpolated Libor rates, obtained based on the historical Libor rates quoted on May 5th 2011, May 13th 2011, and May 27th 2011, at various tenors that correspond to the times to maturity of the option contracts considered. The quoted Libor rates are first converted from the discrete interest rates convention to continuously compounded convention prior to interpolation. A subset of the interpolated rates depicted in Table 1 is used as proxy for the discount rates in the empirical analysis reported in this

section.

Using two sets of option prices observed on May 5th 2011 that correspond to the European vanilla call option contracts expiring on either Sept. 30th 2011 or Mar. 30th 2012, we compare the intervals of implied volatility estimation uncertainty in the presence of discount rate uncertainty across the same horizon for these option contracts. The proxy for discount rates pertaining to these two sets of option contracts at the spot time are interpolated from the Libor term structure quoted on May 5th 2011 while the proxy for future discount rates pertaining to the same sets of option contracts are interpolated from the Libor term structure quoted on May 13th 2011. These discount rates are used to construct the future discount rate uncertainty intervals in order to calculate the corresponding intervals of implied volatility estimation uncertainty. For option contracts expiring on Sept. 30th 2011, we obtain $\rho_{min} = 0.003409$, and $\rho_{max} = 0.003663$. For option contracts expiring on Mar. 30th 2012, we obtain $\rho_{min} = 0.006576$, and $\rho_{max} = 0.006854$. We depict the corresponding estimated implied volatilities in Table 2. In this sample, the implied volatilities for the into-the-money (ITM) option contracts tend to exhibit a wider interval of estimation uncertainty than those for the out-of-the-money (OTM) option contracts. This trend is more obvious for the set of option contracts expiring on Mar. 30th 2012, but less so for those expiring on Sept. 30th 2011. Additionally, for a given range of discount rate uncertainty and for a given strike price, the option contract with longer time to maturity tend to exhibit wider interval of implied volatility estimation uncertainty.

We also analyse the impact of future discount rate uncertainty across different horizons ahead of the spot time based on option contracts with the same time to maturity. In the lower panel of Table 2, for example, we compare and contrast the intervals of implied volatility estimation uncertainty in the presence of discount rate uncertainty across the two different time intervals considered based on a set of option contracts expiring on Mar. 30th 2012. The shorter time interval mimics the future discount rate uncertainty between the spot date, May 5th 2011, and a subsequent date, May 13th 2011, where we obtain $\rho_{min} = 0.006576$, and $\rho_{max} = 0.006854$ by interpolating the Libor rates quoted on these two dates. The longer time interval mimics the future discount rate uncertainty between the spot date and a subsequent date, May 27th 2011, where we obtain $\rho_{min} = 0.006228$, and $\rho_{max} = 0.006854$ by interpolating the Libor rates quoted on these corresponding dates. The interval of implied volatility estimation uncertainty is wider for the scenario simulating the future discount rate uncertainty across a longer time interval in this particular example as the longer time interval considered is associated with a wider range of discount rate uncertainty. This is a sample dependent phenomenon as the evolution of interest rate

across time is stochastic and non-monotonic, and as such it may turn out that, for some other time frames, the interval between the spot rate and the rate more distant into the future may instead be narrower than that between the spot rate and an interest rate at a time in the nearer future. Henceforth, suffice to note that the range of discount rate uncertainty between the spot time and any two different time points ahead may be different.

In order to provide an idea of the impact of 10% change in the magnitude of the discount rate of choice would have on the corresponding inferred implied volatilities using the empirical dataset analysed in this section, we repeat the calculations carried out for Table 2. Instead of constructing the discount rate uncertainty interval using *ex post* Libor discount rates, we use 90%, 100%, and 110% of the contemporaneously quoted Libor rates for the appropriate tenor on May 5th 2011 to construct the discount rate uncertainty ranges and report the corresponding results in Table 3. The findings are qualitatively similar to those of Table 2.

2.6 Numerical analysis using longitudinal S&P500 call options data

In this section, we analyse the size of the implied volatility estimation uncertainty interval for a set of option contracts across a number of consecutive trading days with respect to a given, fixed interval of future discount rate uncertainty throughout these trading days considered. Admittedly, the interval of future discount rate uncertainty may change from day to day. However, the combined effect of the fluctuation of future discount rate uncertainty, and the reduction of time to maturity of the option contracts across different trading dates on the implied volatility estimation uncertainty is complicated and difficult to interpret. The current approach, albeit simple, allows us to concentrate on the analysis of the size of implied volatility estimation uncertainty intervals as the times to maturity of the option contracts decrease, conditional on some fixed interval of discount rate uncertainty.

For this purpose, we use the historical data of two sets of S&P500 index European vanilla call option contracts expiring on either Sept. 30th 2011 or Mar. 30th 2012 traded on CBOE between May 3rd 2011 and May 31st 2011 inclusive. The proxy for the discount rates at spot time for the corresponding times to maturity of the option contracts concerned are interpolated from the Libor rates quoted on May 3rd 2011, while the proxy for the discount rates at a future date for the corresponding times to maturity of these option contracts are interpolated from the Libor rates quoted on May 31st 2011. For option

contracts expiring on Sept. 30th 2011, we obtain $\rho_{min} = 0.003021$, and $\rho_{max} = 0.003740$. For option contracts expiring on Dec. 21st 2013, we obtain $\rho_{min} = 0.007269$, and $\rho_{max} = 0.007578$.

Let $\sigma_{min}(t)$ and $\sigma_{max}(t)$ be the implied volatilities estimated based on (2.6) by inverting the Black-Scholes option pricing formula assuming that the discount rate is either $\rho_{min} = 0.007269$ or $\rho_{max} = 0.007578$ respectively. Let $\Delta(t) = \sigma_{max}(t) - \sigma_{min}(t)$, where t denotes the trading date on which the option prices $C(t; \tau_j, K_{j,\ell})$ are observed. The time series of $\Delta(t)$ for these two sets of option contracts are tabulated in Table 4, and depicted in Figure 3. The non-monotonic trend of $\Delta(t)$ across different trading dates may, in part, be attributed to the stochastic nature of the underlying asset price evolution. For this sample, the day-to-day variability of $\Delta(t)$ appears to be less marked for longer dated option contracts.

With an aim to provide an idea of the impact of 10% increase in the magnitude of the discount rate would have on the inferred implied volatilities using the empirical dataset analysed in this section, we repeat the afore-mentioned calculations based on which Table 4 is produced. Instead of constructing the discount rate uncertainty intervals using *ex post* Libor discount rate fluctuation range, we use 100% and 110% of the contemporaneously quoted Libor rates for the appropriate tenor quoted on on May 2nd 2011 to construct the discount rate uncertainty ranges and report the corresponding results in Table 5.

2.7 Discussion

Assuming that both the implied volatilities and the discount rates are unknown parameters, we construct an under-defined system of nonlinear equations by mapping a cross-sectional set of European vanilla call options prices to the corresponding discount rates and implied volatilities via the Black-Scholes option pricing formula. We then use this system of equations to perform sensitivity analysis of implied volatility estimation uncertainty with respect to discount rate uncertainty. We apply this strategy to the historical data of a set of S&P500 index European vanilla call option contracts to perform sensitivity analysis of implied volatility estimation uncertainty with respect to discount rate uncertainty.

In the empirical analyses reported in Section 2.5 and Section 2.6, we construct proxy for discount rates by interpolation of the contemporaneously quoted Libor rates. Our choice of using the Libor rates as a basis for our analysis is motivated by the fact that the Libor rates tend to reflect the average inter-bank credit risk. Admittedly, other interest rate term structures that reflect different extent of liquidity and credit risks may be used instead

for sensitivity analysis for different contexts of applications.

Chapter 3

Estimation of the implied discount rates and the implied volatilities from option prices via an over-defined system of nonlinear equations

3.1 Introduction

While Chapter 2 concerns the utilization of an under-defined system of equations to analyse the sensitivity of implied volatility calculation with respect to discount rate uncertainty and highlights the potential consequences of discount rate uncertainty in implied volatility calibration, the theme of the current chapter concerns the utilization of an over-defined system of equations to develop a strategy in order to infer the discount rates and the implied volatilities simultaneously from a set of option prices, thereby circumventing the need to make *a priori*, and potentially erroneous, assumption on the discount rate that may affect the accuracy of implied volatility calibration from option prices.

Motivated by the considerations outlined in Section 1.1.5, we propose, in this chapter, a strategy to infer, from the prices of a set of European vanilla call option contracts, the market participants' aggregate choice of the discount rate, and the market participants' aggregate expectation of the underlying asset price volatility for the remaining lifespan of these option contracts. Working within the Black-Scholes option pricing framework, we relax the assumption of *a priori* known risk-free rate, and assume that both the discount

rate and the implied volatility are unknown parameters. We use the Black-Scholes option pricing formula as a mapping tool to construct an over-defined system of nonlinear equations. Approximate numerical solution of this system allow us to map a set of option prices to their corresponding pairs of discount rates and implied volatilities. The set of discount rates may be regarded as the implied discount rates with respect to this set of option prices. We suggest to regard the set of implied discount rates as model-based estimates of the market participants' aggregate choice of discount rate, and the set of implied volatilities estimated jointly with the implied discount rates as model-based estimates of the market participants' aggregate expectation of the underlying asset price volatility for the remaining lifespan of these option contracts.

The rest of the chapter is organized as follows. Section 3.2 reviews the relevant literature and discusses the motivation of the work reported in this chapter. Section 3.3 describes the theoretical framework that maps the implied discount rates and the implied volatilities to the prices of a set of European vanilla call option contracts in the extended Black-Scholes option pricing model where the discount rates and implied volatilities are regarded as unknown model parameters. Section 3.4 describes the proposed algorithm for estimating implied discount rates and implied volatilities jointly from a set of option prices. Section 3.5 reports the numerical performance of the proposed algorithm on two synthetic test data sets. Section 3.6 reports the numerical results obtained by applying the proposed algorithm to analyse the historical prices of the S&P500 index option contracts sampled between 2004 and 2013 inclusive. Section 3.7 discusses related issues.

3.2 Literature review and motivation of study

The choice of the risk-free rate proxy made by market participants in the context of contingent claim valuation tend to reflect their corresponding credit and liquidity risk. The demand from market participants for the flexibility of being able to choose different reference rates as proxy to risk-free rate corresponding to different tenors for different applications is recognized in a recent report by the Bank of International Settlement (Bank of International Settlement, 2013). The said report goes further to indicate the need to make available more diverse reference interest rates that better match the individual needs of the market participants. In practice, a combination of reference rates that reflect different levels of risk premia at different tenors may be used to construct the discount rate term structure for the appropriate context.

One such example is the calculation of volatility indexes. In the calculation of the volatility index based on S&P500 equity index (VIX) quoted by CBOE, the bond-equivalent yields of the U.S. Treasury-bill, which contain near zero credit risk, are used as proxy for the risk-free rates (CBOE, 2013). In the calculation of the volatility index based on DAX equity index (VDAX) quoted by Deutsche Börse, the proxy to risk-free rates are obtained by linear interpolated between Euro OverNight Index Average (EONIA) rate and 1 month Euribor, the London Interbank Offer Rate for the Euro denomination (Deutsche Börse, 2007). In the calculation of the volatility index based on ASX200 equity index (S&P/ASX200 VIX) quoted by the Australian Stock Exchange, the proxy for the risk-free rates are obtained by linear interpolated between overnight Reserve Bank of Australia (RBA) rate and 1 month Australian Financial Markets Association (AFMA) Bank Bill Swap (BBSW) benchmark rate (S&P Dow Jones Indices, 2013). While EONIA and RBA rates are virtually free of bank credit risk, one month Euribor and the AFMA BBSW reflect the average bank credit risk premia.

While Palandri (2014) reported that the risk-free rate has relevant predictive information with respect to the conditional variance of individual stock return, and that interest rate changes have different effects for different assets, Brenner and Galai (1986), Leibowitz et al. (1989) and Adams and Booth (1995), among others, emphasized the importance of the choice of risk-free rate proxy, or discount rate, in contingent claim valuation. In fact, not only would the choice of discount rate affect the calculation of net present value of contingent claims from a pricing perspective, it would affect the magnitude of the implied volatility inferred from the historical price of an option contract from an econometric perspective. On this theme, Section 2.4 offers a discussion on the relationship between the discount rate and the implied volatility estimated jointly from the price of a European vanilla call option contract.

The estimation of implied volatilities from historical option prices is an area of active research as the implied volatility is a financial parameters that has many practical applications. For example, the implied volatility estimated from the European vanilla options can be used to forecast future realized volatility of the underlying asset (see, e.g., Christensen and Prabhala, 1998; Poon and Granger, 2003b; Busch et al., 2011), to construct market benchmarks that reflect the market sentiment of the future realized volatility of certain asset classes (see, e.g., Deutsche Börse, 2007; Jiang and Tian, 2007; Carr and Wu, 2010; CBOE, 2013; S&P Dow Jones Indices, 2013), to provide input for the coherent pricing of exotic contingent claims with the same underlying asset for trading and risk management purposes (see, e.g., da Fonseca and Grasselli, 2011), and to carry out pricing of credit

default swap (CDS) contracts that are related to the same underlying asset of the option contracts from which the implied volatilities are estimated from (see, e.g., Cao, Yu and Zhong, 2010; 2011).

Thus far, the extant literature appear to suggest that the implied volatilities, i.e., both the Black-Scholes (Black and Scholes, 1973) model-based implied volatility, and the model-free implied volatility (Britten-Jones and Neuberger, 2000), appear to be better predictors of the future realized volatility of the underlying asset for the remaining lifespan of the option contract than the historical volatility of the underlying asset. Some empirical results on the forecast performance of the Black-Scholes model implied volatility can be found in, e.g., Christensen and Prabhala (1998), and Christoffersen, Heston and Jacobs (2006), while Jiang and Tian (2005), Jiang and Tian (2007), and Carr and Wu (2009), among others, report forecast performance of the model-free implied volatility. While the Heterogeneous Autoregressive model of Realized Volatility (HAR-RV) proposed by Corsi (2009) appears to be a serious contender of the implied volatility in the forecast of future realized volatility, there is currently no definitive empirical evidence pointing one way or the other.

It has long been reported in the literature that there exists a noticeable difference between the implied and realized volatilities. This difference is larger when the index return distribution is more negatively skewed and leptokurtic in the presence of investor risk aversion (Bakshi and Madan, 2006). A plethora of theories have been put forth in the attempt to explain this difference, including, among others, the existence of negative variance risk premium that rationalize the willingness of risk-adverse investors to pay a premium for protection against an increase in volatility of asset prices (see, e.g., Carr and Wu, 2009; Bollerslev, Tauchen and Zhou, 2009; Todorov, 2010; Bollerslev and Todorov, 2011). Theoretical underpinning aside, the numerical implementation of the estimators for the implied and realized volatilities may have contributed to the estimated difference between implied and realized volatilities.

The squared-root of the sum of squared log return of an asset is widely regarded as a robust estimator of its historical volatility (see, e.g., Aït-Sahalia, Mykland and Zhang, 2003; Bollerslev, Gibson and Zhou, 2011). This estimator is independent of the risk-free rate proxy used in the pricing of the contingent claims that regard this asset as the underlying asset of these claims. On the contrary, the estimation of both the Black-Scholes model-based implied volatility and the model-free implied volatility require making assumption on the risk-free rate. Given an option price, other things being equal, different choices of risk-free rate proxy maps the same option price to different values of implied

volatility. Therefore, for a given estimate of the realized volatility, different choices of risk free rate proxy will result in different estimates of the difference between implied and realized volatilities. In order to infer the market participants' aggregate expectation of the underlying asset price volatility for the remaining lifespan of the option contract, we have to choose a risk-free rate proxy that matches the market participants' aggregate choice of risk-free rate proxy. This motivates the subject of study in this chapter, i.e., to estimate the discount rate and implied volatility jointly from a set of option prices.

Dokuchaev (2006) and Butler and Schachter (1996) proposed a theoretical framework that relaxes the assumption of *a priori* known risk-free rate, and regards the discount rate and implied volatility in the Black-Scholes option pricing formula as unknown parameters. This idea provides impetus to our development of a strategy to jointly estimate the implied discount rates and the implied volatilities from a set of option prices. A recent paper by Bianconi, MacLachlan and Sammon (2015) proposed a strategy to jointly estimate the implied risk-free rates and the implied volatilities from option prices. While the manuscript that arise from this chapter in the form of Hin and Dokuchaev (2015a) was submitted on Mar. 21st 2014 and accepted on Jan. 23rd 2015, the work by Bianconi et al. (2015) was submitted on May 15th 2014 and accepted on Oct. 16th 2014. Although both Hin and Dokuchaev (2015a) and Bianconi et al. (2015) propose strategies to estimate the implied discount rates or implied risk-free rates, and the implied volatilities from option prices, they differ in terms of model assumptions, numerical implementation, and empirical application.

Firstly, Bianconi et al. (2015) arrange a cross-sectional set of prices of European vanilla call option contracts written on the same underlying asset with the same expiry date in ascending magnitudes of strike, and group the adjacent option contracts into multiple non-overlapping pairs. They assume that each pair of these option contracts with different strike prices but the same expiry date are associated with the same implied risk-free rate and implied volatility. For each pair of option contracts, a set of two nonlinear equations is formulated by mapping both option prices to two unknown parameters, i.e., one implied risk-free rate and one implied volatility, via the Black-Scholes option pricing formula. Specifically, they assume that option contracts with different strike prices that are grouped in the same pair share the same implied volatility, while option contracts with the same expiry date but grouped in different pairs may have different implied risk-free rate.

In contrast, our proposed strategy utilize prices of a set of European vanilla call option contracts written on the same underlying asset with different strike prices and different expiry dates observed on two successive trading days. We assume that the option contracts

with the same time to maturity and expiry date are associated with the same implied discount rate. In this sense, the definition of implied risk-free rate in Bianconi et al. (2015) is different from the definition of implied discount rate in our proposed strategy. We believe our assumption that option contracts sharing the same expiry date are associated with the same discount rate is more in line with the current practice of coherent contingent claim pricing where cash flows at the same time horizon are discounted with the same discount rate. On the other hand, the assumption used by Bianconi et al. (2015) is somewhat at odds with this practice as it seems to allow non-uniqueness of discount rate at the same tenor for the same contingent claim. Additionally, we assume that option contracts with different strike and expiry characteristics may be associated with different implied volatilities. We believe this assumption is less restrictive than requiring option contracts with different strike prices to share the same value of implied volatility on the basis of user-specified pairing of option contracts.

Secondly, Bianconi et al. (2015) utilize a pair of option prices observed at the same instance to formulate a system of two nonlinear equation with two unknown parameters to be solved. In contrast, we utilize prices of a set of option contracts observed at two instances in time to formulate an over-defined system of nonlinear equations and seek numerical approximate solution to this system.

Additionally, Bianconi et al. (2015) seek numerical solution to their system of nonlinear equations by a three stage optimization procedure that minimize a scaled L_2 objective function. Interior point search is first performed based on a pair of user-defined starting values to obtain a first set of solution for implied risk-free rate and implied volatility. One then use this first set of solutions as input to the *patternsearch* algorithm, a derivative-free method in the optimization tool box of MATLAB (The MathWorks, Inc., Natick, Massachusetts, United States) to obtain a second set of solution values. One finally use this second set of solutions as input to the interior point search algorithm again to obtain a third set of solution values. The set of solution among the three that corresponds to the smallest value of objective function is regarded as the solution to the system of equations.

In contrast, we seek numerical solution to our over-defined system of nonlinear equations by the Zhang-Sanderson algorithm (Zhang and Sanderson, 2009), a stochastic-based multi-point direct-search global optimization algorithm that belongs to the differential evolution family of optimization techniques (see, e.g., Storn and Price, 1997) implemented in the `DEoptim` (Ardia, Mullen, Peterson and Ulrich, 2012) package for the `R` computing environment (R Core Team, 2012). Our numerical implementation strategy can accommodate minimization of both L_1 and L_2 metric objective functions. Provision of user-

defined starting values is not required as the algorithm is initialised using pseudo-random numbers.

Thirdly, Bianconi et al. (2015) use the implied risk-free rates and implied volatilities estimated as solutions to their system of equations based on the 2007 to 2008 historical prices of S&P500 index call option contracts to interpolate at-the-money (ATM) implied volatilities based on a seemingly unrelated regression framework. Then the interpolated ATM implied volatilities are used to forecast the VIX index.

In contrast, we apply our proposed strategy to samples from the 2004 to 2013 historical prices of S&P500 index call option contracts in order to analyse the trend of the implied discount rate across time. Specifically, we highlight the difference between the implied discount rates and contemporaneously quoted Libor rates and Overnight Indexed Swap (OIS) rates in these samples.

3.3 The model framework

We consider the Black-Scholes option pricing formula (2.1) described in Section 2.2. To facilitate referencing, we depict (2.2) and (2.3) hereunder. The theoretical price of a European vanilla call option contract evaluated using the Black-Scholes option pricing formula, assuming zero dividend rate, is

$$\begin{aligned} C_{BS}(t,T,S(t),\sigma(t),\rho(t),K) &= S(t)\mathscr{N}(d_+(t,T,S(t),\sigma(t),\rho(t),K)) \\ &\quad - Ke^{-\rho\tau}\mathscr{N}(d_-(t,T,S(t),\sigma(t),\rho(t),K)) \,, \\ d_+(t,T,S(t),\sigma(t),\rho(t),K) &= \left[\log(S(t)/K) + \rho(t)\tau\right]/(\sigma(t)\sqrt{\tau}) + (\sigma(t)\sqrt{\tau})/2 \,, \\ d_-(t,T,S(t),\sigma(t),\rho(t),K) &= d_+(t,T,S(t),\sigma(t),\rho(t),K) - \sigma(t)\sqrt{\tau} \,, \end{aligned}$$

for some fixed $0 < t < T$, where $\tau = T - t$, $\mathscr{N}(d) \triangleq \frac{1}{\sqrt{2\pi}}\int_{-\infty}^{d} e^{-x^2/2}dx$, $K > 0$ is the strike price of the option contract, and where

$$\rho(t) \triangleq \frac{1}{T-t}\int_t^T \widetilde{\rho}(s)ds \,, \quad \text{and} \quad \sigma(t) \triangleq \left(\frac{1}{T-t}\int_t^T \widetilde{\sigma}(s)^2 ds\right)^{1/2}$$

are the discount rate and implied volatility for the time interval $[t,T]$ respectively where $s \in [t,T]$. In practice, $\sigma(t)$ is often estimated by inverting the Black-Scholes option pricing formula with respect to the price of a European vanilla call option contract for some a

priori assumed value of $\rho(t)$ as a solution of the nonlinear equation

$$C_{BS}(t, T, S(t), \sigma(t), \rho(t), K) = \text{Observed option price} .$$

From the relationship between the implied discount rate and the implied volatility for a given, fixed price of a European vanilla call option contract described in Section 2.3, we can see that if we choose a larger value for $\rho(t)$, we will map the observed option price to a smaller estimate of implied volatility.

In the classical Black-Scholes option pricing framework, $\rho(t)$ is assumed to be known, and the implied volatility is regarded as a function of the option price, $\rho(t)$, K, $S(t)$, t, and T. However, this standard definition of the implied volatility ignores the fact that, in reality, the market participants' aggregate choice of the risk-free rate proxy is unknown, and need to be inferred from the option prices, and vice versa.

In order to circumvent the need to make *a priori* assumption on $\rho(t)$ in estimating $\sigma(t)$, we propose a strategy to estimate $\rho(t)$ and $\sigma(t)$ jointly from a set of option prices.

3.4 Joint inference of the implied discount rates and the implied volatilities from an over-defined system of non-linear equations constructed based on longitudinal option prices

Let $C(t_i, T_j, K_{j,\ell}), i = 1, \ldots, p, j = 1, \ldots, m, \ell = 1, \ldots, n_j$, be the prices of a set of European vanilla call option contracts that expire at times T_j and struck at $K_{j,\ell}$ respectively where p, m, and n_j, are some given positive integers. These option prices are observed at times t_i where $t_{i-1} < t_i$. Working within the extended Black-Scholes framework described in Section 3.3, we regard both the implied discount rates and the implied volatilities as unknown parameters that have to estimated from the set of option prices $\{C(t_i, T_j, K_{j,\ell})\}_{i=1,\ldots,p, j=1,\ldots,m, \ell=1,\ldots,n_j}$.

We make the following assumptions.

A.1 **Parameter dependence assumption.** We assume that the price of an option contract $C(t_i, T_j, K_{j,\ell})$ contains information on the implied discount rate $\rho_j(t_i)$ at time t_i for tenor $\tau_{i,j} = T_j - t_i$, and the implied volatility $\sigma_{imp,j,\ell}(t_i)$ for tenor $\tau_{i,j}$ and strike

price $K_{j,\ell}$. The mapping $\tau_{i,j} \to \rho_j(t_i)$ facilitates the construction of an implied discount rate term structure using the techniques proposed in the extant literature such as Hagan and West (2006), Andersen (2007), and Fengler and Hin (2015a) among others. The mapping $(\tau_{i,j}, K_{j,\ell}) \to \sigma_{imp,j,\ell}(t_i)$ facilitates the construction of an implied volatility surface that accommodates the representation of the implied volatility smile across strike prices and the implied volatility term structure across times to maturity, two important features of the implied volatility surface demonstrated by many empirical studies (see, e.g. Rubinstein, 1994; Dupire, 1994; Derman and Kani, 1994; Dumas, Fleming and Whaley, 1998; Cont, 2001; Cont et al., 2002; da Fonseca and Grasselli, 2011; Fengler and Hin, 2015b).

A.2 **Parameter stability assumption.** We assume that, within some reasonable short time intervals $[t_1, t_p]$, there is some stability for the implied volatility and the implied discount rate within these time intervals. Specifically, we assume that

$$\sigma_{imp,j,\ell,[t_1,t_p]} = \sigma_{imp,j,\ell}(t_1) = \cdots = \sigma_{imp,j,\ell}(t_p)\ , \quad \text{and,} \quad \rho_{j,[t_1,t_p]} = \rho_j(t_1) = \cdots = \rho_j(t_p)\ .$$

In practice, an implicit assumption on the stability in the implied volatility of an option contract over a short time interval is commonly made in the execution of risk management activities in the financial industry. Dynamic hedging of positions in option contracts cannot be carried out continuously due to practical constraints such as transaction costs, and has to be carried out at discrete time intervals (see, e.g., Boyle and Emanuel, 1980; Hayashi and Mykland, 2005). The discrete rebalancing of dynamic hedge positions for option contracts implicitly assume that, for practical purpose, the implied volatility remains the same within the time period between two successive rebalancing activities. Additionally, the reference interest rates used as proxy for the risk-free rates are usually quoted on a daily basis, except on weekends and business holidays. This implies that the risk-free rate, or discount rate, term structure may be assumed to remain the same between two successive announcements of this set of reference rates.

Based on these two assumptions, we map the set of observed option prices $C(t_i, T_j, K_{j,\ell})$ to $\sigma_{imp,j,\ell,[t_1,t_p]}$ and $\rho_{j,[t_1,t_p]}$ via the Black-Scholes option pricing formula (2.3) in order to construct a system of nonlinear equations

$$\begin{aligned} &C_{BS}(t_i, T_j, S(t_i), \sigma_{imp,j,\ell,[t_1,t_p]}, \rho_{j,[t_1,t_p]}, K_{j,\ell}) = C(t_i, T_j, K_{j,\ell}), \\ &i = 1, \ldots, p, \quad j = 1, \ldots, m, \quad \ell = 1, \ldots, n_j. \end{aligned} \tag{3.1}$$

If $p = 1$, then (3.1) is under-defined because there are $m + \sum_{j=1}^{m} n_j$ unknown variables to be solved for only $\sum_{j=1}^{m} n_j$ nonlinear equations present in the system since $m \geq 1$.

In this chapter, we consider the $p > 1$ specification of (3.1) where there are $m+\sum_{j=1}^{m} n_j$ unknown variables to be solved based on $p \times \sum_{j=1}^{m} n_j$ equations. Since $m \leq \sum_{j=1}^{m} n_j$, we have $p\times\sum_{j=1}^{m} n_j > m+\sum_{j=1}^{m} n_j$. The situation where $m = \sum_{j=1}^{m} n_j$ occurs only in the unusual theoretical situation where there is only one option contract for every expiry time in the data set. In practice, we usually have at least several option contract for each available expiry date where $m < \sum_{j=1}^{m} n_j$. Henceforth, assuming that $m < \sum_{j=1}^{m} n_j$, (3.1) becomes an over-defined system of nonlinear equations for $p > 1$.

Let

$$\Psi(\boldsymbol{\theta}) = \sum_{i=1}^{p} \sum_{j=1}^{m} \sum_{\ell=1}^{n_j} \left(C(t_i, T_j, K_{j,\ell}) - C_{BS}(t_i, T_j, S(t_i), \sigma_{imp,j,\ell,[t_1,t_p]}, \rho_{j,[t_1,t_p]}, K_{j,\ell}) \right)^2 , \quad (3.2)$$

where $\boldsymbol{\theta} = (\boldsymbol{\sigma}, \boldsymbol{\rho})$, $\boldsymbol{\sigma} = \left(\sigma_{imp,1,1,[t_1,t_p]}, \ldots, \sigma_{imp,m,n_m,[t_1,t_p]} \right)$, $\boldsymbol{\rho} = \left(\rho_{1,[t_1,t_p]}, \ldots, \rho_{m,[t_1,t_p]} \right)$, $\sigma_{imp,j,\ell,[t_1,t_p]} > 0$, and $\rho_{j,[t_1,t_p]} > 0$, $j = 1, \ldots, m, \ell = 1, \ldots, n_j$. Since there is no exact solution for the over-defined system (3.1), we seek approximate solution of $\boldsymbol{\sigma}$ and $\boldsymbol{\rho}$ in the following optimization problem

$$\begin{aligned} &\text{Minimize} \quad \Psi(\boldsymbol{\theta}) \quad \text{over} \quad \boldsymbol{\theta} \qquad (3.3)\\ &\text{subject to} \\ &\sigma_{imp,j,\ell,[t_1,t_p]} > 0 , \qquad j = 1, \ldots, m, \ell = 1, \ldots, n_j, \\ &\rho_{j,[t_1,t_p]} > 0 , \qquad j = 1, \ldots, m, \ell = 1, \ldots, n_j. \end{aligned}$$

The solution of (3.3) represents an approximate solution of (3.1).

Since objective function (3.2) is not convex with respect to $\rho_{j,[t_1,t_p]}$ and $\sigma_{imp,j,\ell,[t_1,t_p]}$, gradient-based optimization strategies cannot be used due to potential trapping in the local minima. The appropriate method of choice is from among the class of direct-search optimization strategies. We choose to seek numerical solution of (3.2) via the Zhang-Sanderson's algorithm (Zhang and Sanderson, 2009). This algorithm belongs to a class of stochastic-based multi-point direct-search optimization techniques known as differential evolution (Storn and Price, 1997) designed to locate the global minimum in the presence of multiple co-existing local minima without the need to evaluate the path of steepest descent. Classical differential evolution strategies require explicit specification of control parameters to accelerate convergence. Specification of these parameters are known to

be problem dependent and sometimes require tedious trial and error to arrive at the appropriate values for the problem at hand. In contrast, the Zhang-Sanderson's algorithm incorporates self-adaptive control parameters that render the specification of these control parameters insensitive to different optimization problems, making it an attractive numerical solution algorithm for our optimization problem at hand.

3.4.1 Implementation of the Zhang-Sanderson's algorithm to estimate implied discount rates and implied volatilities from option prices

We follow the exposition style of Zhang and Sanderson (2009) in describing the implementation of the Zhang-Sanderson's algorithm for numerical solution of (3.2). Let $g = 1, \ldots, G$, be successive iteration steps with $g = 0$ representing the initialization stage.

1. **Initialization stage**: Generate N_p D-dimensional random vectors, $\boldsymbol{\theta}_{I,0}, I = 1, \ldots, N_p$, where $\boldsymbol{\theta}_{I,0} = \{\theta_{J,I,0}\}_{J=1}^{D}$, and where $\theta_{J,I,0}$ is a pseudo-random number generated from the uniform distribution $U[\theta_J^{Lower}, \theta_J^{Upper}]$, and where $[\theta_J^{Lower}, \theta_J^{Upper}]$ is a user specified parameter interval for each of the D parameters to be estimated, indexed by J, within which θ_J is assumed to be located.

2. **Iteration stage**: Successive iterations are indexed by $g = 1, \ldots, G$. Each iteration consists of three steps.

   (a) **Mutation step for iteration stage** g: We construct N_p D-dimensional mutation vectors

   $$\mathbf{v}_{I,g} = \left\{v_{J,I,g}\right\}_{J=1}^{D} = \boldsymbol{\theta}_{I,g} + F_{I,g}\left(\boldsymbol{\theta}_{best,g}^{p} - \boldsymbol{\theta}_{I',g}\right), \quad I = 1, \ldots, N_p,$$

   where $\boldsymbol{\theta}_{best,g}^{p}$ is randomly chosen from the subset of $\left\{\boldsymbol{\theta}_{I,g}, I = 1, \ldots, N_p\right\}$ where $\Psi\left(\boldsymbol{\theta}_{best,g}^{p}\right)$ is in the lowest p-percentiles of $\left\{\Psi\left(\boldsymbol{\theta}_{I,g}\right), I = 1, \ldots, N_p\right\}$, $\boldsymbol{\theta}_{I',g} = \boldsymbol{\theta}_{I,g} - \boldsymbol{\theta}_{I_1,g} + \boldsymbol{\theta}_{I_2,g}, I \neq I_1 \neq I_2$, while $F_{I,g}$ is a pseudo-random variable generated from the Cauchy distribution with location parameter $\mu_{F,g}$ and scale parameter 0.1, and then to be either truncated to 1 if $F_{I,g} \geq 1$ or regenerated if $F_{I,g} \leq 0$. This construction of the mutation vectors corresponds to the non-archive-assisted DE/current-to-$p$best/1 implementation of the Zhang-Sanderson algorithm (Eqn. 6, Zhang and Sanderson, 2009) implemented in the `DEoptim` (Ardia et al., 2012) package for the `R` computing environment (R Core Team, 2012). Additionally, let $\mu_{F,0} = 0.5$, let $\mu_{F,g+1} = (1 - c)\,\mu_{F,g} + c\mu_{L,S_{F,g},g}$, where

c is a user specified parameter, $S_{F,g} = \left\{F_{I,g} : \boldsymbol{\theta}_{I,g} \neq \boldsymbol{\theta}_{I,g+1}\right\}$, and $\mu_{L,S_{F,g},g} = \sum_{F_{I,g} \in S_{F,g}} F_{I,g}^2 \Big/ \sum_{F_{I,g} \in S_{F,g}} F_{I,g}$. Any element $v_{J,I,g}$ that falls outside the interval $[\theta_J^{Lower}, \theta_J^{Upper}]$ will be reset to a value within the interval by

$$v_{J,I,g} = \begin{cases} \theta_J^{Lower} + \zeta_{J,I,g}\left(\theta_J^{Upper} - \theta_J^{Lower}\right) , & if\ v_{J,I,g} < \theta_J^{Lower} , \\ \theta_J^{Upper} - \zeta_{J,I,g}\left(\theta_J^{Upper} - \theta_J^{Lower}\right) , & if\ v_{J,I,g} > \theta_J^{Upper} , \end{cases}$$

where $\zeta_{J,I,g}$ is a pseudo-random number generated from uniform distribution $U[0, 1]$.

(b) **Crossover step for iteration stage** g: We construct N_p D-dimensional crossover vectors $\mathbf{u}_{I,g} = \left\{u_{J,I,g}\right\}_{J=1}^{D}, I = 1, \ldots, N_p$, by the rule

$$u_{J,I,g} = \begin{cases} v_{J,I,g}, & \text{if} \quad \xi_{J,I,g} \leq CR_{I,g} , \\ \theta_{J,I,g}, & \text{otherwise} , \end{cases}$$

where $\xi_{J,I,g}$ is a pseudo-random number generated from uniform distribution $U[0, 1]$, while $CR_{I,g}$ is generated by truncating a pseudo-random number generated from a Gaussian distribution $\mathcal{N}\left(\mu_{CR,g}, 0.01\right)$ with respect to a floor of 0 and a ceiling of 1. Additionally, let $\mu_{CR,0} = 0.5$, and let $\mu_{CR,g+1} = (1 - c)\mu_{CR,g} + c\mu_{A,CR,g}$, where c is a user specified parameter and where $\mu_{A,CR,g}$ is the arithmetic mean of the set of all successful crossover probabilities.

(c) **Selection step for iteration stage** g: We update $\boldsymbol{\theta}_{I,g+1}$ by the rule

$$\boldsymbol{\theta}_{I,g+1} = \begin{cases} \mathbf{u}_{I,g} , & if \quad \Psi\left(\mathbf{u}_{I,g}\right) < \Psi\left(\boldsymbol{\theta}_{I,g}\right) , \\ \boldsymbol{\theta}_{I,g} , & otherwise . \end{cases}$$

The selection for member vector I is regarded as successful if $\boldsymbol{\theta}_{I,g+1} \neq \boldsymbol{\theta}_{I,g}$.

3. **Algorithm termination**: The parameter vector $\boldsymbol{\theta}_{best,G} = \left(\boldsymbol{\sigma}_{best,G}, \boldsymbol{\rho}_{best,G}\right)$ that corresponds to $\min\left\{\Psi\left(\boldsymbol{\theta}_{I,G}\right), I = 1, \ldots, N_p\right\}$ is the best estimate of the parameters in the set of parameter vector population $\left\{\boldsymbol{\theta}_{I,G}\ , I = 1, \ldots, N_p\right\}$, and that $\boldsymbol{\theta}_{best,G}$ is regarded as the approximate solution of (3.1) by minimization of objective function (3.2) over a given number of iteration steps G.

For the numerical experiment reported in Section 3.5 we set $c = 0.2$, $p = 0.01$, $N_p = 50 \times D$ and $G = 5,000$, whereas for the empirical data analysis reported in Section 3.6, we set $c = 0.15$, $p = 0.01$ and $N_p = 25 \times D$. Additionally, for both the numerical

studies considered in Section 3.5 and Section 3.6, we used the Zhang-Sanderson algorithm implemented in the `DEoptim` (Ardia et al., 2012) package for the `R` computing environment (R Core Team, 2012). We used 48 parallel cores provided by the National eResearch Collaboration Tools and Resources (NeCTAR) cloud computing infrastructure to carry out all the calculations reported in this paper to accelerate the speed of computation. The computational acceleration achieved is considerable. For example, completion of the two numerical experiments described in Section 3.5 took 5.68 and 5.74 hours respectively on a single core, but only took 1.23 and 1.24 hours respectively instead on 48 parallel cores, leading to an approximately 78% reduction in computation time in this particular example.

3.4.2 Construction of the estimation uncertainty bounds for the estimated implied discount rates and implied volatilities

Since the estimated parameters $\boldsymbol{\sigma}_{best,G}$ and $\boldsymbol{\rho}_{best,G}$ are approximate solutions to (3.1), some measures of in-sample goodness-of-fit assessment can give us an idea of the solution accuracy of the system of nonlinear equations. It was pointed out by an anonymous referee during the review process of the paper by Hin and Dokuchaev (2015a) that while the standard error is a error measure of choice for statistical and financial econometric inference, bootstrap procedures for standard error estimation are too computationally intensive to be implemented given the complexity of the problem at hand. We propose, as an alternative to the classical goodness-of-fit measures such as mean squared error, to perform empirical assessment of the distribution properties of the member vectors at algorithm termination and their corresponding objective function value to quantify the uncertainty bound for $\boldsymbol{\sigma}_{best,G}$ and $\boldsymbol{\rho}_{best,G}$ as a model-free in-sample goodness-of-fit assessment.

The N_p D-dimensional member vectors $\{\boldsymbol{\theta}_{I,G}, I = 1, \ldots, N_p\}$ are the result of iterative stochastic perturbation of the random initialization vectors $\{\boldsymbol{\theta}_{I,0}, I = 1, \ldots, N_p\}$ via the Zhang-Sanderson's algorithm. In this sense, $\{\boldsymbol{\theta}_{I,G}, I = 1, \ldots, N_p\}$ may be regarded as a set of random variables. For each $\boldsymbol{\theta}_{I,G}$, there exists the mapping $\boldsymbol{\theta}_{I,G} \rightarrow \Psi(\boldsymbol{\theta}_{I,G})$. If the number of iterative loops G is sufficiently large for the set of member vectors to converge to, hopefully, the global minimum, then one would expect the value of $\min\{\Psi(\boldsymbol{\theta}_{I,G}), I = 1, \ldots, N_p\}$ to be small in absolute terms. Additionally, the range and percentiles of the distribution of $\{\Psi(\boldsymbol{\theta}_{I,G}), I = 1, \ldots, N_p\}$ may be used as an empirical gauge to quantify the

dispersion of $\{\Psi(\boldsymbol{\theta}_{I,G}), I = 1, \ldots, N_p\}$, such that the narrower the interval

$$[\Psi_{Lower}(\boldsymbol{\theta}_{I,G}), \Psi_{Upper}(\boldsymbol{\theta}_{I,G})] \stackrel{\Delta}{=} \left[\min\{\Psi(\boldsymbol{\theta}_{I,G}), I = 1, \ldots, N_p\}, \max\{\Psi(\boldsymbol{\theta}_{I,G}), I = 1, \ldots, N_p\}\right], \tag{3.4}$$

the more likely that the member vectors are converging towards a minimum. From the percentiles of $\{\Psi(\boldsymbol{\theta}_{I,G}), I = 1, \ldots, N_p\}$, one can infer additional information on the shape of the empirical error distribution.

We may also view the set $\{\rho_{I,G:j,[t_1,t_p]}, I = 1, \ldots, N_p\}$ as the set of random possible solutions of $\rho_{j,[t_1,t_p]}$, $j = 1, \ldots, m$, and $\{\sigma_{I,G:imp,j,\ell,[t_1,t_p]}, I = 1, \ldots, N_p\}$ as the set of random possible solutions of $\sigma_{imp,j,\ell,[t_1,t_p]}$, for each (j, ℓ) pair where $j = 1, \ldots, m, \ell = 1, \ldots, n_j$. We suggest to use

$$\left[\rho_{Lower:j,[t_1,t_p]}, \rho_{Upper:j,[t_1,t_p]}\right] \stackrel{\Delta}{=} \left[\min\{\rho_{I,G:j,[t_1,t_p]}, I = 1, \ldots, N_p\}, \max\{\rho_{I,G:j,[t_1,t_p]}, I = 1, \ldots, N_p\}\right], \tag{3.5}$$

as a gauge to quantify the parameter estimation uncertainty interval of $\rho_{best,G:j,[t_1,t_p]}$ as an estimator of $\rho_{j,[t_1,t_p]}$ for each j where $j = 1, \ldots, m$, and to use

$$\begin{aligned}&\left[\sigma_{Lower:imp,j,\ell,[t_1,t_p]}, \sigma_{Upper:imp,j,\ell,[t_1,t_p]}\right] \\ &\stackrel{\Delta}{=} \left[\min\{\sigma_{I,G:imp,j,\ell,[t_1,t_p]}, I = 1, \ldots, N_p\}, \max\{\sigma_{I,G:imp,j,\ell,[t_1,t_p]}, I = 1, \ldots, N_p\}\right],\end{aligned} \tag{3.6}$$

as a gauge to quantify the parameter estimation uncertainty interval of $\sigma_{best,G:imp,1,1,[t_1,t_p]}$ as an estimator of $\sigma_{imp,j,\ell,[t_1,t_p]}$ for each (j, ℓ) pair where $j = 1, \ldots, m, \ell = 1, \ldots, n_j$.

Our construction of (3.4), (3.5), and (3.6) to quantify the parameter estimation uncertainty of (3.3) is inspired by Ben Hamida and Cont (2005) who suggested using the probabilistic approach to the model calibration problem within the stochastic-based differential evolution optimization framework. After a sufficiently large number of iteration steps, the population of member vectors converges to the set of global minima of pricing errors (see, e.g., Ben Hamida and Cont, 2005; Hu et al., 2013). However, at the termination of the optimization algorithm, each of the member vectors may still be associated with a different value of pricing error. This results in the existence of a set of pricing model parameters that may be compatible with the contingent claim prices in question, up to a magnitude of in-sample goodness-of-fit error. Our empirical parameter estimation uncertainty interval builds on this notion of model parameter uncertainty. This strategy relies on neither the large sample results nor the assumption of independently and identically distributed errors across options.

The Zhang-Sanderson algorithm that we used to estimate the parameters belongs to the family of stochastic-based differential evolution optimization algorithms considered in Ben Hamida and Cont (2005). Our estimation of the implied discount rates and implied volatilities from the option prices is similar in spirit to the notion of model calibration as defined in Ben Hamida and Cont (2005). As such, it appears that their interpretation of the member vectors as a family of pricing model parameters compatible with observed contingent claim prices may be applicable to our framework as well.

Adapting the Ben Hamida-Cont notion of model parameter uncertainty to our context, we may regard $\{\rho_{I,G:j,[t_1,t_p]}, I = 1,\ldots,N_p\}$, as a family of possible estimated values of $\rho_{j,[t_1,t_p]}$ for each j $j = 1,\ldots,m$, and may regard $\{\sigma_{I,G:imp,j,\ell,[t_1,t_p]}, I = 1,\ldots,N_p\}$, as a family of possible estimated values of $\sigma_{imp,j,\ell,[t_1,t_p]}$ for each (j,ℓ) pair where $j = 1,\ldots,m, \ell = 1,\ldots,n_j$, based on a set of population vectors at algorithm termination. Additionally, we may quantify the global goodness-of-fit uncertainty of the solution for the entire system of nonlinear equations using $[\Psi_{Lower}(\boldsymbol{\theta}_{I,G}), \Psi_{Upper}(\boldsymbol{\theta}_{I,G})]$, and may quantify the model parameter estimation uncertainty of $\rho_{j,[t_1,t_p]}$ and $\sigma_{imp,j,\ell,[t_1,t_p]}$ using $\left[\rho_{Lower:j,[t_1,tp]}, \rho_{Upper:j,[t_1,tp]}\right]$ and $\left[\sigma_{Lower:imp,j,\ell,[t_1,tp]}, \sigma_{Upper:imp,j,\ell,[t_1,tp]}\right]$ respectively.

3.5 Numerical experiment with synthetic test data

In this section, we construct two sets of synthetic test data sets to assess the performance of our proposed parameter estimation strategy in terms of convergence profile, the parameter estimation performance of the proposed strategy, and the effect of the choice of objective function on the parameter estimation performance.

3.5.1 Construction of synthetic test data sets

Two sets of synthetic test data sets are constructed. Each of these data sets simulate the prices of a set of European vanilla call option contracts quoted on two successive days. The hypothetical prices in both test data sets are synthesized using the same set of hypothetical times to maturity, spot and strike prices, and implied volatilities as input values to (2.3), setting the dividend rate to be zero. They differ only in the input of the hypothetical discount rates to (2.3).

For the set of synthetic test data that simulate an up-sloping discount rate term structure, the hypothetical discount rates corresponding to the unique times to maturity at in-

creasing tenors are 0.002, 0.004, 0.006, 0.012, 0.015 and 0.019 respectively. For the set of test data that simulate the inverted discount rate term structure, the hypothetical discount rates corresponding to the unique times to maturity at increasing tenors are 0.002, 0.004, 0.019, 0.015, 0.012, and 0.006 respectively.

We set the hypothetical times to maturity corresponding to the hypothetical prices observed at the first instance to be 0.17, 0.42, 0.69, 0.94, 1, and 1.5 years and set those observed at the second instance to be 0.17 - δ_τ, 0.42 - δ_τ, 0.69 - δ_τ, 0.94 - δ_τ, 1 - δ_τ, and 1.5 - δ_τ, where $\delta_\tau = 1/365$. For simplicity, we set the spot underlying asset price to be \$590 on both instances, and set the strike to spot ratio to be 0.85, 0.9, 0.95, 1, 1.05, 1.1, 1.15, 1.2, 1.3, and 1.4 on both instances as well. The hypothetical implied volatilities are adapted from the implied volatilities of the European call options on the S&P500 equity index quoted in October 1995 and reported in Table 1 of Andersen and Brotherton-Ratcliffe (1997). They are chosen to provide a volatility surface with smile that constitute a system of nonlinear equations that is numerically challenging to solve. Figure 4 depicts a graphical profile of this set of implied volatilities.

Each data set consists of 120 synthetic data points; 60 of them are regarded as the hypothetical prices of 60 option contracts observed at one instance in time while the remaining 60 are regarded as the hypothetical prices of the same set of hypothetical option contracts quoted one day later. For each synthetic test data set, we construct an over-defined system of 120 nonlinear equations based on (3.1). In each of these systems, there are 66 unknown parameters, i.e., 60 implied volatilities and 6 implied discount rates, to be solved for based on the corresponding hypothetical option prices where $p = 2, m = 6$, and $n_j = 10$.

3.5.2 The convergence profile and the parameter estimation accuracy profile pertaining to the synthetic test data sets

In order to seek numerical approximate solution to the two over-defined systems of nonlinear equations formulated using the synthetic test data sets, we minimize the L_2-metric loss function (3.2) via (3.3) for each of them in turn. We suggest to use $\Psi(\boldsymbol{\theta}_{best,G})/(p\times\sum_{j=1}^{m} n_j)$ as a gauge of the overall in-sample goodness-of-fit at termination of the Zhang-Sanderson's algorithm. For an L_2-metric loss function in the likes of (3.2), this gauge may be regarded as the average residual sum of squares. We suggest to examine the trend of average residual sum of squares at iteration g, i.e., $\Psi(\boldsymbol{\theta}_{best,g})/(p \times \sum_{j=1}^{m} n_j)$, against the corresponding number of iterations g in order to elucidate the speed of convergence and the number of

iterations required to achieve a reasonable level of the overall in-sample goodness-of-fit. For these two synthetic test data sets, $p = 2$ and $\sum_{j=1}^{m} n_j = 60$. For both synthetic test data sets, the average residual sum of squares decrease to the order of 1×10^{-6} in approximately 2,000 iterations. Since the convergence profiles for both test data sets are similar, only that for the up-sloping term structure is depicted in Panel A of Figure 5.

Let $\left\{\rho_{j,[t_1,t_2]}^{TRUE,Test\ data}\right\}_{j=1,\ldots,6}$ and $\left\{\sigma_{imp,j,\ell,[t_1,t_2]}^{TRUE,Test\ data}\right\}_{j=1,\ldots,6,\ell=1,\ldots,10}$ be, respectively, the hypothetical values of the discount rates and the implied volatilities used to generate the hypothetical option prices in the synthetic test data sets where t_1 is the hypothetical spot time, and $t_2 = t_1 + \delta_\tau$ as described in Section 3.5.1. Let

$$\text{Error}\left(\rho_{j,[t_1,t_2]}^{Test\ data}\right) = \left| \rho_{best,G:j,[t_1,tp]}^{Test\ data} - \rho_{j,[t_1,t_2]}^{TRUE,Test\ data} \right|$$

be the absolute value of the solution error pertaining to the estimated implied discount rates $\rho_{best,G:j,[t_1,tp]}^{Test\ data}$ with respect to $\rho_{j,[t_1,t_2]}^{TRUE,Test\ data}$ for each j where $j = 1, \ldots, 6$, and let

$$\text{Error}\left(\sigma_{imp,j,\ell,[t_1,t_2]}^{Test\ data}\right) = \left| \sigma_{best,G:imp,j,\ell,[t_1,t_2]}^{Test\ data} - \sigma_{imp,j,\ell,[t_1,t_2]}^{TRUE,Test\ data} \right|$$

be the absolute value of the solution error pertaining to the estimated implied volatilities $\sigma_{best,G:imp,j,\ell,[t_1,t_2]}^{Test\ data}$ with respect to $\sigma_{imp,j,\ell,[t_1,t_2]}^{TRUE,Test\ data}$ for each (j,ℓ) pair where $j = 1, \ldots, 6, \ell = 1, \ldots, 10$, respectively.

The profiles of the absolute values of parameter estimation error pertaining to the numerical solutions of the implied discount rates are depicted in Table 6. For both hypothetical implied discount rate term structures, the absolute parameter estimation error pertaining to the implied discount rates are in general small in the order of 10^{-3}.

The profiles of the absolute values of parameter estimation error pertaining to the numerical solutions of the implied volatilities are depicted in Table 7. For both synthetic test data sets, the solution error pertaining to the implied volatilities are in general small in the order of magnitude ranging from 10^{-1} to 10^{-4} across all available strikes and times to maturity. The estimation errors appear to be smaller for the hypothetical OTM options than for the ITM options in general. One plausible explanation is that the values of OTM options are smaller, facilitating the numerical algorithm to perform optimizing search in the parameter space.

Table 8 depicts the summary statistics for the set of objective function values $\{\Psi(\boldsymbol{\theta}_{I,G}), I = 1, \ldots, 3300, G = 5000\}$ that correspond to the 3,300 member parameter vectors at algorithm termination. The $[\Psi_{Lower}(\boldsymbol{\theta}_{I,G}), \Psi_{Upper}(\boldsymbol{\theta}_{I,G})]$ intervals, constructed using (3.4), are

narrow for both synthetic test data sets. We obtain $[1.882 \times 10^{-4}, 1.977 \times 10^{-4}]$ for the synthetic data set that simulate up-sloping discount rate scenario, and $[1.959 \times 10^{-4}, 2.051 \times 10^{-4}]$ for the synthetic test data set that simulate inverted discount rate scenario. This is an indication that our proposed parameter estimation strategy produce similar overall in-sample goodness-of-fit for both synthetic test data sets.

Table 9 depicts $\left[\rho^{Test\ data}_{Lower:j,[t_1,t_2]}, \rho^{Test\ data}_{Upper:j,[t_1,t_2]}\right]$, the uncertainty bounds for the estimated implied discount rates $\rho^{Test\ data}_{best,G:j,[t_1,t_p]}$ for all j, $j = 1, \ldots, 6$, constructed using (3.5). The range parameter estimation uncertainty bounds for $\rho^{Test\ data}_{best,G:j,[t_1,t_p]}$ appear to be narrow. The values of estimated hypothetical discount rate for any of the hypothetical option contracts estimated using different member vectors in the population differ by a magnitude of less than 4×10^{-4}.

Table 10 depicts $\left[\sigma^{Test\ data}_{Lower:imp,j,\ell,[t_1,t_2]}, \sigma^{Test\ data}_{Upper:imp,j,\ell,[t_1,t_2]}\right]$, the parameter uncertainty bounds for the estimated implied volatilities $\sigma^{Test\ data}_{best,G:imp,j,\ell,[t_1,t_2]}$ for all (j, ℓ) pair, $j = 1, 6, \ell = 1, \ldots, 10$, constructed using (3.6). The parameter estimation uncertainty bounds for $\sigma^{Test\ data}_{best,G:imp,j,\ell,[t_1,t_2]}$ appear to be narrow. The values of estimated hypothetical implied volatilities for any of the synthetic option contracts estimated using different member vectors in the population differ by a magnitude of less than 1×10^{-2}.

3.5.3 Effect of objective function choice on the convergence profile and the parameter estimation accuracy profile

We have, thus far, performed model parameter estimation based on the the synthetic test data sets by minimization of (3.2), an L_2-metric loss function. The L_2-metric loss function loss function is a popular objective function widely used in the estimation of the model parameters from option prices (see, e.g., Ben Hamida and Cont, 2005; Detlefsen and Härdle, 2007b; Detlefsen and Härdle, 2008). However, it is well known that, the parameter estimation based on minimization of the L_1-metric loss function may confer significant robustness advantages over the parameter estimation based on minimization of the L_2-metric loss function (see, e.g., Portnoy and Koenker, 1997; Cadzow, 2002). In order to investigate whether the estimation of $\boldsymbol{\theta}$ based on the test dataset is sensitive to the choice of loss function, we have also performed the parameter estimation based on the same synthetic test data sets using a L_1-loss function in the form of

$$\Psi_{L_1}(\boldsymbol{\theta}) = \sum_{i=1}^{p} \sum_{j=1}^{m} \sum_{\ell=1}^{n_j} \left| C(t_i, T_j, K_{j,\ell}) - C_{BS}(t_i, T_j, S(t_i), \sigma_{imp,j,\ell,[t_1,t_p]}, \rho_{j,[t_1,t_p]}, K_{j,\ell}) \right| . \quad (3.7)$$

Since the convergence profiles for both test data sets are similar, only that for the upsloping term structure for minimization of $\Psi_{L_1}(\boldsymbol{\theta})$ is depicted in Panel B of Figure 5. Comparison of the convergence profiles for $\Psi_{L_1}(\boldsymbol{\theta})$ and $\Psi(\boldsymbol{\theta})$ gives an impression that convergence rate tends to be slower for L_1 minimization.

The corresponding error profiles for the estimated implied discount rates and estimated implied volatilities obtained by minimizing (3.7) are depicted in Table 11 and Table 12 respectively. Comparing the absolute error profiles for the estimated hypothetical implied discount rates as depicted in Table 6 and Table 11, and comparing the absolute error profiles for the estimated hypothetical implied volatilities as depicted in Table 7 and Table 12, it appears that the estimated hypothetical implied discount rates and the estimated hypothetical implied volatilities estimated using the L_1-loss function or the L_2-loss function as the objective function are in general similar. For the rest of this chapter, we use the L_2-loss function (3.2) for the estimation of the implied discount rates and the implied volatilities.

3.6 Numerical analysis using historical S&P500 call options data

Section 3.6.1 describes the data used for the empirical analysis reported in this section. Section 3.6.2 reports the implied discount rates and the implied volatilities estimated from four sets of S&P500 options data sampled approximately one year apart from 2010 to 2013 inclusive in order to analyse the spreads between implied discount rates and the contemporaneously quoted Libor and OIS rates, and examine the sensitivity of implied volatility estimation with respect to different choices of discount rate proxy. Section 3.6.3 reports the implied discount rates estimated from ten sets of S&P500 options data sampled approximately one year apart from 2004 to 2013 in order to investigate the trend of the spreads between the implied discount rates and the contemporaneously quoted Libor rates.

3.6.1 Data description

For the empirical analysis reported in this section, we use the historical day-close prices of S&P500 index European vanilla call option contracts traded at the CBOE obtained from Market Data Express LLC. We consider OTM options with moneyness between 1 and 1.2 because this set of OTM option contracts are not "too far" out of the money. Aït-Sahalia and Lo (1998), and Jiang and Tian (2005), among others, recommended the

use of OTM option contracts for the empirical study of implied volatility because ITM option contracts are more expensive and often less liquid than the OTM option contracts. Additionally, Cont and da Fonseca (2002) noted that OTM options that are not "too far" out of the money are suitable for implied volatility and risk-free rate analysis because far OTM options are low in liquidity and are associated with higher numerical uncertainty on implied volatility.

We use the option contracts with remaining times to maturity between 150 and 320 days in our empirical analysis. Option contracts with remaining times to maturity less than 60 days are excluded from this study as the information content of these options in terms of volatility is questionable, as demonstrated by Ben Hamida and Cont (2005) using empirical options data. Option contracts with remaining times to maturity greater than 320 days are excluded from this study as long dated option are potentially less liquid and thus may contain less contemporaneous information on the market participants' aggregate choice of discount rate, and aggregate expectation of the underlying asset price volatility for the remaining lifespan of the option contracts.

The estimated implied discount rates inferred from the historical option prices are compared with the contemporaneously quoted USD Libor and OIS rates. While the USD Libor rates are quoted uncollateralized interbank reference rates designed to reflect the average credit risk among different banks, the USD OIS rates are OTC-quoted interest rate swap rates the floating legs of which are based on discrete daily compounded effective Federal Funds rate and is virtually free of credit risk by construction. We obtained the historical time series data of the Libor rates from the Economic Research Division, Federal Reserve Bank of St. Louis. We obtained the historical data of the Libor-OIS spread rates, the difference between the Libor reference rates and the OTC-quoted US Dollar OIS rates, from the Thomson Reuters Tick History (TRTH) supplied by the Securities Industry Research Centre of Asia-Pacific (SIRCA). We subtract the Libor-OIS spread rates from the contemporaneous Libor rates for the corresponding tenors to recovers the contemporaneous OIS rates. In order to facilitate comparison with the implied discount rate, these Libor and OIS rates were converted from the discrete interest rates convention to continuously compounded convention prior to analysis.

While both the Libor reference rates and Libor-OIS spread rates are quoted at 11am London time, the day-close option prices are quoted at 3.15pm Chicago time, a few hours behind the London time. Due to the fact that there exists a significant time lag between the publication of these reference interest rates, and the availability of the option price data from which the implied discount rates are estimated, one would not expect the im-

plied discount rates to match either the Libor or the OIS rates exactly as the arrival of new information during this lag time period may influence the market participants to alter their choices of the implied discount rates and to modify their expectation of the future underlying asset price volatility. Additionally, the market participants may choose a set of discount rates tailored to their own credit and liquidity risk profile but are different from the Libor and OIS rates.

3.6.2 Results of analysis

We report in this subsection the analysis results based on four samples of historical option prices, each comprises of the day-close prices of a set of option contracts quoted on two consecutive business days. Specifically, these four sets of option prices are quoted on May 18th & 19th 2010, May 18th & 19th 2011, May 23rd & 24th 2012, and May 22nd & 23rd 2013 respectively. We construct, for each of the four samples, a system of over-defined nonlinear equations using (3.1), and estimate the implied discount rates and implied volatilities by minimization of (3.2) using the estimation strategy described in Section 3.4.

We depict in Table 14 and Figure 7 the estimated implied discount rates and the contemporaneously quoted Libor and OIS rates. Due to the fact that the tenors corresponding to the implied discount rates differ from sample to sample, and are in general different from the fixed tenors of the contemporaneously quoted Libor and OIS rates, we apply the interest rate interpolation technique previously used in Sections 2.5 in order to obtain, in the present context, the interpolated Libor and OIS rates corresponding to the tenors of the implied discount rates in order to facilitate the tenor-matched numerical comparison depicted in Table 14.

Specifically, we first fit smoothing spline curves to the Libor and OIS rates where the smoothing parameters are estimated using generalized cross-validation, and then obtain the corresponding interpolated Libor and OIS rates from the spline curves at the respective tenors that correspond to the tenors of the implied discount rates. In order to do so, we used the smoothing spline modelling algorithm implemented as the in-build function `smooth.spline()` for the `R` computing environment (R Core Team, 2012). This suffice for our current purpose of obtaining interpolated Libor and OIS rates for comparative purposes. However, more sophisticated financial and econometric purposes such as coherent pricing and hedging of contingent claims, and econometric analysis may warrant the use of more sophisticated arbitrage-free interpolation techniques such as those proposed by

Hagan and West (2006), Laurini and Moura (2010), and Fengler and Hin (2015a), among others.

We select subsets of option contracts in each of the four samples that have comparable moneyness characteristics, i.e., spot to strike ratio, for comparison of their estimated implied volatilities. Option contracts with strike price of USD1,150, USD1,400, USD1,370, or USD1,725 are selected from the samples of option data observed on May 18th & 19th 2010, May 18th & 19th 2011, May 23rd & 24th 2012, and May 22nd & 23rd 2013 respectively for this purpose. They are use to construct Table 15 and Figure 8 to illustrate the sensitivity of implied volatility estimation with respect to the choice of discount rate from among the implied discount rate, and the contemporaneously quoted Libor and OIS rates pertaining to the samples of option prices considered. Specifically, we estimate the implied volatilities from the same sets of option prices by inverting (2.3), using the estimated implied discount rates, or the tenor matching interpolated values with respect to the contemporaneously quoted Libor or OIS rates (Table 14) as the risk-free rate proxy.

Table 16 depict the parameter estimation uncertainty intervals of the implied discount rates and implied volatilities estimated from these four samples constructed using (3.6) and (3.5) respectively. It appears that the depicted parameter estimation uncertainty intervals are narrow, suggesting that the member vectors at algorithm termination produce comparable overall goodness-of-fit to the systems of equations.

Figure 6 depict the convergence profiles for the four data samples as the trend of average residual sum of squares, $\Psi(\boldsymbol{\theta}_{best,g})/(p \times \sum_{j=1}^{m} n_j)$, against the number of iterations g. After approximately 2,000 iterations, the average residual sum of squares reached a value that is smaller than one. This magnitude of average residual sum of squares corresponds to a pricing discrepancy between observed and model prices of the option that is comparable to the size of the bid-ask spread. We believe that this may be considered as an acceptable level of precision because, in reality, the observed option price jumps between the bid and ask prices, and attempt to achieve higher precision than the bid-ask spread may not be of substantial practical significance (Ben Hamida and Cont, 2005).

3.6.2.1 The differences among implied discount rates, and contemporaneously quoted Libor & OIS rates

In Table 14, we depict the implied discount rates estimated from the four samples, and the tenor matching interpolated values of the contemporaneous Libor and OIS rates. The interpolated Libor and OIS rates on the dates corresponding to the consecutive sampling

dates of these four samples of option prices are found to exhibit small day-to-day fluctuation amounting to approximately 10^{-4} in magnitude. For the data samples considered, it appears that the implied discount rates are higher than the contemporaneous Libor and OIS rates. For example, the differences between implied discount rates estimated based on option prices quoted on May 19th 2011 and the interpolated contemporaneous Libor and OIS rates can be as large as 0.03 depending on the tenor.

Gefang, Koop and Potter (2011) suggested that the higher the bank credit risk premium, the higher the discount rate at the long end of the tenor. Table 14 and Figure 7 depict that, at the available tenors considered that range between 150 and 320 days, the implied discount rates appear to be higher than the contemporaneously quoted Libor and OIS rates in these samples. This may imply that the credit risk for some market participants may be higher than the average bank credit risk.

Additionally, the differences between the implied discount rates and the tenor matching interpolated values of the contemporaneously quoted OIS rates depicted in Table 14 appear to be comparable in magnitude to the credit default swap (CDS) spreads of US firms with an average Moody's and S&P ratings between BBB and BB, as depicted in Table II of Longstaff, Mithal and Neis (2005) and Table 1 of Wang, Zhou and Zhou (2013). This finding concur with a comment made by an anonymous referee during the review process of the paper by Hin and Dokuchaev (2015a) that the difference between the implied discount rate and standard risk-free rate proxy should, to some extent, reflect the premium paid by agents to fund their investment.

The estimated implied discount rates inferred from the data span narrow ranges of tenor, and are too few in number to be used as input for the construction of an arbitrage-free discount curve using interpolation methods such as those proposed by Hagan and West (2006), Andersen (2007), Laurini and Moura (2010), and Fengler and Hin (2015a), among others, in order to obtain interpolated values that are coherent with the salient features of the discount curve term structure. However, in order to perform Mincer-Zarnowitz type regression to study the relationship between implied discount rates and the standard risk-free rate proxies in a regression framework, either the standard risk-free rate proxies or the implied discount rates need to interpolated to construct a set of interpolated standard risk-free rate proxies and implied discount rates that corresponding to a set of common tenors for this purpose. In the presence of a small number of estimated discount rates that cluster within a narrow tenor range, potential numerical error and loss of information incurred by suboptimal interpolation may jeopardize the accuracy of the econometric analysis performed based on these interpolated data.

3.6.2.2 The sensitivity of implied volatility estimation with respect to the magnitude of the risk-free rate proxy

In Table 15 and Figure 8, we depict the estimated implied volatilities that correspond to the prices of the subsets of option contracts from these four samples. These subsets are chosen based on their similarity in moneyness characteristics to facilitate comparison across these option chains. For each subset of data, the implied volatilities estimated jointly with the implied discount rates are smaller than the implied volatilities calculated by inverting (2.3) and using either the tenor matching interpolated values of the contemporaneously quoted Libor or OIS rates as risk-free rate proxy. By virtue of (2.5) in Section 2.3 that higher discount rates map a given European vanilla call option price to lower implied volatilities, the comparatively higher implied discount rates relative to the tenor matching interpolated contemporaneous Libor and OIS rates (Table 14) in these samples map the option prices to lower implied volatilities. This is a sample dependent phenomenon. If the implied discount rates are lower than the tenor matching interpolated contemporaneous Libor and OIS rates instead, then the implied volatilities estimated jointly with the implied discount rates will be higher than those estimated using the contemporaneous Libor and OIS rates as discount rates.

Currently, there is no consensus on the choice of discount rate, or risk-free rate proxy, among the extant empirical studies that are aimed at investigating the information content of the implied volatility and its role as a predictor of the realized volatility. Some popular choices of discount rate include the average of the daily Eurodollar deposit rate and the daily broker call rate (Canina and Figlewski, 1993b), one month LIBOR rate (Christensen and Prabhala, 1998), daily Treasury bill yields (Jiang and Tian, 2005), and the US Eurodollar deposit one-month middle rate quote (Busch et al., 2011). That said, the market participants' aggregate choice of discount rate may differ from the choices of discount rate commonly used in the literature.

If the implied discount rate were a better estimate of the true market participants' aggregate choice of discount rate than the commonly used risk-free rate proxies, then we would expect the Black-Scholes implied volatility calculated based on the implied discount rate to be a better estimate of the true market participants' aggregate expectation of the underlying asset price volatility for the remaining lifespan of the option contract compared to those estimated based on these commonly used proxies. It follows that the choice of discount rate will affect the performance of the econometric methods used to investigate the information content of the implied volatilities such as the univariate and encompassing

regression used in Canina and Figlewski (1993b), Christensen and Prabhala (1998), and Jiang and Tian (2005), and the in-sample Mincer and Zarnowitz (1969) forecasting regressions used in Busch et al. (2011), among others. If the chosen discount rate overestimates the market participants' aggregate choice of discount rate, then the corresponding implied volatility underestimates the market participants' aggregate expectation of the underlying asset return volatility, and vice versa. Specifically, if we regress the realized volatilities against the implied volatilities estimated based on a risk-free rate proxy that is different from the true market participants' aggregate choice of discount rate, it may lead to error in the quantification of the implied volatility information content expressed in terms of regression summary statistics such as the R-squared values of these regression analyses.

In an ideal world, one would like to verify whether the implied discount rate is an accurate estimator of the true market participants' aggregate choice of the discount rate, or, equivalently, whether the implied volatility estimated jointly with the implied discount rate is an accurate estimator of the market participants' aggregate expectation of the underlying asset price volatility for the remaining lifespan of the option contract. However, both the market participants' aggregate choice of discount rate and aggregate expectation of future realized volatility are latent, unobservable state variables, and it is unclear how one should construct an econometric test to verify the accuracy of these estimates. That said, from the numerical experiment results reported in Section 3.5, it appears that our proposed estimation strategy is capable of estimating the implied discount rates and implied volatilities used to generate the synthetic option prices with reasonable accuracy. While these experimental results raise the prospect that the application of our estimation strategy to historical data may be capable of estimating the market participants' aggregate choice of discount rates and aggregate expectation of future realized volatilities, these parameter estimates need to be examined carefully in terms of the proposed in-sample goodness-of-fit measures, and in terms of the econometric plausibility of the magnitude of these estimates.

The implied volatilities of option prices reflect the volatility risk premium (see, e.g., Carr and Wu, 2009; Andersen, Fusari and Todorov, 2015). In order to investigate the role of implied volatility in the forecast of the realized volatility, one may need to consider to first disentangle the volatility risk premium from the implied volatility. While there exists empirical evidence suggesting that the variance risk premium is negative (see, e.g., Carr and Wu, 2009; Bakshi and Kapadia, 2003), which reflects the risk averse nature of investors and inflates the magnitude of the implied volatility, there is currently no consensus on the functional form of the variance risk premium. Additionally, Todorov (2010)

pointed out that in order to capture the salient features of the variance risk premium, it would be necessary to model the dynamics of asset price evolution in a framework that take into consideration stochastic volatility and jumps. The fact that our strategy is constructed based on a framework that models the asset price dynamics with a log-normal diffusion process limits our ability to model the variance risk premium along the line of Todorov (2010).

Alternatively, one may instead estimate the model-free implied volatility which is defined as a weighted portfolio of European vanilla option prices and forward contracts (see, e.g., Britten-Jones and Neuberger, 2000; Jiang and Tian, 2005; 2007). However, the estimation of the model-free implied volatility also requires *a priori* specification of the risk-free rate proxy. While the implied discount rate can be estimated jointly with the Black-Scholes model-based implied volatility, it is unclear how to infer the implied discount rate within the model-free implied volatility framework. Additionally, whether the implied discount rate estimated jointly with the model-based implied volatility can be plugged into the model-free implied volatility expression is an open research question.

In order to investigate, using the aforementioned regression-based methods, the information content of the implied volatilities that have being estimated jointly with the implied discount rates, it would be necessary to used the ATM implied volatilities in these regression analyses because the ATM implied volatilities have the highest correlation with the realized volatility (see, e.g., Jiang and Tian, 2005). We have confined our empirical analysis to the OTM European vanilla call option contracts due to the fact that the OTM options contain more information on the implied volatility than the ITM options (see, e.g., Cont and da Fonseca, 2002). In order to accurately interpolate the ATM implied volatilities, it would be necessary to first refine our proposed numerical solution strategy so that we can estimate the implied volatilities of the ITM and OTM option contracts with the same degree of accuracy.

One plausible approach is to construct the system of nonlinear equations using (3.1) based on ITM and OTM European vanilla call options. However, there are two potential pitfalls. Firstly, since it is known that the ITM options contain less information on the implied volatility than the OTM options, it is possible that the inclusion of the ITM options in the estimation procedure may compromise the accuracy of implied volatility and implied discount rate estimation. Secondly, the implied volatility estimation error profiles depicted in Tables 7 and 12 reveal that the estimation errors for the ITM implied volatilities are slightly higher than the estimation errors for the OTM implied volatilities. This asymmetric error profile may introduce error in the interpolation of ATM implied

volatilities.

The other plausible approach is to include the relevant OTM European put options and OTM European call options to construct a larger system of nonlinear equations in order to estimate the implied discount rates, and the implied volatilities that correspond to the ITM and OTM option contracts. This approach requires making the assumption that the put-call parity no-arbitrage relation holds among the option contracts considered. The put-call parity, formalized by Stoll (1969), implies that, in the absence of arbitrage, European vanilla put and call options with the same strike price and the same expiry date are associated with the same implied volatility at the same spot time. While, on average, the put-call parity do hold for European vanilla options, substantial violation of the put-call parity have been observed in empirical studies of option prices, suggesting the existence of underpricing and overpricing of both call and put options (see, e.g., Kamara and Miller, 1995). These empirical findings raise the question whether OTM put and call option prices contain comparable amount of market information on discount rate and implied volatility, and whether this plausible approach is an optimal way to estimate the implied discount rates along with the implied volatilities that correspond to the ITM and OTM option contracts.

3.6.3 The differences between the implied discount rates and the contemporaneously quoted Libor rates

The analysis results reported in Section 3.6.2 suggest that the implied discount rates estimated from the historical options data sampled between 2010 and 2013 inclusive appear to be higher than the contemporaneously quoted Libor rates. In this section, we seek to investigate whether this trend is persistent across a longer time frame.

We obtain ten samples of historical option prices quoted between 2004 and 2013 inclusive, each containing the day-close prices of a set of of option contracts quoted on two consecutive business days. Using these ten data samples, we construct, for each of them, a system of over-defined nonlinear equations using (3.1), and estimate the corresponding implied discount rates and implied volatilities by minimization of (3.2) using the numerical strategy described in Section 3.4. In Figures 9 and 10, we depict the estimated implied discount rates and the contemporaneously quoted Libor rates. For the option prices sampled between 2004 and 2007 inclusive, the implied discount rates appear to be comparable to or slightly lower than the contemporaneously quoted Libor rates. In contrast, for option prices sampled between 2008 and 2013 inclusive, the implied discount rates appear to be higher than the contemporaneously quoted Libor rates. One plausible explanation for this

change in the relative magnitudes between the implied discount rates and the contemporaneous Libor rates is that since the sub-prime mortgage crisis in 2007 the Libor rates have been reduced substantially, as depicted in Figures 1 and 2, and that the market participants may have become more aware of their liquidity risk and credit risk, hence taking into account these premiums in their choices of risk-free rate proxy.

We also investigate whether the estimation of the implied discount rates are numerically stable with respect to day-to-day variation of the samples of the option prices used to construct these over-defined systems of nonlinear equations. For each of the ten aforementioned samples of option prices, we obtained an additional sample of option prices pertaining to the same set of option contracts from another two consecutive trading days by rolling the sampling window one trading day further down the line. We construct, for each of these ten additional samples of option prices, a system of over-defined nonlinear equations using (3.1), and estimated the implied discount rates and implied volatilities by minimization of (3.2). The implied discount rates and the contemporaneously quoted Libor rates are depicted in Figures 9 and 10, and the results suggests that the implied discount rates are, in general, numerically stable with respect to day-to-day variation across each pair of samples considered.

3.7 Discussion

In this chapter, we have proposed a strategy to estimate the implied discount rates and implied volatilities pertaining to the prices of a set of European vanilla call option contracts as approximate solution to an over-defined system of nonlinear equations constructed using the Black-Scholes option pricing formula as a mapping tool.

Results of numerical experiments based on synthetic test data sets appear to suggest that our proposed algorithm is reasonably accurate in the recovery of the hypothetical implied discount rates and implied volatilities that are used to generate these test data sets. Albeit possibly data dependent, these results may be viewed as a small initial step towards the construction of an econometric procedure to estimate and analyse the market participants' aggregate choice of discount rate. Granted, a more general framework may be required to more effectively capture the information on implied discount rates and implied volatilities for ITM as well as OTM option contracts with the same degree of accuracy, and accommodate the existence of underlying asset price jumps and stochastic nature of instantaneous volatility of the price process dynamics.

The differences in the implied volatilities estimated from the same sets of option prices with respect to different choices of discount rates, including the estimated implied discount rates, reported in Section 3.6.2 may be viewed as a sensitivity analysis of implied volatility estimation uncertainty with respect to discount rate choice uncertainty. In this sense, the empirical analysis reported in Section 3.6.2 may be viewed as an implied volatility estimation uncertainty sensitivity analysis from a perspective that is complimentary to that of the sensitivity analysis reported in Chapter 2 the primarily focus of which is on plausible future discount rate uncertainty.

The time series of estimated implied discount rates depicted in Figures 9 and 10 demonstrate an interesting relative relationship between the estimated implied discount rates and the contemporaneously quoted Libor rates, and demonstrate that the timing of an apparent change in such a relationship roughly coincides with the timing of a major financial event. While it is premature to attach econometric significance on the estimated implied discount rates in its present form, our current empirical results appear to point towards a perspective from which inference of market participants' aggregate choice of discount rate from option prices may be plausible.

The strategy we have proposed in this chapter to jointly infer implied discount rates and implied volatilities from a cross-sectional set of European vanilla call option prices belongs to the family of model calibration techniques. For the strategy to be applicable, the data pertaining to the option contracts must be reliable. Currently, there is no consensus on the optimal interval for the remaining lifespan of option contracts within which the prices of these options contain the most accurate information on the market participants' aggregate choice of discount rate and expectation of implied volatility. Short of that, we appeal to the extant literature for guidance.

We outline, among many others, several examples that utilize S&P500 European vanilla index options data, the same options data we use for the empirical analysis reported in this chapter. Constantinides, Jackwerth and Savov (2011) pointed out that the short maturity options tend to move erratically close to expiration while the long maturity options lack volume and open interest. On this ground, they removed all options with remaining lifespan of less than 7 or more than 180 calendar days to perform econometric analysis of S&P500 index options return. Aït-Sahalia and Lo (1998) include S&P500 index option contracts with remaining lifespan of at most 350 days to perform nonparametric inference of the implied state price density from the cross-sectional sets of option prices, while Fengler and Hin (2015b) included S&P500 index option contracts with remaining lifespan of less than 7 or more than 180 calendar days to infer the implied state price density from the

cross-sectional sets of option prices within a constrained tensor-product B-spline framework. Hurn, Lindsay and McClelland (2015) include S&P500 index option contracts with remaining lifespan of less than 90 days for calibration of stochastic volatility models.

One may read into the choices of options data inclusion range with respect to the time to maturity of the option contracts from the aforementioned literature that the S&P500 index options data with a remaining lifespan exceeding one calendar year are in general excluded for model calibration purposes, likely due to the reason that the long maturity options lack transaction volume and open interest as pointed out by Constantinides et al. (2011). It is on this ground that we have restricted our empirical analysis to option contracts with remaining times to maturity between 150 and 320 days. Therefore, we envisage our proposed technique to be applicable in this context to option contracts with remaining lifespan not exceeding one year.

When confronted with the recovery of parameters involving prices of option contracts with medium to long tenors, there may be several possible avenues that one may explore.

For example, one may build on the insight provided by Gefang et al. (2011) that the higher the bank credit risk premium, the higher the discount rate at the long end of the tenor, alongside the results of our empirical analysis presented in Section 3.6.2.1 to construct a discount curve term structure for medium to long tenors by offsetting the risk-free OIS interest rate term structure with the appropriate interest rate spread that reflects the credit risk pertaining to the respective tenors. For this purpose, information on the credit risk at longer tenors may be inferred from the CDS contracts that match the appropriate credit rating level (see, among many others, Cao et al., 2010; 2011; Pak and Kim, 2012).

Alternatively, one may construct an arbitrage-free constrained discount curve using the strategy proposed in Fengler and Hin (2015a) in order to construct an arbitrage-free discount curve that match the available implied discount rates as closely as possible. By setting the support of the co-incidental boundary knots of the B-spline support to encompass the tenors of interest, one may obtain the discount rate by interpolation within the support of the boundary knots, a technique popularised by Eilers and Marx (1996), among others.

Should it be of interest to infer the market participants' aggregate choice of discount rates and implied volatilities from the exchange-traded American options, the Black-Scholes pricing formula for European vanilla call options in (3.2) need to be replaced by the American vanilla call option counterpart. If the model calibration framework assumes the absence of dividend payout, then, the American vanilla call option has the same

value as a European vanilla call option that has identical contractual characteristics except the right for early exercise (Throrem 2, Merton, 1973).

However, if the model calibration framework assumes the presence of dividend payout, then, the American vanilla call option has no closed-form solution and an approximation of the American call option must be sought. This can be achieved numerically via lattice methods (see, e.g., Cox, Ross and Rubinstein, 1979; Cassimon, Engelen, Thomassen and van Wouwe, 2007; Ehrhardt and Mickens, 2008; Nelson and Arthur, 2013), via finite difference solution of partial differential equations (see, e.g., Dempster and Hutton, 1997; Dempster and Richards, 2000; Rindell, 2005), or via Riesz decomposition of the American option price into a European option price and an early exercise premium based on the results established by El Karoui and Karatzas (1991) where the early exercise premium may be approximated by numerical integration across the immediate exercise boundary spanning the remaining lifespan of the American option in question. An approximation of the immediate exercise boundary may be sought as recursive backward step-wise approximate solution of a non-linear integral equation (see, e.g., Kim, 1990; Jacka, 1991; Carr, Jarrow and Myeneni, 1992). Alternatively, one may restrict attention to a class of exercise policies that are easy to evaluate and choose the best from within the class in order to obtain an approximated lower bound for the exercise boundary as proposed by Broadie and Detemple (1996).

While it is straight forward to invoke the put-call parity to modify the numerical strategy proposed in Section 3.4 to infer jointly the implied discount rates and the implied volatilities from a cross-sectional set of European vanilla put options, there is no put-call parity for American vanilla options and one must implement the numerical approximation for the American vanilla put option to calibrate against the market prices of the American put options in an appropriately modified version of (3.2). Worthy of note is that while the American and European vanilla call prices are the same in the absence of dividend payouts, the American vanilla put always worth more than the European counterpart.

Chapter 4

Forecast of short rate based on the CIR model implemented in the multiple yield curve framework

4.1 Introduction

While Chapters 2 utilize the framework of an under-defined system of equation to investigate the impact of discount rate uncertainty on implied volatility calibration accuracy, and while Chapter 3 utilize the framework of an over-defined system of equation to develop a strategy for joint calibration of discount rates and implied volatilities from a cross-sectional set of option prices, the present chapter utilize the framework of a well-defined system of equation to develop a strategy for short-rate forecast.

Motivated by the multi-curve approach for yield curve modelling discussed in Section 1.2.3, we propose, in this chapter, a strategy to model and forecast the short rate using the information implied from a cross-sectional set of zero coupon bond prices, and investigate the effect of the term risk premium on its forecast performance. Instead of following the classical interest rate modelling approach that assumes the existence of a unique yield curve that spans the entire tenor, our strategy is inspired by the recently proposed multi-curve approach of modelling the yield curve.

Contrary to the classical paradigm, the multi-curve approach of modelling the yield curve builds different yield curves for different tenors (see, e.g., Mercurio, 2010; Madan and Schoutens, 2012). In our context, we model different segments of the yield curve that

correspond to different tenor intervals using different short rate processes.

We arrange a set of cross-sectional zero coupon bonds in ascending order of tenor, organize adjacent bonds into multiple non-overlapping triplets that correspond to different non-overlapping tenor intervals, and use a separate single-factor Cox-Ingersoll-Ross (CIR, Cox et al., 1985) process to model the short rate process associated with each tenor interval. We use the CIR zero coupon bond pricing formula as a mapping tool to construct a system of nonlinear equations. Approximate numerical solution of this system enable us to map the prices of each triplet to a set of implied CIR model parameters. We suggest to regard these sets of implied CIR model parameters as the model-based representation of the market participants' aggregate view of the future short rate at forecast horizons that are comparable to the tenors of the corresponding triplets. We propose an algorithm to forecast the future short rate based on these implied CIR model parameters.

Although inspired by the literature on the multi-curve approach of modelling the yield curve, our proposed approach differ from the multi-curve HJM model (Moreni and Pallavicini, 2014), and the multi-curve LIBOR market model (Mercurio, 2010) in that we considering modelling the tenor specific short rate processes instead of modelling the tenor specific basis spreads. Despite the fact that our strategy and that of Madan and Schoutens (2012) both use the tenor specific single-factor CIR model to pin down different segments of the yield curve, our work differ from that of Madan and Schoutens (2012) in two ways. Firstly, Madan and Schoutens (2012) consider a two-price economy whereas we work within the framework of a one-price economy. Secondly, Madan and Schoutens (2012) consider contingent claim pricing within the multi-curve framework whereas we consider short rate forecast within the multi-curve framework.

We apply our proposed algorithm to infer the market participants' aggregate view of the future short rate from the historical prices of the United States Separately Traded Registered Interest and Principal Securities (US STRIPS) sampled between 2001 and 2014 inclusive, and use this information to forecast the US effective Federal Funds rate.

The rest of the chapter is as follows. Section 4.2 reviews the relevant literature and discuss the motivation of this study. Section 4.3 describes some characteristics of the single-factor CIR short rate process. Section 4.4 constructs the estimator of CIR model parameters in the multi-curve framework, describes the parameter estimation algorithm, and derives the predictor for future short rate and the estimator for the forward variance of the integrated CIR process. Section 4.5 reports the application of the proposed strategy to the historical US STRIPS prices and effective Federal Funds rate. Section 4.6 discusses related issues.

4.2 Literature review and motivation of study

The classical asset pricing paradigm, i.e., the single-curve framework , assumes the existence of a unique yield curve to forecast interest rates, and to discount cash flows. It is well known that the multi-factor short rate models perform better than their single-factor counterparts in capturing the salient features of the yield curve and forecasting the interest rates in the single-curve framework. Additionally, under some circumstances, regime-switching extension of the single-factor affine term structure models may improve in-sample model fit and out-of-sample forecast performance of the corresponding single-factor affine term structure models. The vast extant literature in this area include the factor models that attempt to model the dynamics of the entire yield curve using the principal components of the yield curve time series data (see, e.g., Litterman and Scheinkman, 1991; Diebold and Li, 2006), the affine term structure models that facilitates modelling of each affine state variable of the short rate by either a Gaussian or squared-root process (see, e.g., Duffie and Kan, 1996; Dai and Singleton, 2002), various generalizations of the affine term structure models including the essentially affine term structure model (Duffee, 2002) and the unspanned stochastic volatility model (see, e.g., Collin-Dufresne and Goldstein, 2002; Collin-Dufresne et al., 2008; Trolle and Schwartz, 2009) that facilitate joint modelling of the interest rate and its volatility, and the regime-switching models that relax the the restriction of time-invariant long-term interest rate in affine term structure models (see, e.g., Ang and Bekaert, 2002; Zhou and Mamon, 2012). While the models proposed by Diebold and Li (2006), Diebold et al. (2008), Moench (2008), and Guidolin and Timmermann (2009), among others, are designed to forecast interest rates based on time-series data of the yield curve, i.e., under the physical measure, those proposed by de Munnik and Schotman (1994), and Bams and Schotman (2003), among others, are designed to forecast interest rates based on cross-sectional data of the yield curve, i.e., under the risk neutral measure, in the single-curve framework.

Since the subprime mortgage crisis of 2007, the quoted interest rates are no longer consistent with one another. For example, the forward rates implied by the prices of two consecutive zero coupon bonds are no longer comparable to the forward rate agreement rate quotes or the forward rates implied by the OIS rate quotes, (see, e.g., Mercurio, 2009; 2010; Moreni and Pallavicini, 2014; Baviera and Cassaro, 2015). This segmentation of interest rates in the market violate the usual no-arbitrage relationships of the interest rate term structure and pose difficulty in maintaining a coherent framework for the pricing of contingent claims based on interest rate and discounting cash flows.

The inconsistencies of the quoted interest rates that ushered in the practice of multi-curve interest rate modelling framework may be viewed as an empirical example of the 'Market Segmentation Hypothesis' that hypothesize that different groups of market participants may prefer to invest in interest rate related instruments with different maturities. The reasons for the heterogeneity of their investment preferences may include investment horizon preferences and regulatory constraints (see, e.g., Culberston, 1957; Modigliani and Sutch, 1966; Van Horne, 1980).

From a practical perspective, recognizing that the classical single-curve framework is not capable of capturing the interest rate market segmentation, the financial industry begin to adopt an empirical approach of modelling the interest rate term structure. This approach, referred to as the multi-curve framework, pins down different segments of the yield curve by constructing as many yield curves as possible rate tenors to forecast future interest rates, and allows considerable flexibility in cash flow discounting by constructing a different set of curves to discount future cash flows at different horizons into the future (see, e.g., Mercurio, 2010; Moreni and Pallavicini, 2014). Central to this approach is the assumption that interest rates corresponding to different tenors are associated with different yield curves. A different perspective of interpreting this assumption is that since, in the multi-curve framework, we assume that interest rates that correspond to different tenors are associated with different yield curves, we may use different short rate processes to model these different yield curves. This motivates our choice of using tenor-specific CIR processes to model short rate processes associated with different triplets in a cross-sectional set of zero coupon bonds in the multi-curve framework.

We use the single-factor CIR process to model the short rate process associated with each triplet of zero coupon bonds because this is the simplest possible model that guarantees positivity of the short rate, and that its zero coupon bond pricing formula is available in closed form. Madan and Schoutens (2012) also used the single-factor CIR model in the multi-curve framework for similar reasons, but in the context of a two-price economy instead. We also draw support for our choice from the empirical results in the single-curve framework reported in Aït-Sahalia (1996b) that for short rate of magnitude less than 0.09, the CIR model is a good approximation model for the seven-day Eurodollar deposit short rate dynamics. We conjecture that this benefit may carry through to the multi-curve setting.

The role of the CIR model in interest rate modelling bears resemblance to the role of the Black-Scholes option pricing formula in the pricing of contingent claim pertaining to the equity asset class in that it has been used by many researchers as a starting point in

the single-curve framework from which more sophisticated models are constructed with an aim to better capture the salient features of the interest rate term structure (see, e.g., Hull and White, 1990; Jamshidian, 1995; Maghsoodi, 1996; Schlögl and Schlögl, 2000; Ahn and Thompson, 1988; Deng, 2014). As far as we are aware, the segmented CIR model (Schlögl and Schlögl, 2000) that models the long range interest rate parameter as a piecewise-continuous constant is probably one of the earliest literature aimed at capturing the salient features of different segments of the yield curve by the use of tenor specific short rate model parameters. That said, our proposed approach differs from the segmented CIR model in several aspects.

Firstly, our approach is designed for the multi-curve framework, while the segmented CIR model is designed for the single-curve framework. Secondly, we model different segments of the yield curve corresponding to different tenors are using different single-factor CIR processes that give rise to different sets of implied CIR model parameters, whereas the segmented CIR model model the entire yield curve using one single-factor CIR process, keeping the same speed of mean reversion fixed across all tenors, specifying the volatilities as exogenous input based on the volatility parameters of some contingent claims of interest, and estimating the long-range mean short rate as a piece-wise constant that span the time intervals between the maturity dates of two adjacent zero coupon bonds arranged in increasing tenor. Thirdly, while our parameter estimation procedure ensures that all the estimated CIR model parameters are positive, the segmented CIR model model encounters some numerical instability issue where strongly downward sloping initial forward rate curves can lead to negative values of long-range mean short rate.

As far as we are aware, there are no previous published literature on interest rate forecast based on the multi-curve framework except Hin and Dokuchaev (2015b), a recently accepted paper derived from the work reported in this chapter. We attempt to contribute to the literature by proposing a strategy to forecast short rate within the multi-curve framework using the information of the market participants' aggregate view on future short rate inferred from a cross-sectional set of zero coupon bond prices. The performance of this strategy on some historical data set may give us some idea on the feasibility of constructing short rate forecast strategy within the multi-curve framework, and the effect of term risk premium on the forecast performance of such a strategy.

The extant literature on interest rate forecast in the single-curve framework appears to suggest that the effect of term premium on interest rate forecast performance becomes noticeable beyond some forecast horizon. On the one hand, Fama (1976) noted that the forward rates calculated from T-Bill rates do not perform well in predicting short rate at

forecast horizons beyond two years unless adjustment is made to account for the term premium. On the other hand, Longstaff (2000) reported that the effect of term premium for short-term repurchase rates is negligible for tenors up to three months. Since these empirical studies considered two different sets of interest rates, the forecast horizon beyond which the term premium start to show noticeable effect on the performance of future short rate predictor constructed from the same set of interest rates is not entirely clear. This motivates us to investigate the effect of term premium on short rate forecast in the multi-curve framework using our proposed algorithm as a test model.

Although some existing literature recommends disentangling the expected future short rate from the expected term premium to improve the forecast performance of short rate predictors (see, e.g., Fama, 1976; Fama and Bliss, 1987; Huang and Lin, 1996; Dai and Singleton, 2002; Tzavalis, 2004; Cochrane and Piazzesi, 2005), the difficulty in the practical implementation of this recommendation lies in the lack of consensus on the functional form of the term premium. In fact, many different definitions and parametric expressions of the term premium have been suggested, and numerous different numerical strategies have proposed to estimate them (see, e.g., Fama and Bliss, 1987; Cochrane and Piazzesi, 2005; Collin-Dufresne, Goldstein and Jones, 2009; Gil-Alana and Moreno, 2012; Rudebusch, 2012; Dewachter et al., 2014). To make the matter even more challenging, the estimation of the term premium is sensitive to the choice of estimator and is data dependent. Kim (2007) pointed out that it is this lack of robustness in existing methodologies that renders it less appealing to practitioners to adjust for the term premium in their analysis of interest rates.

The current chapter focus on the construction of a strategy to forecast the short rate, and do not consider the proposition of a strategy to forecast volatility of the short rate. This is because the one-factor CIR model that we have chosen as our working model is not capable of of capturing potential jumps and stochastic components in the volatility of the effective Federal Funds rate (see, e.g., Das, 2002; Piazzesi, 2005; Wright and Zhou, 2009). Our focus of study in this chapter is to propose, using a simple working model, a strategy to extract information on the market participants' expectation of the future short rate in a multi-curve framework.

Additionally, recent empirical studies (see, e.g., Duffee, 2011; Collin-Dufresne et al., 2009; Andersen and Benzoni, 2010) suggest that the cross-sectional interest rate term structure does not contain information on the short rate volatility. In this light, our model framework may not be an appropriate construct to analyse short rate volatility. Instead, one should extract this information from the time series of the interest rates in order to

forecast the realized volatility of the short rate.

In order to estimate the realized variance of a short rate process, one may need to construct a more sophisticated model that takes into account stochastic volatility and jump of the short rate process (see, e.g., Duffee, 2002; Collin-Dufresne and Goldstein, 2002; Piazzesi, 2005) or adopt time series modelling strategies such as the extended EGARCH-type model (see, e.g., Andersen and Benzoni, 2010).

As an alternative, one may, instead, use the Heterogeneous Autoregressive model of Realized Volatility (HAR-RV, Corsi, 2009) to forecast the realized volatility of yield by linear projection of the historical volatilities that are estimated at different lags. The out-of-sample forecast performance of the HAR-RV model is comparable to that of the extended EGARCH-type model (Andersen and Benzoni, 2010). Additionally, it is superior to that of the lag-1 and the lag-3 Autoregressive models, and the Autoregressive Fractional Integrated Moving Average (ARFIMA) model (Corsi, 2009). Refinements of the HAR-RV model in the extant literature include the modification by Andersen, Bollerslev and Diebold (2007) to forecast the realized volatility of affine jump-diffusion stochastic processes, and the extension proposed by McAleer and Medeiros (2008) to capture non-linearities and long-range dependence in the time series dynamics via a flexible multiple regime smooth transition model.

4.3 The model framework

Let $(\Omega, \mathscr{F}, \mathbb{P})$ be a standard probability space where Ω is a set of elementary events, $\mathscr{F}$ is a complete sigma algebra of events, and $\mathbb{P}$ is a probability measure. Let $\mathscr{F}_t$ be a complete sigma algebra of events generated by the data observed at time t. Let the short rate process $r(u), u \in [t, T], t < T$, be a stochastic process adapted to the filtration $\{\mathscr{F}_t\}$, where $\{\mathscr{F}_t\}$ is some filtration generated by the flow of the currently observed market data, $r(u)$ is non-negative, or at least that the process $\min(r(u), 0)$ is bounded, $\mathbf{E}\left[\int_t^T r(u)^2 du \,\middle|\, \mathscr{F}_t\right] < +\infty, t < T$, where $\mathbf{E}$ is the expectation taken over $r(u)$ under some probability measure $\mathbb{P}$, and the case when the filtration $\{\mathscr{F}_t\}$ is generated by the process $r(u)$ is not excluded. The price of a zero-coupon bond at the current time t and with maturity time T is defined by the conditional expectation

$$P(t, T) = \mathbf{E}\left[e^{-\int_t^T r(u)du} \,\middle|\, \mathscr{F}_t\right] . \tag{4.1}$$

4.3.1 General setting

Let

$$\rho(t;s,T) \stackrel{\Delta}{=} \mathbf{E}\left[\frac{1}{T-s}\int_s^T r(u)du \;\middle|\; \mathscr{F}_t\right], \tag{4.2}$$

where $u \in [s,T]$, $s < T$, be the 'expected average integrated short rate' observed at time t for the time interval $[s,T]$, and let $\gamma(t;s,T) = (T-s)\rho(t;T_1,T_2)$. Let

$$\eta(t,T) = -\frac{1}{T-t}\log P(t,T) \tag{4.3}$$

be the yield-to-maturity of the zero coupon bond maturing at the tenor $T-t$, and let

$$J(t,T) = \rho(t;t,T) - \eta(t,T) \tag{4.4}$$

be the corresponding 'convexity adjustment' term, (see, e.g. Fisher and Gilles, 1998). Since e^{-x}, $x \in \mathbb{R}$, is a convex function, we obtain, by the Jensen's inequality,

$$\mathbf{E}\left[e^{-\int_t^T r(u)du} \;\middle|\; \mathscr{F}_t\right] \geq e^{-\mathbf{E}\left[\int_t^T r(u)du \;\middle|\; \mathscr{F}_t\right]},$$

and it follows from (4.2) and (4.3) that $J(t,T) \geq 0$. If the short rate process $r(u)$, $u \in [t,T]$, is non-random, then $J(t,T) = 0$.

Let $\eta(t,T_1)$ and $\eta(t,T_2)$ be the yield-to-maturities with respect to two different zero coupon bonds $P(t,T_1)$ and $P(t,T_2)$ respectively where $t < T_1 < T_2$. Based on $P(t,T_1)$ and $P(t,T_2)$, we can infer the forward rate in the interval $[T_1,T_2]$ by

$$F(t;T_1,T_2) = \frac{-\log P(t,T_2) + \log P(t,T_1)}{T_2-T_1} = \frac{(T_2-t)\,\eta(t,T_2) - (T_1-t)\,\eta(t,T_1)}{T_2-T_1}. \tag{4.5}$$

It follows from (4.4) and (4.5) that

$$\rho(t;T_1,T_2) - F(t;T_1,T_2) = \frac{(T_2-t)\,J(t,T_2) - (T_1-t)\,J(t,T_1)}{T_2-T_1}. \tag{4.6}$$

Further let $\gamma(t;s,T) = (T-s)\rho(t;s,T)$, and let

$$\Gamma(t;s,T) = \mathbf{E}\left[\left(\int_s^T r(u)du\right)^2 \;\middle|\; \mathscr{F}_t\right],$$

where $u \in [s,T]$, and $t \leq s < T$. We expand $e^{-\int_t^{T_q} r(u)du}$, $q = 1,2$, up to the second order to

obtain an approximation expression of the zero coupon bond pricing formula (4.1)

$$P(t,T_q) \approx 1 - \gamma(t;t,T_q) + \frac{1}{2}\Gamma(t;t,T_q)\,, \qquad q = 1,2,$$

and then obtain the approximation expression of $\log P(t,T_q)$ using this expression by expanding the log term up to the second order and discarding the terms higher than the second order to obtain

$$\begin{aligned}
\log P(t,T_q) &\approx \log\left(1 - \gamma(t;t,T_q) + \frac{1}{2}\Gamma(t;t,T_q)\right) \\
&\approx -\gamma(t;t,T_q) + \frac{1}{2}\Gamma(t;t,T_q) - \frac{1}{2}\left(-\gamma(t;t,T_q) + \frac{1}{2}\Gamma(t;t,T_q)\right)^2 \\
&\approx -\gamma(t;t,T_q) + \frac{1}{2}\left(\Gamma(t;t,T_q) - \gamma(t;t,T_q)^2\right) \\
&= -\gamma(t;t,T_q) + \frac{1}{2}\left(\mathbf{E}\left[\left(\int_t^{T_q} r(u)du\right)^2 \,\middle|\, \mathscr{F}_t\right] - \mathbf{E}\left[\int_t^{T_q} r(u)du \,\middle|\, \mathscr{F}_t\right]^2\right) \\
&= -\gamma(t;t,T_q) + \frac{1}{2}\,\mathrm{Var}\left[\int_t^{T_q} r(u)du \,\middle|\, \mathscr{F}_t\right]\,, \qquad q = 1,2, \qquad (4.7)
\end{aligned}$$

where, in the last two lines, we have used the identity $\mathrm{Var}[x] = \mathbf{E}[x^2] - \mathbf{E}[x]^2, x \in \mathbb{R}$. Substituting (4.7) into (4.5), we obtain

$$\begin{aligned}
F(t;T_1,T_2) &= \rho(t;T_1,T_2) - \frac{\delta(t;T_1,T_2)}{2(T_2-T_1)} + \mathscr{R}\left(P(t,T_1) - P(t,T_2)\right) \\
&\approx \rho(t;T_1,T_2) - \frac{\delta(t;T_1,T_2)}{2(T_2-T_1)}\,, \qquad (4.8)
\end{aligned}$$

where

$$\delta(t;T_1,T_2) = \mathrm{Var}\left[\int_t^{T_2} r(u)du \,\middle|\, \mathscr{F}_t\right] - \mathrm{Var}\left[\int_t^{T_1} r(u)du \,\middle|\, \mathscr{F}_t\right]\,,$$

and $\mathscr{R}\left(P(t,T_1) - P(t,T_2)\right)$ represents the collection of all the higher order terms in the exponential expansions of $P(t,T_q), q = 1,2$, and the higher order terms in the logarithmic expansions of $\log P(t,T_q), q = 1,2$, which we disregard in obtaining the approximation (4.8). Let

$$\Delta(t;T_1,T_2) = 2\left(\rho(t;T_1,T_2) - F(t;T_1,T_2)\right) \approx \frac{\delta(t;T_1,T_2)}{T_2-T_1}\,, \qquad (4.9)$$

be the 'approximate average forward variance', an expression that we may regard as a gauge of the average volatility of the integrated short rate in the interval $[T_1,T_2]$ for some $t < T_1 < T_2$ that may be approximated using $\delta(t;T_1,T_2)$.

4.3.2 The CIR model

The expressions (4.1) to (4.9) do not rely on a particular model for the short rate process. Although we do not assume that a particular short rate model can capture all the salient features of the interest rate term structure, for the reasons outlined in Section 4.2, we choose to use the one-factor CIR process to model the dynamics of the tenor specific short rate processes in a multi-curve framework.

Let $r_{CIR}(u), u \in [t, T], t < T$, be a one-factor CIR process where

$$r_{CIR}(T) = r_{CIR}(t) + \kappa\theta(T-t) - \kappa \int_t^T r_{CIR}(u)du + \sigma \int_t^T r_{CIR}(u)^{1/2} dW(u) \,, \tag{4.10}$$

where κ is the speed of mean-reversion of the short rate, θ is the long-range short rate, σ is the volatility of the process, $r_{CIR}(t) = r(t)$ where $r(t)$ is the short rate at time t, and $W(u)$ is the standard Wiener process. If $\kappa = 0$ or $\theta = 0$, $r_{CIR}(T)$ reaches zero almost surely and the point zero is absorbing. If $2\kappa\theta \geq \sigma^2$, $r_{CIR}(T)$ is a transient process that stays positive and never reaches zero. If $0 < 2\kappa\theta < \sigma^2$, $r_{CIR}(T)$ is instantaneously reflective at point zero (Feller, 1951).

Taking expectation across (4.10) conditional on $\mathscr{F}_t$ with respect to $r_{CIR}(T)$, we obtain

$$\mathbf{E}\left[r_{CIR}(T) \,|\mathscr{F}_t\right] = r_{CIR}(t) + \kappa\theta(T-t) - \kappa \int_t^T \mathbf{E}\left[r_{CIR}(u) \,|\mathscr{F}_t\right] du \,.$$

Differentiate with respect to T,

$$\frac{d\mathbf{E}\left[r_{CIR}(T) \,|\mathscr{F}_t\right]}{dT} = \kappa\left(\theta - \mathbf{E}\left[r_{CIR}(T) \,|\mathscr{F}_t\right]\right) \,.$$

Let $\mathbf{E}\left[r_{CIR}(T) \,|\mathscr{F}_t\right] = \Phi(T)$, we solve the variable separable first order first degree ordinary differential equation

$$\frac{d\Phi(T)}{dT} = \kappa\left(\theta - \Phi(T)\right) \,,$$

and since $\Phi(t) = r(t)$, we obtain

$$\mathbf{E}[r_{CIR}(T)|\mathscr{F}_t] = \theta + \left(r(t) - \theta\right) e^{-\kappa(T-t)} \,. \tag{4.11}$$

It follows from (4.11) that

$$\begin{aligned}\gamma_{CIR}(t;t,T) &= \mathbf{E}\left[\int_t^T r_{CIR}(u)du \;\middle|\; \mathscr{F}_t\right] \\ &= \int_t^T \mathbf{E}[r_{CIR}(u)|\mathscr{F}_t]\, du \\ &= \theta(T-t) + \left(\frac{r(t)-\theta}{\kappa}\right)\left(1-e^{-\kappa(T-t)}\right) . \end{aligned} \tag{4.12}$$

and, using (4.2), we obtain

$$\rho_{CIR}(t;t,T) = \frac{\gamma_{CIR}(t;t,T)}{T-t} = \theta + \frac{r(t)-\theta}{\kappa(T-t)}\left(1-e^{-\kappa(T-t)}\right) . \tag{4.13}$$

and it follows that, for some $t < T_1 < T_2$,

$$\rho_{CIR}(t;T_1,T_2) = \theta + \left(\frac{r(t)-\theta}{\kappa(T_2-T_1)}\right)\left(e^{-\kappa(T_1-t)} - e^{-\kappa(T_2-t)}\right) , \tag{4.14}$$

where, as $T_1 \to \infty$ and $T_2 \to \infty$, $\rho_{CIR}(t;T_1,T_2) \to \theta$. Using (4.4), we may define $\rho_{CIR}(t;t,T) = \eta(t,T) + J_{CIR}(t,T)$, and express the relation between $\rho_{CIR}(t;T_1,T_2)$ and $F(t;T_1,T_2)$ as

$$\rho_{CIR}(t;T_1,T_2) - F(t;T_1,T_2) = \frac{(T_2-t)\, J_{CIR}(t,T_2) - (T_1-t)\, J_{CIR}(t,T_1)}{T_2-T_1} . \tag{4.15}$$

Using (4.9), and (4.15), we define

$$\Delta_{CIR}(t;T_1,T_2) = 2\left(\rho_{CIR}(t;T_1,T_2) - F(t;T_1,T_2)\right) \approx \frac{\delta_{CIR}(t;T_1,T_2)}{T_2-T_1} , \tag{4.16}$$

and may use this expression as an estimator of the approximate average forward variance when the short rate dynamics is modelled using the CIR process where

$$\delta_{CIR}(t;T_1,T_2) = \mathrm{Var}_{CIR}\left[\int_t^{T_2} r_{CIR}(u)du \;\middle|\; \mathscr{F}_t\right] - \mathrm{Var}_{CIR}\left[\int_t^{T_1} r_{CIR}(u)du \;\middle|\; \mathscr{F}_t\right] ,$$

and $\mathrm{Var}_{CIR}(\cdot)$ denote the variance expressions for the integrated CIR process.

4.4 Inference of the implied CIR model parameters based on cross sectional zero coupon bond prices

We arrange a set of cross-sectional zero coupon bond in ascending order of tenor, and organize the adjacent bonds into multiple triplets that correspond to different non-overlapping tenor intervals. We assume each triplet that corresponds to a different tenor interval is associated with a different short rate process, and model each of these short rate processes using a separate one-factor CIR process specific for each of the tenor intervals considered.

Since the zero coupon bond pricing formula for a one-factor CIR process under the risk-neutral measure is given by

$$P_{CIR}(t, T; \kappa, \theta, \sigma, r(t)) = e^{B_1 - B_2 r(t)} , \tag{4.17}$$

where

$$\begin{aligned} B_1 &= \frac{\kappa\theta}{\sigma^2}\left[(\kappa + B_3)(T-t) - 2\log\left(1 + \frac{(\kappa + B_3)(e^{B_3(T-t)} - 1)}{2B_3}\right)\right] , \\ B_2 &= \frac{2\left(e^{B_3(T-t)} - 1\right)}{(\kappa + B_3)\left(e^{B_3(T-t)} + 2B_3\right)} , \\ B_3 &= \left(\kappa^2 + 2\sigma^2\right)^{1/2} , \end{aligned}$$

and $r(t)$ is the initial short rate, we construct, for each triplet, a set of three nonlinear equations with three unknown parameters by mapping the corresponding triplet of cross section zero coupon bond prices to their respective set of implied CIR model parameters via (4.17). Based on this mapping, we extract the information on the market participants' aggregate view of the future short rate at various forecast horizons from the triplets with comparable tenors, and represent this information as sets of implied CIR parameters for the the one-factor CIR processes associated with different tenors.

4.4.1 Numerical framework for the inference

Let $\left\{P(t, T_{j,k})\right\}_{j=1,\ldots,n,k=1,2,3}$ denote the prices of a set of zero coupon bonds observed at time t maturing at $T_{j,k}$ where $T_{j,k+1} > T_{j,k} > t$, and $T_{j+1,1} > T_{j,3} > t$, $j = 1, \ldots, n$. We assume that each triplet of prices $\left\{P(t, T_{j,k})\right\}_{k=1}^{3}$, indexed by $j = 1, \ldots, n$, that corresponds to a different non-overlapping tenor interval $(T_{j-1,3} - t, T_{j,3} - t]$, $j = 1, \ldots, n$, is associated with a different short rate process, while $T_{j-1,3} - t = 0$ for $j - 1 = 0$, and this triplet can be

mapped to a set of CIR model parameters $(\kappa_j(t), \theta_j(t), \sigma_j(t))$. Using (4.17) as a mapping tool, we construct a system of nonlinear equations

$$P_{CIR}(t, T_{j,k}; \kappa_j(t), \theta_j(t), \sigma_j(t), r(t)) = P(t, T_{j,k}) \,, \quad j = 1, \ldots, n, \quad k = 1, 2, 3, \tag{4.18}$$

where $(\kappa_j(t), \theta_j(t), \sigma_j(t))$ is the set of CIR model parameters inferred from $\left\{P(t, T_{j,k})\right\}_{k=1}^{3}$. Specifically, there are n sets of equations in this system, each set comprising of 3 nonlinear equations and three unknown parameters.

The initial short rate $r(t)$ is being regarded as a latent variable by Brown and Dybvig (1986), de Munnik and Schotman (1994), among others, and is treated as an unknown parameter and estimated alongside $\kappa_j(t)$, $\theta_j(t)$, and $\sigma_j(t)$. On the other hand, Aït-Sahalia (1996b), Chapman, Long and Pearson (1999), Chapman and Pearson (2001), among others, choose interest rates observed in the market as proxies for $r(t)$. While Schlögl and Schlögl (2000) are concerned that using a market rate, such as an overnight rate, as a proxy for $r(t)$ may not match the term structure implied by the CIR model parameters well, Chapman et al. (1999) demonstrated that accurate estimates of the drift and diffusion terms of the short-rate process can be obtained in an affine bond price model such as the single-factor CIR model even using interest rates maturities as long as three months for US data as proxies for $r(t)$.

We use an observable overnight interest rate in the same economy as $P(t, T_{j,k})$ that reflect the credit and liquidity risk levels that are comparable to those of $P(t, T_{j,k})$ as a proxy for $r(t)$. Specifically, we assume that, in a multi-curve framework, the proxy short rate process can be used to model the true short rate process in the tenor interval $[T_{j,1} - t, T_{j,3} - t]$ corresponding to the triplet $\left\{P(t, T_{j,k})\right\}_{k=1}^{3}$.

Let $\boldsymbol{\kappa}(t) = (\kappa_1(t), \ldots, \kappa_n(t))$, $\boldsymbol{\theta}(t) = (\theta_1(t), \ldots, \theta_n(t))$, $\boldsymbol{\sigma}(t) = (\sigma_1(t), \ldots, \sigma_n(t))$, and let

$$\boldsymbol{\Psi}\left(\boldsymbol{\Xi}(t)\right) = \sum_{j=1}^{n} \sum_{k=1}^{3} \Big(P(t, T_{j,k}) - P_{CIR}(t, T_{j,k}; \kappa_j(t), \theta_j(t), \sigma_j(t), r(t))\Big)^2 \tag{4.19}$$

be an L_2 metric loss function where, $\kappa_j(t) > 0$, $\theta_j(t) > 0$, $\sigma_j(t) > 0$, in order to fulfil the condition of $2\kappa_j(t)\theta_j(t) \geq \sigma_j(t)^2$, $j = 1, \ldots, n$, so that the short rate process is a transient process that always stays positive. Let $\boldsymbol{\Xi}(t) = (\Xi_1(t), \ldots, \Xi_{3n}(t)) = (\boldsymbol{\kappa}(t), \boldsymbol{\theta}(t), \boldsymbol{\sigma}(t))$, we

seek approximate solution to (4.18) as the optimization problem

$$\begin{aligned} &\text{Minimize} \qquad \boldsymbol{\Psi}\left(\boldsymbol{\Xi}(t)\right) \quad \text{over} \quad \boldsymbol{\Xi}(t) \\ &\text{subject to} \\ &\qquad\qquad \kappa_j(t) > 0\,, \qquad j = 1, \ldots, n, \\ &\qquad\qquad \theta_j(t) > 0\,, \qquad j = 1, \ldots, n, \\ &\qquad\qquad \sigma_j(t) > 0\,, \qquad j = 1, \ldots, n, \end{aligned} \tag{4.20}$$

where the solution of (4.20) represents an approximation to (4.18). Since (4.19) is not convex with respect to $\kappa_j(t)$, $\theta_j(t)$, and $\sigma_j(t)$, we seek numerical approximation to $\boldsymbol{\Xi}(t)$ via the Zhang-Sanderson's differential evolution algorithm (Zhang and Sanderson, 2009) that is designed to locate the global minimum in the presence of multiple co-existing local minima.

4.4.2 Implementation of the Zhang-Sanderson's algorithm to estimate the implied CIR model parameters from zero coupon bond prices

We follow the exposition style of Zhang and Sanderson (2009) in describing the implementation of the Zhang-Sanderson's algorithm for numerical solution of (4.20). Let $g = 1, \ldots, G$, be successive iteration steps with $g = 0$ representing the initialization stage.

1. **Initialization stage**: Generate N_p $3n$-dimensional random vectors $\boldsymbol{\Xi}_{I,0}(t), I = 1, \ldots, N_p$, where $\boldsymbol{\Xi}_{I,0}(t) = \{\Xi_{J,I,0}(t)\}_{J=1}^{3n}$, and where $\Xi_{J,I,0}(t)$ is a pseudo-random number generated from the uniform distribution $U[\Xi_J^{Lower}(t), \Xi_J^{Upper}(t)]$, and where $[\Xi_J^{Lower}(t), \Xi_J^{Upper}(t)]$ is a user specified interval for each of the $3n$ parameters, indexed by J, to be estimated within which $\Xi_J(t)$ is assumed to be located.

2. **Iteration stage**: Successive iterations are indexed by $g = 1, \ldots, G$. Each iteration consists of three steps.

   (a) **Mutation step for iteration stage** g: We construct N_p $3n$-dimensional mutation vectors

   $$\mathbf{v}_{I,g}(t) = \left\{v_{J,I,g}(t)\right\}_{J=1}^{3n} = \boldsymbol{\Xi}_{I,g}(t) + F_{I',g}(t)\left(\boldsymbol{\Xi}^p_{best,g}(t) - \boldsymbol{\Xi}_{I',g}(t)\right)\,, \quad I = 1, \ldots, N_p,$$

   where $\boldsymbol{\Xi}^p_{best,g}(t)$ is randomly chosen from the subset of $\left\{\boldsymbol{\Xi}_{I,g}(t)\,, I = 1, \ldots, N_p\right\}$ such that $\Psi\left(\boldsymbol{\Xi}^p_{best,g}(t)\right)$ is in the lowest p-percentiles of $\left\{\Psi\left(\boldsymbol{\Xi}_{I,g}(t)\right), I = 1, \ldots, N_p\right\}$,

$\boldsymbol{\Xi}_{I',g}(t) = \boldsymbol{\Xi}_{I,g}(t) - \boldsymbol{\Xi}_{I_1,g}(t) + \boldsymbol{\Xi}_{I_2,g}(t), I \neq I_1 \neq I_2$, while $F_{I,g}(t)$ is a pseudo-random number generated from the Cauchy distribution with location parameter $\mu_{F,g}(t)$ and scale parameter 0.1, and then to be either truncated to 1 if $F_{I,g}(t) \geq 1$ or regenerated if $F_{I,g}(t) \leq 0$. This construction of the mutation vectors corresponds to the non-archive-assisted DE/current-to-$p$best/1 implementation of the Zhang-Sanderson algorithm (Eqn. 6, Zhang and Sanderson, 2009) implemented in the `DEoptim` (Ardia et al., 2012) package for the `R` computing environment (R Core Team, 2012). Additionally, let $\mu_{F,0}(t) = 0.5$, let $\mu_{F,g+1}(t) = (1-c)\,\mu_{F,g}(t) + c\mu_{L,S_{F,g},g}(t)$, where c is a user specified parameter, $S_{F,g}(t) = \left\{F_{I,g}(t) : \boldsymbol{\Xi}_{I,g}(t) \neq \boldsymbol{\Xi}_{I,g+1}(t)\right\}$, and $\mu_{L,S_{F,g},g}(t) = \sum_{F_{I,g} \in S_{F,g}} F_{I,g}^2(t) \Big/ \sum_{F_{I,g} \in S_{F,g}} F_{I,g}(t)$. Any element $v_{J,I,g}(t)$ that falls outside the interval $[\Xi_J^{Lower}(t), \Xi_J^{Upper}(t)]$ will be reset to a value within the interval by the rule

$$v_{J,I,g}(t) = \begin{cases} \Xi_J^{Lower}(t) + \zeta_{J,I,g}(t)\left(\Xi_J^{Upper}(t) - \Xi_J^{Lower}(t)\right) , & if\ v_{J,I,g}(t) < \Xi_J^{Lower}(t) , \\ \Xi_J^{Upper}(t) - \zeta_{J,I,g}(t)\left(\Xi_J^{Upper}(t) - \Xi_J^{Lower}(t)\right) , & if\ v_{J,I,g}(t) > \Xi_J^{Upper}(t) , \end{cases}$$

where $\zeta_{J,I,g}(t)$ is a pseudo-random number generated from uniform distribution $U[0,1]$.

(b) **Crossover step for iteration stage** g: We construct N_p $3n$-dimensional crossover vectors $\mathbf{u}_{I,g}(t) = \left\{u_{J,I,g}(t)\right\}_{J=1}^{3n}, I = 1, \ldots, N_p$, by the rule

$$u_{J,I,g}(t) = \begin{cases} v_{J,I,g}(t), & \text{if} \quad \xi_{J,I,g}(t) \leq CR_{I,g} , \\ \Xi_{J,I,g}(t), & \text{otherwise} , \end{cases}$$

where $\xi_{J,I,g}(t)$ is a pseudo-random number generated from uniform distribution $U[0,1]$, while $CR_{I,g}(t)$ is generated by truncating a pseudo-random number generated from a Gaussian distribution $\mathcal{N}\left(\mu_{CR,g}(t), 0.01\right)$ with respect to a floor of 0 and a ceiling of 1. Additionally, let $\mu_{CR,0}(t) = 0.5$, and let $\mu_{CR,g+1}(t) = (1-c)\mu_{CR,g}(t) + c\mu_{A,CR,g}(t)$, where c is a user specified parameter and where $\mu_{A,CR,g}$ is the arithmetic mean of the set of all successful crossover probabilities.

(c) **Selection step for iteration stage** g: We update $\boldsymbol{\Xi}_{I,g+1}(t)$ by the rule

$$\boldsymbol{\Xi}_{I,g+1}(t) = \begin{cases} \mathbf{u}_{I,g}(t) , & if \quad \Psi\left(\mathbf{u}_{I,g}(t)\right) < \Psi\left(\boldsymbol{\Xi}_{I,g}(t)\right) , \\ \boldsymbol{\Xi}_{I,g}(t) , & otherwise . \end{cases}$$

The selection for member vector I is regarded as successful if $\boldsymbol{\Xi}_{I,g+1}(t) \neq \boldsymbol{\Xi}_{I,g}(t)$.

3. **Algorithm termination**: The parameter vector $\boldsymbol{\Xi}_{best,G}(t)$ that corresponds to the objective function value $\min\left\{\Psi\left(\boldsymbol{\Xi}_{I,G}(t)\right), I = 1, \ldots, N_p\right\}$ is is the best estimate of the parameters in the set of parameter vector population $\left\{\boldsymbol{\Xi}_{I,G}(t)\ , I = 1, \ldots, N_p\right\}$, and that $\boldsymbol{\Xi}_{best,G}(t)$ is regarded as the approximate solution of (4.18) by minimization of objective function (4.19) over a given number of iteration steps G. In all numerical applications in this chapter, we set $G = 2,000$, $c = 0.15$, $p = 0.05$, and $N_p = 25{\times}3n$.

Here, $\boldsymbol{\Xi}_{best,G}(t) = \left\{\Xi_{best,G,j}(t)\right\}_{j=1}^{3n} = \left(\boldsymbol{\kappa}_{best,G}(t), \boldsymbol{\theta}_{best,G}(t), \boldsymbol{\sigma}_{best,G}(t)\right)$, where $\boldsymbol{\kappa}_{best,G}(t) = \left\{\kappa_{best,G,j}(t)\right\}_{j=1}^{n}$, $\boldsymbol{\theta}_{best,G}(t) = \left\{\theta_{best,G,j}(t)\right\}_{j=1}^{n}$, $\boldsymbol{\sigma}_{best,G}(t) = \left\{\sigma_{best,G,j}(t)\right\}_{j=1}^{n}$, are the implied CIR model parameters estimated based on the corresponding zero coupon prices along the respective tenors $\left\{T_{j,3} - t\right\}_{j=1}^{n}$. The triplets $\left(\kappa_{best,G,j}(t), \theta_{best,G,j}(t), \sigma_{best,G,j}(t)\right)$ are regarded as the sets of estimated CIR model parameters for the short rate process that span the tenors $T_{j,3} - t$. The estimated parameters $\boldsymbol{\Xi}_{best,G}(t)$ are approximate solutions to (4.20). Uncertainty bound for estimated parameters may be constructed based on $\left\{\kappa_{I,G,j}(t)\right\}_{I=1}^{N_p}$, $\left\{\theta_{I,G,j}(t)\right\}_{I=1}^{N_p}$,and $\left\{\sigma_{I,G,j}(t)\right\}_{I=1}^{N_p}$ for each $j, j = 1, \ldots, n$, based on the strategy detailed in Section 3.4.2, and Hin and Dokuchaev (2015a).

A typical set of cross-sectional US STRIPS zero coupon bond prices used in the numerical analysis reported in Section 4.5 contains more than 120 data points with which we can construct approximately 40 sets of nonlinear equations, each based on a non-overlapping triplet of zero coupon bonds. In order to accelerate the numerical computation involved in simultaneous approximate solution of such a large system of equations, we use the Zhang-Sanderson algorithm implemented in the `DEoptim` (Ardia et al., 2012) package for the `R` computing environment (R Core Team, 2012). We used 48 parallel cores provided by the NeCTAR cloud computing infrastructure to carry out all the calculations reported in this Section 4.5 in order to accelerate the speed of computation. The computational acceleration achieved is considerable. As an example to give an idea of the extent of computational acceleration, we estimated the CIR model parameters based on day-close US STRIPS prices quoted on Jan. 2nd 2001. There are 168 parameters to be estimated from the system of equations constructed from that set of zero coupon bond prices. Using one processor, it took 3 hours and 10 minutes to carry out 2000 iterations. Using 48 parallel processors, it took 46 minutes instead, leading to a 76% reduction in computation time. This is comparable to the computational acceleration achieved in the numerical experiment reported in Section 3.4 and Hin and Dokuchaev (2015a).

4.4.3 Forecast of short rate using the implied CIR model parameters

We propose a set of predictors in Section 4.4.3.1 to forecast the short rate. They are designed for the multi-curve framework where different sets of implied CIR model parameters that correspond to different triplets of zero coupon bond prices are used to predict short rate at different forecast horizons.

In order to compare the performance of our proposed predictors with that of a set of short rate predictors implemented in the single-curve framework, we construct, in Section 4.4.3.2, a separate set of predictors that utilize only the set of implied CIR model parameters corresponding to the shortest tenor to forecast short rate at horizons beyond its tenor, which may be regarded as a 'naive' short rate predictor within the single-curve framework.

4.4.3.1 Forecast within the multi-curve framework

Assuming that the estimated implied CIR model parameters $\{\kappa_{best,G,j}(t), \theta_{best,G,j}(t), \sigma_{best,G,j}(t)\}$ contain some information on the market participants' expectation of the future short rate at forecast horizon $T_{j,3} - t$, we propose to formulate the forecast strategy by using the estimated implied CIR model parameters $\{\kappa_{best,G,j}(t), \theta_{best,G,j}(t), \sigma_{best,G,j}(t)\}$ to model the short rate process associated with the triplet $\left\{P(t, T_{j,k})\right\}_{k=1}^{3}$. We then use the non-linear projection of the future short rate based on the corresponding tenor-specific short rate curve in order to forecast $r(T_{j,3})$, the realized short rate at time $T_{j,3}$.

Based on (4.12), we may predict $\gamma_{CIR}(t; t, T_{j,3})$ at the forecast horizons $\left\{T_{j,3} - t\right\}_{j=1}^{n-1}$ using

$$\hat{\gamma}_{CIR}(t; t, T_{j,3}) = \theta_{best,G,j}(t)\left(T_{j,3} - t\right) + \frac{r(t) - \theta_{best,G,j}(t)}{\kappa_{best,G,j}(t)}\left(1 - e^{-\kappa_{best,G,j}(t)}\right), \quad j = 1, \ldots, n. \tag{4.21}$$

Using (4.14) and (4.21), we may predict $\rho_{CIR}(t; T_{j,3}, T_{j+1,3})$ within the time intervals $[T_{j+1,3}, T_{j,3}]$, $j = 1, \ldots, n-1$, using

$$\hat{\rho}_{CIR}(t; T_{j,3}, T_{j+1,3}) = \frac{\hat{\gamma}_{CIR}(t; t, T_{j+1,3}) - \hat{\gamma}_{CIR}(t; t, T_{j,3})}{T_{j+1,3} - T_{j,3}}, \quad j = 1, \ldots, n-1. \tag{4.22}$$

We suggest to use (4.22) to forecast short rates $\left\{r(T_{j,3})\right\}_{j=1}^{n-1}$ at forecast horizons $\left\{T_{j,3} - t\right\}_{j=1}^{n-1}$ for each j, $j = 1, \ldots, n-1$, respectively.

Additionally, based on (4.5), we may calculate

$$F(t;T_{j,3},T_{j+1,3}) = \frac{\log P(t,T_{j,3}) - \log P(t,T_{j+1,3})}{T_{j+1,3}-T_{j,3}}\,, \quad j=1,\ldots,n-1. \tag{4.23}$$

as the forward rates in the intervals $[T_{j,3},T_{j+1,3}]$ respectively.

4.4.3.2 Forecast within the single-curve framework

We construct a separate set of predictors based on a one-factor CIR process in a single-curve framework to compare with the aforementioned set of predictors. They are different from our proposed multi-curve strategy implemented in (4.21) to (4.35). In formulating this set of predictors, we use the estimated CIR model parameters $\{\kappa_{best,G,1}(t),\theta_{best,G,1}(t),\sigma_{best,G,1}(t)\}$ implied from the triplet $\{P(t,T_{1,k})\}_{k=1}^{3}$ corresponding to the shortest available tenors in the set of cross section zero coupon bond prices to model the short rate process and to forecast the short rate at different forecast horizons that may span beyond $T_{1,3}-t$.

Based on (4.12), we construct the single-curve predictor for $\gamma_{CIR}(t;t,T_{j,3})$ at the forecast horizons $\left\{T_{j,3}-t\right\}_{j=1}^{n-1}$ using

$$\hat{\gamma}_{CIR,1}(t;t,T_{j,3}) = \theta_{best,G,1}(t)\left(T_{j,3}-t\right) + \frac{r(t)-\theta_{best,G,1}(t)}{\kappa_{best,G,1}(t)}\left(1-e^{-\kappa_{best,G,1}(t)}\right)\,, \quad j=1,\ldots,n. \tag{4.24}$$

Using (4.14) and (4.24), we construct the single-curve predictor for $\rho_{CIR}(t;T_{j,3},T_{j+1,3})$ for the time intervals $[T_{j+1,3},T_{j,3}]$, $j=1,\ldots,n-1$, as

$$\hat{\rho}_{CIR,1}(t;T_{j,3},T_{j+1,3}) = \frac{\hat{\gamma}_{CIR,1}(t;t,T_{j+1,3}) - \hat{\gamma}_{CIR,1}(t;t,T_{j,3})}{T_{j+1,3}-T_{j,3}}\,, \quad j=1,\ldots,n-1. \tag{4.25}$$

We use (4.25) as a naive predictor of future short rate $\left\{r(T_{j,3})\right\}_{j=1}^{n-1}$ at the forecast horizons $\left\{T_{j,3}-t\right\}_{j=1}^{n-1}$ in the single-curve framework for comparison purpose only.

4.5 Numerical analysis using the historical US STRIPS data and the effective Federal Funds rate

4.5.1 Data description

We use the day-close prices of the US STRIPS zero coupon bonds from Jan. 2nd 2001 to Apr. 28th 2014 for the empirical assessment of our proposed forecast algorithm. This set of historical data is retrieved from the Thomson Reuters Tick History (TRTH) supplied by the Securities Industry Research Centre of Asia-Pacific (SIRCA). The US STRIPS are zero coupon bonds that are created by stripping the Treasury notes and bonds. If so desired, they can be reconstituted to form the original Treasury notes and bonds (see, e.g., Gregory and Livingston, 1992; Grinblatt and Longstaff, 2000). The market for the US STRIPS zero coupons is highly liquid. Additionally, these zero coupons contain negligible credit risk. Specifically, we use the average of the day close bid and ask prices to construct the system of nonlinear equations in order to estimate the implied CIR model parameters.

The historical data of the US effective Federal Funds rate was downloaded from the Board of Governors of the Federal Reserve System and converted to continuously compound convention to be used as proxy for the short rate process to provide input for $r(t)$ in the CIR model.

Our choice of short rate proxy is made on grounds that the credit and the liquidity risk profiles of the effective Federal Funds rate, a weighted average of the uncollateralized overnight borrowing rate for a group of federal funds broker, are comparable to those of the US STRIPS, a highly liquid financial instrument derived from the uncollateralized US Treasuries.

Empirical findings reported by Garfinkel and Thornton (1995) suggest that the effective Federal Funds rate and the daily three-month T-bills rate are cointegrated, and exhibit bidirectional Granger causality at various lags. Anderson (1997), Hall, Anderson and Granger (1992), Rudebusch (1995), and Sarno and Thornton (2003), among others, reported that the effective Federal Funds rate and US Treasury bill (T-bill) rates tend to move together. Additionally, the T-bill rates have been used in some studies to predict the effective Federal Funds rates (see, e.g., Hardouvelis, 1988; Simon, 1990; Roberds, Runkle and Whiteman, 1996; Guidolin and Timmermann, 2009). We envisage that, since the US STRIPS are derived from the US T-bills and T-bonds, this instrument may contain information for the prediction of the effective Federal Funds rate as well.

In Section 4.5.2 and Section 4.5.3, we let $t = t_i, i = 1, \ldots, 3234$, index the date of the cross section day close prices of the US STRIPS for each of the 3,234 trading days between Jan. 2nd 2001 and Apr. 28th 2014 denoted by $\left\{P(t_i, T_{i,j,k})\right\}_{k=1,2,3}$, $i = 1, \ldots, 3234$, $j = 1, \ldots, n_i$, where $T_{i,j,k}$ is the maturity date of the corresponding zero coupon bond that is observed at t_i, and $r(T_{i,j,k})$ is the effective Federal Funds rate on the same day. For each t_i, we construct a system of nonlinear equations using (4.18), and estimate the term structure of CIR model parameters using the numerical strategy described in Section 4.4.2.

In the empirical example data set analysed and reported in this section, the day-close prices of the US STRIPS zero coupon bonds from Jan. 2nd 2001 to Apr. 28th 2014 are used. These zero coupon bonds mature at various different tenors, ranging from less than one year all the way out to 30 years. However, since the most recent historical data of the US effective Federal Funds rate available at the date of study is Apr. 28th 2014, the empirical analysis reported in Section 4.5 can only include US STRIPS zero coupon bonds with tenors spanning approximately 10 years out. Therefore, the results reported herein reflect the performance of the fixed-income instruments, in this case US STRIPS zero coupon bonds, having maturities of more than one year. In fact, they span maturities up to 10 years.

4.5.2 Term structure of implied CIR model parameters

Let the term structure of implied CIR model parameters estimated from the US STRIPS day-close prices from Jan. 2nd 2001 to Apr. 28th 2014 be indexed by their respective observation dates t_i as $\boldsymbol{\kappa}_{best,G}(t_i) = \{\kappa_{best,G,j}(t_i)\}_{j=1}^{n_i}$, $\boldsymbol{\theta}_{best,G}(t_i) = \{\theta_{best,G,j}(t_i)\}_{j=1}^{n_i}$, and $\boldsymbol{\sigma}_{best,G}(t_i) = \{\sigma_{best,G,j}(t_i)\}_{j=1}^{n_i}$. The sets of parameters $(\kappa_{best,G,j}(t_i), \theta_{best,G,j}(t_i), \sigma_{best,G,j}(t_i))$ are regarded as the sets of implied CIR model parameters for the one-factor CIR processes estimated from $\left\{P(t_i, T_{i,j,k})\right\}_{k=1,2,3}$ that span the tenors $\left\{T_{i,j,3} - t_i\right\}_{j=1}^{n_i}$. We group $\boldsymbol{\kappa}_{best,G}(t_i)$, $\boldsymbol{\theta}_{best,G}(t_i)$, and $\boldsymbol{\sigma}_{best,G}(t_i)$ with respect to the tenor ranges they are associated with into 100 intervals of tenors $(\tau_\ell, \tau_{\ell+1}]$, where τ_ℓ is the ℓ-th percentile of tenors in the data for $\ell = 0, \ldots, 99$, and regard these tenor interval specific groups as 'buckets'.

In Figure 11, we depict the term structure of these bucket-specific average CIR model parameters with respect to these 100 intervals. The average estimated implied CIR model parameters exhibit nonlinear relationship with respect to the tenor. This nonlinearity appears to suggest that a one-factor CIR process, driven by one set of CIR model parameters, is inadequate for modelling the entire yield curve because, on average, different subsets of cross-sectional zero coupon bond prices in the form of triplets spanning different tenors

appear to map to different sets of implied CIR model parameters. If a one-factor CIR process is adequate in modelling the entire yield curve, then the implied CIR model parameters estimated from these subsets of zero coupon bond prices should not demonstrate highly nonlinear relationship with respect to tenor as depicted in Figure 11.

Instead, if we work in the multi-curve framework, each segment of the term structure that corresponds to a different tenor is modelled using a different short rate process. As such, we can afford the flexibility of modelling these short rate processes using multiple one-factor CIR processes with different sets of CIR model parameters to capture the features of different segments of the yield curve. We may consider this modelling flexibility an impetus to model the yield curve in a multi-curve framework.

Figure 11 reveals that the values of $\hat{\kappa}$ and $\hat{\theta}$ are high at the short end of the tenor, rapidly decreases until tenor of about one year, then increases until tenor of up to 20 years, and finally decreases again. This "snake shape" profile of the $\hat{\kappa}$ and $\hat{\theta}$ with respect to tenor bears resemblance to the volatility term structure of the Libor and swap rates depicted in Figure 6 of Piazzesi (2005). This is somewhat surprising considering that $\hat{\kappa}$ and $\hat{\theta}$ are inferred from the US STRIP prices and the effective Federal Funds rate, two sets of observable financial state variables that reflect credit and liquidity risk profiles that are different from those of the Libor rates.

Piazzesi (2005) reported higher levels of interest rate volatility at the shorter end of the yield curve. The implication of this empirical finding may be that market participants' tend to have more diverse views on the expectation of future short rate at shorter tenors, and it is possible that, at the shorter end of the yield curve, the sensitivity of expected future short rate with respect to tenor is higher. This may possibly explain, in part, the observation that the sensitivities of $\hat{\kappa}$ and $\hat{\theta}$ with respect to the tenor are higher at shorter tenor in Figure 11.

The bucket-wise standard deviation of $\hat{\kappa}$ and $\hat{\theta}$ are widest at tenor between 1.5 to 2 years, corresponding to the "hump" of the volatility term structure depicted in Figure 6 of Piazzesi (2005), and in Figure 3 of Dai and Singleton (2000). This may reflect the existence of a wider range of $\hat{\kappa}$ and $\hat{\theta}$ across all t_i in order to capture the more diverse views on the expectation of future short rate among market participants. The wide bucket-wise standard deviation of $\hat{\theta}$ may be interpreted as a reflection of the market participants' heterogeneous views of the long-term interest rate. The increasing trend of $\hat{\sigma}$ with respect to tenor may reflect the market participants' perception that interest rate risk tend to increases as tenor increases.

4.5.3 Backtesting the forecast algorithms using historical US STRIPS data and effective Federal Funds rate

4.5.3.1 Short rate prediction in the multi-curve framework

We consider the forecast performance of using $\hat{\rho}_{CIR}(t_i; T_{i,j,3}, T_{i,j+1,3})$, defined in (4.22), to forecast. $r(T_{i,j,3})$, $j = 1, \ldots, n_i - 1$, for each t_i, $i = 1, \ldots, 3234$. Let

$$\text{Error}\left(t_i; r(T_{i,j,3}), \hat{\rho}_{CIR}(t_i; T_{i,j,3}, T_{i,j+1,3})\right) = r(T_{i,j,3}) - \hat{\rho}_{CIR}(t_i; T_{i,j,3}, T_{i,j+1,3}) \ , \quad j = 1, \ldots, n_i - 1, \tag{4.26}$$

be the differences between the realized short rates, $r(T_{i,j,3})$, and the predicted short rates, $\hat{\rho}_{CIR}(t_i; T_{i,j,3}, T_{i,j+1,3})$. Additionally, let

$$\text{Error}\left(t_i; r(T_{i,j,3}), F(t_i; T_{i,j,3}, T_{i,j+1,3})\right) = r(T_{i,j,3}) - F(t_i; T_{i,j,3}, T_{i,j+1,3}) \ , \quad j = 1, \ldots, n_i - 1, \tag{4.27}$$

be the differences between the $r(T_{i,j,3})$ and the forward rates, $F(t_i; T_{i,j,3}, T_{i,j+1,3})$, at forecast horizons $\left\{T_{i,j,3} - t_i\right\}_{j=1}^{n-1}$. Following Duffee (2002), and Diebold and Li (2006), among others, we use the random walk as a benchmark to evaluate the short rate forecast accuracy where the short rate $r(t_i)$ is used as the forecast of the future short rate at the forecast horizon. Let

$$\text{Error}\left(t_i; r(T_{i,j,3}), RW\right) = r(T_{i,j,3}) - r(t_i) \ , \quad j = 1, \ldots, n_i - 1, \tag{4.28}$$

be the differences between the realized short rates, $r(T_{i,j,3})$, and the random walk prediction of future short rate, which is simply $r(t_i)$, at forecast horizons $\left\{T_{i,j,3} - t_i\right\}_{j=1}^{n-1}$. The random walk benchmark is known to be a tough benchmark to match, and it is known to perform better than the one-factor affine term structure models in the single-curve framework in some studies (see, e.g., Duffee, 2002).

We group the results evaluated using (4.26) and (4.27) into 100 non-overlapping intervals, or 'buckets', with respect to the forecast horizon similar to the grouping of estimated implied CIR parameters in Section 4.5.2. Specifically, we choose 100 intervals of forecast horizons $(\tau_\ell, \tau_{\ell+1}]$, where τ_ℓ is the ℓ-th percentile of the set of forecast horizons denoted by $\left\{T_{i,j,3} - t_i, i = 1, \ldots, 3234, j = 1, \ldots, n_i - 1\right\}$ and $\ell = 0, \ldots, 99$. For each $(\tau_\ell, \tau_{\ell+1}]$, we compute the forecast horizons interval specific, i.e., bucket-specific, root mean squared

error (RMSE) for $\hat{\rho}_{CIR}(t_i; T_{i,j,3}, T_{i,j+1,3})$

$$\text{RMSE}_\ell\left(\hat{\rho}_{CIR}\right) = \left\{\frac{1}{n_\ell}\sum_{i=1}^{3234}\sum_{j}^{n_i}\mathbf{1}_{\tau_\ell < T_{i,j,3}-t_i \leq \tau_{\ell+1}}\ \text{Error}\left(t_i; r(T_{i,j,3}), \hat{\rho}_{CIR}(t_i; T_{i,j,3}, T_{i,j+1,3})\right)^2\right\}^{1/2}, \tag{4.29}$$

for $F(t_i; T_{i,j,3}, T_{i,j+1,3})$

$$\text{RMSE}_\ell\left(F\right) = \left\{\frac{1}{n_\ell}\sum_{i=1}^{3234}\sum_{j}^{n_i}\mathbf{1}_{\tau_\ell < T_{i,j,3}-t_i \leq \tau_{\ell+1}}\ \text{Error}\left(t_i; r(T_{i,j,3}), F(t_i; T_{i,j,3}, T_{i,j+1,3})\right)^2\right\}^{1/2}, \tag{4.30}$$

and for the random walk benchmark

$$\text{RMSE}_\ell\left(RW\right) = \left\{\frac{1}{n_\ell}\sum_{i=1}^{3234}\sum_{j}^{n_i}\mathbf{1}_{\tau_\ell < T_{i,j,3}-t_i \leq \tau_{\ell+1}}\ \text{Error}\left(t_i; r(T_{i,j,3}), RW\right)^2\right\}^{1/2}. \tag{4.31}$$

We also compute the bucket-specific mean absolute error (MAE) for $\hat{\rho}_{CIR}(t_i; T_{i,j,3}, T_{i,j+1,3})$

$$\text{MAE}_\ell\left(\hat{\rho}_{CIR}\right) = \frac{1}{n_\ell}\sum_{i=1}^{3234}\sum_{j}^{n_i}\mathbf{1}_{\tau_\ell < T_{i,j,3}-t_i \leq \tau_{\ell+1}}\ \left|\text{Error}\left(t_i; r(T_{i,j,3}), \hat{\rho}_{CIR}(t_i; T_{i,j,3}, T_{i,j+1,3})\right)\right|, \tag{4.32}$$

for $F(t_i; T_{i,j,3}, T_{i,j+1,3})$

$$\text{MAE}_\ell\left(F\right) = \frac{1}{n_\ell}\sum_{i=1}^{3234}\sum_{j}^{n_i}\mathbf{1}_{\tau_\ell < T_{i,j,3}-t_i \leq \tau_{\ell+1}}\ \left|\text{Error}\left(t_i; r(T_{i,j,3}), F(t_i; T_{i,j,3}, T_{i,j+1,3})\right)\right|, \tag{4.33}$$

and for the random walk benchmark

$$\text{MAE}_\ell\left(RW\right) = \frac{1}{n_\ell}\sum_{i=1}^{3234}\sum_{j}^{n_i}\mathbf{1}_{\tau_\ell < T_{i,j,3}-t_i \leq \tau_{\ell+1}}\ \left|\text{Error}\left(t_i; r(T_{i,j,3}), RW\right)\right|, \tag{4.34}$$

where $n_\ell = \sum_{i=1}^{3234}\sum_{j}^{n_i}\mathbf{1}_{\tau_\ell < T_{i,j,3}-t_i \leq \tau_{\ell+1}}$, and $\mathbf{1}$ is the indicator function. For this set of data, $\min\left(\{n_\ell\}_{\ell=0}^{99}\right) = 449$, $\max\left(\{n_\ell\}_{\ell=0}^{99}\right) = 584$, and $\sum_{\ell=0}^{99} n_\ell = 20963$.

We depict, in Panels A and B of Figure 12, $\text{RMSE}_\ell\left(\hat{\rho}_{CIR}\right)$, $\text{RMSE}_\ell\left(F\right)$, $\text{RMSE}_\ell\left(RW\right)$, $\text{MAE}_\ell\left(\hat{\rho}_{CIR}\right)$, $\text{MAE}_\ell\left(F\right)$ and $\text{MAE}_\ell\left(RW\right)$ for the prediction of $r(T_{i,j,3})$. Both the predictors $\hat{\rho}_{CIR}(t_i; T_{i,j,3}, T_{i,j+1,3})$ and $F(t_i; T_{i,j,3}, T_{i,j+1,3})$ appear to be reasonably good predictors of future short rate up to a forecast horizon of one year (Panel B, Figure 12). However, progressive deterioration of the forecasting performance becomes noticeable beyond a forecast horizon of one year, possibly due to factors such as the effect of term premium

on forecasting ability of both $\hat{\rho}_{CIR}(t_i; T_{i,j,3}, T_{i,j+1,3})$ and $F(t_i; T_{i,j,3}, T_{i,j+1,3})$. This observation bears resemblance to the findings reported by Fama (1976) and Longstaff (2000). Additionally, the corresponding ℓ-interval specific MSE and MAE for the random walk are depicted in Figure 12 for comparison.

The values of the forecast horizon interval specific RMSE and MAE for the multi-curve predictor $\hat{\rho}_{CIR}(t_i; T_{i,j,3}, T_{i,j+1,3})$ and the forward rate $F(t_i; T_{i,j,3}, T_{i,j+1,3})$ for the corresponding tenors are comparable up to forecast horizons of 2 years, beyond which those of $\hat{\rho}_{CIR}(t_i; T_{i,j,3}, T_{i,j+1,3})$ become noticeably larger than those of $F(t_i; T_{i,j,3}, T_{i,j+1,3})$ (Figure 12). We briefly analyse the relationship between $\text{RMSE}_\ell\,(\hat{\rho}_{CIR})$ and $\text{RMSE}_\ell\,(F)$, and that between $\text{MAE}_\ell\,(\hat{\rho}_{CIR})$ and $\text{MAE}_\ell\,(F)$.

Based on (4.22) and $F(t_i; T_{i,j,3}, T_{i,j+1,3})$, the estimated average variance of the integrated CIR process within the time interval $[T_{i,j,3}, T_{i,j+1,3}]$ can be expressed as

$$\begin{aligned}\hat{\Delta}_{CIR}(t_i; T_{i,j,3}, T_{i,j+1,3}) &= 2\left(\hat{\rho}_{CIR}(t_i; T_{i,j,3}, T_{i,j+1,3}) - F(t_i; T_{i,j,3}, T_{i,j+1,3})\right) \\ &\approx \frac{\hat{\delta}_{CIR}(t_i; T_{i,j,3}, T_{i,j+1,3})}{T_{i,j+1,3} - T_{i,j,3}}\,, \end{aligned} \tag{4.35}$$

where

$$\hat{\delta}_{CIR}(t_i; T_{i,j,3}, T_{i,j+1,3}) = \widehat{\text{Var}}_{CIR}\left[\int_{t_i}^{T_{i,j+1,3}} r_{CIR}(u)du \,\middle|\, \mathscr{F}_{t_i}\right] - \widehat{\text{Var}}_{CIR}\left[\int_{t_i}^{T_{i,j,3}} r_{CIR}(u)du \,\middle|\, \mathscr{F}_{t_i}\right]\,,$$

and where $\widehat{\text{Var}}_{CIR}(\cdot)$ represents the variance of the integrated short rate within the multi-curve construct where the short rate process $r_{CIR}(u)$ in the time interval $[T_{i,j,3}, T_{i,j+1,3}]$ is associated with the one-factor CIR processed modelled using the estimated implied parameters $\theta_{best,G,j}(t_i)$, $\kappa_{best,G,j}(t_i)$, and $\sigma_{best,G,j}(t_i)$. From (4.35), we obtain

$$\begin{aligned}\frac{1}{2}\hat{\Delta}_{CIR}(t_i; T_{i,j,3}, T_{i,j+1,3}) &= \hat{\rho}_{CIR}(t_i; T_{i,j,3}, T_{i,j+1,3}) - F(t_i; T_{i,j,3}, T_{i,j+1,3}) \\ &= \left(\hat{\rho}_{CIR}(t_i; T_{i,j,3}, T_{i,j+1,3}) - r(T_{i,j,3})\right) - \left(F(t_i; T_{i,j,3}, T_{i,j+1,3}) - r(T_{i,j,3})\right) \\ &= \text{Error}\left(t_i; r(T_{i,j,3}), \hat{\rho}_{CIR}(t_i; T_{i,j,3}, T_{i,j+1,3})\right) - \text{Error}\left(t_i; r(T_{i,j,3}), F(t_i; T_{i,j,3}, T_{i,j+1,3})\right) \\ &\approx \frac{\hat{\delta}_{CIR}(t_i; T_{i,j,3}, T_{i,j+1,3})}{2(T_{i,j+1,3} - T_{i,j,3})}\,. \end{aligned} \tag{4.36}$$

Taking squares on both sides of

$$\begin{aligned}\text{Error}\left(t_i; r(T_{i,j,3}), \hat{\rho}_{CIR}(t_i; T_{i,j,3}, T_{i,j+1,3})\right) \approx \text{Error}\left(t_i; r(T_{i,j,3}), F(t_i; T_{i,j,3}, T_{i,j+1,3})\right) \\ + \frac{\hat{\delta}_{CIR}(t_i; T_{i,j,3}, T_{i,j+1,3})}{2(T_{i,j+1,3} - T_{i,j,3})} ,\end{aligned}$$

then multiply both sides by $\mathbf{1}_{\tau_\ell < T_{i,j,3} - t_i \leq \tau_{\ell+1}}$ and sum across $i, i = 1, \ldots, 3234$, and $j, j = 1, \ldots, n_i$, and finally divide both sides by n_ℓ before rearranging, we obtain

$$\begin{aligned}&\text{RMSE}_\ell\left(\hat{\rho}_{CIR}\right)^2 - \text{RMSE}_\ell\left(F\right)^2 \\ &\approx \frac{1}{n_\ell}\sum_{i=1}^{3234}\sum_{j}^{n_i} \mathbf{1}_{\tau_\ell < T_{i,j,3} - t_i \leq \tau_{\ell+1}} \text{Error}\left(t_i; r(T_{i,j,3}), F(t_i; T_{i,j,3}, T_{i,j+1,3})\right) \frac{\hat{\delta}(t_i; T_{i,j,3}, T_{i,j+1,3})}{T_{i,j+1,3} - T_{i,j,3}} \\ &+ \frac{1}{n_\ell}\sum_{i=1}^{3234}\sum_{j}^{n_i} \mathbf{1}_{\tau_\ell < T_{i,j,3} - t_i \leq \tau_{\ell+1}} \left(\frac{\hat{\delta}(t_i; T_{i,j,3}, T_{i,j+1,3})}{2\left(T_{i,j+1,3} - T_{i,j,3}\right)}\right)^2 . \qquad (4.37)\end{aligned}$$

Since $\hat{\delta}(t_i; T_{i,j,3}, T_{i,j+1,3}) > 0$, the sign of $\text{RMSE}_\ell\left(\hat{\rho}_{CIR}\right)^2 - \text{RMSE}_\ell\left(F\right)^2$ depends on the sign and magnitude of $\text{Error}\left(t_i; r(T_{i,j,3}), F(t_i; T_{i,j,3}, T_{i,j+1,3})\right)$. Panel A of Figure 12 depicts that there appears to be a progressively increasing trend of $\text{RMSE}_\ell\left(\hat{\rho}_{CIR}\right) - \text{RMSE}_\ell\left(F\right)$ along the forecast horizons.

Let $\mathscr{R}\left(P(t_i, T_{i,j,3}), P(t_i, T_{i,j+1,3})\right)$ represents the collection of all the higher order terms in the exponential expansions of $P(t_i, T_{i,j,3})$ and $P(t_i, T_{i,j+1,3})$ and the higher order terms in the logarithmic expansions of $\log P(t_i, T_{i,j,3})$ and $\log P(t_i, T_{i,j+1,3})$ which we disregard in obtaining the approximation of (4.35) following the derivation of (4.8). From (4.8) and (4.35), we obtain

$$\begin{aligned}&\hat{\rho}_{CIR}(t_i; T_{i,j,3}, T_{i,j+1,3}) - F(t_i; T_{i,j,3}, T_{i,j+1,3}) \\ &= \left(\hat{\rho}_{CIR}(t_i; T_{i,j,3}, T_{i,j+1,3}) - r(T_{i,j,3})\right) - \left(F(t_i; T_{i,j,3}, T_{i,j+1,3}) - r(T_{i,j,3})\right) \\ &= \frac{\hat{\delta}_{CIR}(t_i; T_{i,j,3}, T_{i,j+1,3})}{2(T_{i,j+1,3} - T_{i,j,3})} + \mathscr{R}\left(P(t_i, T_{i,j,3}), P(t_i, T_{i,j+1,3})\right) . \qquad (4.38)\end{aligned}$$

Since

$$\begin{aligned}&\left| \frac{\hat{\delta}_{CIR}(t_i; T_{i,j,3}, T_{i,j+1,3})}{2(T_{i,j+1,3} - T_{i,j,3})} + \mathscr{R}\left(P(t_i, T_{i,j,3}), P(t_i, T_{i,j+1,3})\right) + \left(F(t_i; T_{i,j,3}, T_{i,j+1,3}) - r(T_{i,j,3})\right) \right| \\ \leq &\left| \frac{\hat{\delta}_{CIR}(t_i; T_{i,j,3}, T_{i,j+1,3})}{2(T_{i,j+1,3} - T_{i,j,3})} \right| + \left| \mathscr{R}\left(P(t_i, T_{i,j,3}), P(t_i, T_{i,j+1,3})\right) \right| + \left| \left(F(t_i; T_{i,j,3}, T_{i,j+1,3}) - r(T_{i,j,3})\right) \right| ,\end{aligned}$$

we obtain

$$\begin{aligned}
&\left| \hat{\rho}_{CIR}(t_i; T_{i,j,3}, T_{i,j+1,3}) - r(T_{i,j,3}) \right| - \left| \left(F(t_i; T_{i,j,3}, T_{i,j+1,3}) - r(T_{i,j,3}) \right) \right| \\
\leq &\left| \frac{\hat{\delta}_{CIR}(t_i; T_{i,j,3}, T_{i,j+1,3})}{2(T_{i,j+1,3} - T_{i,j,3})} \right| + \left| \mathscr{R}\left(P(t_i, T_{i,j,3}), P(t_i, T_{i,j+1,3}) \right) \right| . \qquad (4.39)
\end{aligned}$$

Multiply both sides of (4.39) by $\mathbf{1}_{\tau_\ell < T_{i,j,3} - t_i \leq \tau_{\ell+1}}$ and sum across $i, i = 1, \ldots, 3234$, and $j, j = 1, \ldots, n_i$, and finally divide both sides by n_ℓ before using (4.32) and (4.33), we obtain

$$\begin{aligned}
&\mathrm{MAE}_\ell(\hat{\rho}_{CIR}) - \mathrm{MAE}_\ell(F) \\
&\leq \frac{1}{n_\ell} \sum_{i=1}^{3234} \sum_{j}^{n_i} \mathbf{1}_{\tau_\ell < T_{i,j,3} - t_i \leq \tau_{\ell+1}} \left| \frac{\hat{\delta}_{CIR}(t_i; T_{i,j,3}, T_{i,j+1,3})}{2(T_{i,j+1,3} - T_{i,j,3})} \right| \\
&+ \frac{1}{n_\ell} \sum_{i=1}^{3234} \sum_{j}^{n_i} \mathbf{1}_{\tau_\ell < T_{i,j,3} - t_i \leq \tau_{\ell+1}} \left| \mathscr{R}\left(P(t_i, T_{i,j,3}), P(t_i, T_{i,j+1,3}) \right) \right| . \qquad (4.40)
\end{aligned}$$

Additionally, we calculate the interval specific Theil's inequality coefficient U (Theil, 1966; Bliemel, 1973) to assess the forecast performance of the two predictors of future short rate considered for each interval $(\tau_\ell, \tau_{\ell+1}], \ell = 0, \ldots, 99$. The Theil's U is bounded between zero and one. The nearer the Theil's U statistic is to zero, the better the forecast performance. Let

$$\mathrm{U}_\ell\left(\hat{\rho}_{CIR}\right) = \frac{\mathrm{RMSE}_\ell\left(\hat{\rho}_{CIR}\right)}{\mathrm{RMSS}_\ell\left(\hat{\rho}_{CIR}\right) + \mathrm{RMSS}_\ell\left(r(T_{i,j,3})\right)} \qquad (4.41)$$

be the interval specific Theil's U for $\hat{\rho}_{CIR}(t_i; T_{i,j,3}, T_{i,j+1,3})$ where $\mathrm{RMSE}_\ell\left(\hat{\rho}_{CIR}\right)$ is defined in (4.29),

$$\mathrm{RMSS}_\ell\left(\hat{\rho}_{CIR}\right) = \left\{ \frac{1}{n_\ell} \sum_{i=1}^{3234} \sum_{j}^{n_i} \mathbf{1}_{\tau_\ell < T_{i,j,3} - t_i \leq \tau_{\ell+1}} \, \hat{\rho}_{CIR}(t_i; T_{i,j,3}, T_{i,j+1,3})^2 \right\}^{1/2} ,$$

and

$$\mathrm{RMSS}_\ell\left(r(T_{i,j,3})\right) = \left\{ \frac{1}{n_\ell} \sum_{i=1}^{3234} \sum_{j}^{n_i} \mathbf{1}_{\tau_\ell < T_{i,j,3} - t_i \leq \tau_{\ell+1}} \, r(T_{i,j,3})^2 \right\}^{1/2} .$$

Let

$$\mathrm{U}_\ell\left(F\right) = \frac{\mathrm{RMSE}_\ell\left(F\right)}{\mathrm{RMSS}_\ell\left(F\right) + \mathrm{RMSS}_\ell\left(r(T_{i,j,3})\right)} \qquad (4.42)$$

be the interval specific Theil's U for $F(t_i; T_{i,j,3}, T_{i,j+1,3})$ where $\mathrm{RMSE}_\ell(F)$ is defined in (4.30), and

$$\mathrm{RMSS}_\ell(F) = \left\{ \frac{1}{n_\ell} \sum_{i=1}^{3234} \sum_{j}^{n_i} \mathbf{1}_{\tau_\ell < T_{i,j,3} - t_i \le \tau_{\ell+1}} \; F(t_i; T_{i,j,3}, T_{i,j+1,3})^2 \right\}^{1/2} .$$

Let

$$\mathrm{U}_\ell(RW) = \frac{\mathrm{RMSE}_\ell(RW)}{\mathrm{RMSS}_\ell(RW) + \mathrm{RMSS}_\ell\left(r(T_{i,j,3})\right)} , \tag{4.43}$$

be the interval specific Theil's U for the random walk benchmark where $\mathrm{RMSE}_\ell(RW)$ is defined in (4.31), and

$$\mathrm{RMSS}_\ell(RW) = \left\{ \frac{1}{n_\ell} \sum_{i=1}^{3234} \sum_{j}^{n_i} \mathbf{1}_{\tau_\ell < T_{i,j,3} - t_i \le \tau_{\ell+1}} \; r(t_i)^2 \right\}^{1/2} .$$

We depict, in Figure 13, $\mathrm{U}_\ell(\hat{\rho}_{CIR})$, $\mathrm{U}_\ell(F)$, and $\mathrm{U}_\ell(RW)$ with respect to different forecast horizons $(\tau_\ell, \tau_{\ell+1}]$, $\ell = 0, \ldots, 99$. Both of them show an increasing trend with respect to the forecast horizon, indicating that the forecasting performance is better at shorter forecast horizon. In particular, the values of $\mathrm{U}_\ell(\hat{\rho}_{CIR})$ and $\mathrm{U}_\ell(F)$, are approximately 0.4 or less when the forecast horizons are less than one year, implying that both $\hat{\rho}_{CIR}(t_i; T_{i,j,3}, T_{i,j+1,3})$ and $F(t_i; T_{i,j,3}, T_{i,j+1,3})$ may forecast the future effective Federal Funds rate with higher accuracy up to two year ahead that beyond. This is in keeping with the trend depicted in Figure 12.

We depict in Table 17 the forecast horizon specific performance of $\hat{\rho}_{CIR}(t_i; T_{i,j,3}, T_{i,j+1,3})$, the predictor for the multi-curve framework, and $F(t_i; T_{i,j,3}, T_{i,j+1,3})$, the forward rate for each interval $(\tau_\ell, \tau_{\ell+1}]$, $\ell = 0, \ldots, 99$, and, for comparison, $\hat{\rho}_{CIR,1}(t_i; T_{i,j,3}, T_{i,j+1,3})$, the predictor for the single-curve framework. Duffee (2002) has remarked that the random walk is a tough benchmark for the standard class of affine models to beat. The forward rate in general performs less favourably against the random walk. The predictor for the multi-curve framework $\hat{\rho}_{CIR}(t_i; T_{i,j,3}, T_{i,j+1,3})$ performs marginally better than the random walk at forecast horizons of 0.8 to 1.6 years, but not for forecast horizons shorter than 0.4 years and longer than 1.6 years.

The effective Federal Funds rates are weighted average of the overnight borrowing rates for federal funds brokers guided by the target Federal Funds rates set by the Federal Open Market Committee (FOMC) that meet eight times a year, and whenever necessary. There is a tendency for the effective Federal Funds rates to oscillate around the target

Federal Funds rates. It is possible that at forecast horizons shorter than 0.4 years, the mean reverting nature of the effective Federal Funds at such short time interval may, for this data sample, may, in general, behave like random walk due to the oscillatory nature of the effective Federal Funds rate.

The RMSE and MAE for both $\hat{\rho}_{CIR}(t_i; T_{i,j,3}, T_{i,j+1,3})$ and $F(t_i; T_{i,j,3}, T_{i,j+1,3})$ increase along the forecast horizon, as depicted in Figure 12. We envisage that the forecast performance deterioration at horizons beyond two year is the result of, among other factors, the noticeable effect of the term premium.

Other factors may affect the forecast performance of $\hat{\rho}_{CIR}(t_i; T_{i,j,3}, T_{i,j+1,3})$. The forecast performance assessment of $\hat{\rho}_{CIR}(t_i; T_{i,j,3}, T_{i,j+1,3})$ is a joint test of whether $\rho_{CIR}(t_i; T_{i,j,3}, T_{i,j+1,3})$ is a good predictor of the future short rate, and whether $\hat{\rho}_{CIR}(t_i; T_{i,j,3}, T_{i,j+1,3})$ is a good estimator of $\rho_{CIR}(t_i; T_{i,j,3}, T_{i,j+1,3})$. The former is affected by the model specification risk, the latter by the model estimation risk.

Model specification risk arise as $\rho_{CIR}(t_i; T_{i,j,3}, T_{i,j+1,3})$ is a model-based predictor. While the extant literature suggests that the drift and diffusion coefficients of the short rate process may not be linear (see, e.g., Aït-Sahalia, 1996b; Stanton, 1997; Jones, 2003; Chapman and Pearson, 2000), the one-factor CIR process is nonetheless a relatively good approximation if the short rate process being modelled lies within the range between 0 and 0.09 (Aït-Sahalia, 1996b). The time series of effective Federal Funds rate, our short rate proxy, for the period we consider lies within this boundary. While this lends support to our choice of using CIR process to model this short rate dynamics, the CIR model is nonetheless only an approximate working model.

Model estimation risk arise as $\hat{\rho}_{CIR}(t_i; T_{i,j,3}, T_{i,j+1,3})$ is evaluated using the implied CIR model parameters estimated based on zero coupon bond prices as approximate solutions to a system of nonlinear equations (4.18), thus incurring some uncertainty in the point estimation of $\rho_{CIR,1}(t_i; T_{i,j,3}, T_{i,j+1,3})$. That said, the model estimation risk is an issue faced by all parametric models constructed to model the short rate dynamics due to the necessity for numerical estimation of the model parameters.

4.5.3.2 Short rate prediction in the single-curve framework

The objective of using $\hat{\rho}_{CIR,1}(t_i; T_{i,j,3}, T_{i,j+1,3})$, as a naive one-factor CIR model-based predictor constructed in the single-curve framework to predict $r(T_{i,j,3})$, the future short rate at various forecasting horizons, is to perform a simple comparison between the forecast

performance of the one-factor CIR model-based short rate predictor implemented in the multi-curve framework and that implemented in the single-curve framework.

The evaluation of $\hat{\rho}_{CIR,1}(t_i; T_{i,j,3}, T_{i,j+1,3})$ at each t_i, $i = 1, \ldots, 3234$, is based on the set of implied CIR model parameters $(\kappa_{best,G,1}(t_i), \theta_{best,G,1}(t_i), \sigma_{best,G,1}(t_i))$ inferred from $\{P(t_i, T_{i,1,k})\}_{k=1,2,3}$. Let

$$\text{Error}\left(t_i; r(T_{i,j,3}), \hat{\rho}_{CIR,1}(t_i; T_{i,j,3}, T_{i,j+1,3})\right) = r(T_{i,j,3}) - \hat{\rho}_{CIR,1}(t_i; T_{i,j,3}, T_{i,j+1,3}) \ , \quad j = 1, \ldots, n_i - 1. \tag{4.44}$$

be the differences between the realized short rates, $r(T_{i,j,3})$, and the predicted short rates $\hat{\rho}_{CIR,1}(t_i; T_{i,j,3}, T_{i,j+1,3})$ at forecast horizons $\left\{T_{i,j,3} - t_i\right\}_{j=1}^{n-1}$.

Following the results reporting approach used in Sections 4.5.2, and 4.5.3.1, we group the results evaluated using (4.44) into 100 intervals of forecast horizons $(\tau_\ell, \tau_{\ell+1}]$, where τ_ℓ is the ℓ-th percentiles of the set of forecast horizons $\left\{T_{i,j,3} - t_i\right\}_{i=1,\ldots,3234,\, j=1,\ldots,n_i-1}$, and where $\ell = 0, \ldots, 99$. For each $(\tau_\ell, \tau_{\ell+1}]$, we use (4.26) to compute the forecast horizons interval specific RMSE

$$\text{RMSE}_\ell\left(\hat{\rho}_{CIR,1}\right) = \left\{\frac{1}{n_\ell}\sum_{i=1}^{3234}\sum_{j}^{n_i} \mathbf{1}_{\tau_\ell < T_{i,j,3} - t_i \le \tau_{\ell+1}} \text{Error}\left(t_i; r(T_{i,j,3}), \hat{\rho}_{CIR,1}(t_i; T_{i,j,3}, T_{i,j+1,3})\right)^2\right\}^{1/2} \tag{4.45}$$

and MAE

$$\text{MAE}_\ell\left(\hat{\rho}_{CIR,1}\right) = \frac{1}{n_\ell}\sum_{i=1}^{3234}\sum_{j}^{n_i} \mathbf{1}_{\tau_\ell < T_{i,j,3} - t_i \le \tau_{\ell+1}} \left| \text{Error}\left(t_i; r(T_{i,j,3}), \hat{\rho}_{CIR,1}(t_i; T_{i,j,3}, T_{i,j+1,3})\right) \right| . \tag{4.46}$$

We also calculate the interval specific Theil's U for $\hat{\rho}_{CIR,1}(t_i; T_{i,j,3}, T_{i,j+1,3})$ as

$$\text{U}_\ell\left(\hat{\rho}_{CIR,1}\right) = \frac{\text{RMSE}_\ell\left(\hat{\rho}_{CIR,1}\right)}{\text{RMSS}_\ell\left(\hat{\rho}_{CIR,1}\right) + \text{RMSS}_\ell\left(r(T_{i,j,3})\right)} , \tag{4.47}$$

where $\text{RMSE}_\ell\left(\hat{\rho}_{CIR,1}\right)$ is defined in (4.45), and

$$\text{RMSS}_\ell\left(\hat{\rho}_{CIR,1}\right) = \left\{\frac{1}{n_\ell}\sum_{i=1}^{3234}\sum_{j}^{n_i} \mathbf{1}_{\tau_\ell < T_{i,j,3} - t_i \le \tau_{\ell+1}} \left(\hat{\rho}_{CIR,1}(t_i; T_{i,j,3}, T_{i,j+1,3})\right)^2\right\}^{1/2} .$$

Figure 12 and Table 17 indicate that the forecast performance of $\hat{\rho}_{CIR,1}(t_i; T_{i,j,3}, T_{i,j+1,3})$ is inferior to $\hat{\rho}_{CIR}(t_i; T_{i,j,3}, T_{i,j+1,3})$, $F(t_i; T_{i,j,3}, T_{i,j+1,3})$, and the random walk. Figure 13 depict $\text{U}_\ell\left(\hat{\rho}_{CIR,1}\right)$ for different forecast horizons $(\tau_\ell, \tau_{\ell+1}], \ell = 0, \ldots, 99$. The values of

$\mathrm{U}_\ell\left(\hat{\rho}_{CIR,1}\right)$ are higher than $\mathrm{U}_\ell\left(\hat{\rho}_{CIR}\right)$ and $\mathrm{U}_\ell\left(F\right)$, implying that the forecast performance of $\mathrm{U}_\ell\left(\hat{\rho}_{CIR,1}\right)$ is inferior to $\hat{\rho}_{CIR,1}(t_i; T_{i,j,3}, T_{i,j+1,3})$ and $F(t_i; T_{i,j,3}, T_{i,j+1,3})$ for different forecast horizons.

This comparison verifies the weak forecast performance of one-factor CIR model implemented in a single-curve framework. However, the forecast performance of one-factor CIR model implemented can be improved if it is implemented in a multi-curve framework instead.

4.6 Discussion

In this chapter, we have proposed a strategy to forecast future short rate in the multi-curve framework. We partition the yield curve into segments under the assumption that each segment of the yield curve may be modelled using a separate short rate process. Using the simple one-factor CIR model as a working model, we map each adjacent non-overlapping triplets of zero coupon bond prices arranged in increasing tenor to their respective sets of implied CIR model parameters. We then use these implied parameters to perform short rate forecast.

Our empirical forecast performance assessment involves implementing one-factor CIR model in a multi-curve framework to extract information contained in the US STRIPS prices and use this information to forecast the effective Federal Funds rate. At forecast horizons shorter than 0.4 years, its performance cannot surpass that of the random walk. At forecast horizons longer than 1.6 years, term risk premium, among other factors, leads to progressive deterioration of its forecast performance. That said, the forecast performance of one-factor CIR model implemented in a multi-curve framework is superior to that of one-factor CIR model implemented in a single-curve framework. These empirical findings addressed, to some extent, the motivation of this study as outlined in Section 4.2.

Firstly, it appears to be feasible to construct short rate forecast strategy in the multi-curve framework. In fact, by implementing a simple working model in the likes of one-factor CIR model in a multi-curve framework improves its forecast performance compared to its implementation in a single-curve framework.

Secondly, it appears that, regardless whether the forecast strategy is implemented in multi-curve or single-curve framework, the term risk premium will compromise the forecast accuracy; the further the forecast horizon, the more noticeable the effect.

Chapter 5

Conclusion

In Chapter 2, we investigated the issue of implied volatility calibration sensitivity with respect to discount rate uncertainty via the mathematical framework of seeking an approximate solution to an under-defined system of nonlinear equations. Therein, we used an *ex post* realized interest rate fluctuation range in order to construct realistic empirical interest rate fluctuation ranges for the context of the empirical analysis of the historical S&P500 index European vanilla call option prices reported in Chapter 2. Using this framework as a basis, we see several potential prospects for future research.

Firstly, we may utilize the multi-curve-based short rate forecast techniques proposed in Chapter 4 to construct plausible future interest rate fluctuation intervals, and use these discount rate uncertainty intervals to obtain the corresponding implied volatility estimation uncertainty intervals. The interesting aspect about this potential line of research is that both the future interest rate uncertainty intervals and the implied volatility estimation uncertainties are extracted from cross-sectional data of option prices and zero-coupon bond prices, thereby completely consistent with the risk-neutral probability measure.

Secondly, for the context of risk management, we may utilize time series-based models to forecast future interest rates to construct the plausible future discount rate uncertainty intervals, and, based on these uncertainty intervals, infer the corresponding implied volatility uncertainty intervals that may be used to calculate risk management metrics such as the value at risk, and the expected shortfall, among many others.

Thirdly, one may invert the perspective of the framework used in Chapter 2 where the forecast of the future implied volatility uncertainty may be carried out using factor-based models such that techniques proposed in Fengler et al. (2007), among others, so that we

may first construct implied volatility uncertainty intervals. Then, based on these intervals, we may infer, instead, discount rate uncertainty interval based on these implied volatility uncertainty intervals. Albeit this approach may cast some light on the potential range of discount rates adopted by the market participants' on pricing and trading of equity- or index-linked European vanilla options, further work remained to be done in formalizing its econometric inferential framework.

In Chapter 3, we proposed a strategy to estimate the implied discount rates and implied volatilities from a set of option prices as an approximate solution to an over-defined system of nonlinear equations. The spread between the impled discount rates and the contemporaneously quoted, virtually risk free, OIS rates appears to be comparable to the magnitude of the CDS spread of US firms with an average Moody's and S&P credit ratings between BBB and BB. Using this framework as a basis, we see several potential future research directions.

Firstly, the computational acceleration gained from the implementation of Zhang-Sanderson's differential evolution global optimization algorithm on a high-performance computing framework opens the prospect of relaxing the need for *a priori* risk free rate specification in the existing option pricing formulae as reviewed in Section 1.1. From a numerical perspective, it amounts to introducing one extra parameter in the optimization algorithm. From an econometric point of view, it opens the door for comparison and analysis of implied discount rates inferred from the same set of option prices using different option pricing models, and may contribute towards the strand of literature on mode risk assessment.

Secondly, extensions of the strategy proposed in Chapter 3 may be undertaken such as to cater for call options and put options, and to utilize option prices that are sampled between shorter time intervals to investigate high-frequency characteristics of the market participants' aggregate choice of discount rates.

Thirdly, the strategy proposed in Chapter 3 may be used as an information extraction tool to simultaneously infer the implied volatility surface and the implied discount rate term structures. It would be of interest, from an econometric perspective, to infer the state price density profiles from this joint inference framework, and compare with the state price density profiles constructed from the same set of option prices using the classical approach (see, e.g., Aït-Sahalia and Lo, 1998; Aït-Sahalia and Duarte, 2003; Birke and Pilz, 2009; Constantinides et al., 2011) and analyse the potential reasons leading to the similarities and dissimilarities.

In Chapter 4, we propose a strategy to extract the information on the market participants' aggregate expectation of the future short rate from a cross-sectional set of day-close zero coupon bond prices, to represent this information in the form of implied CIR model parameters in the multi-curve framework, and to use this information to forecast the future short rate. For the dataset used in the empirical analysis reported in Section 4.4.1, the forecast performance of one-factor CIR model implemented in a multi-curve framework appears to be substantially better than the one-factor CIR model implemented in the classical single-curve framework such that, for forecast horizons of 0.8 and 1.6 years, they perform better than the random walk, a considerably difficult benchmark for term structure models to beat. Using this framework as a basis, we see several potential research directions.

Firstly, interest rate forecast using the multi-curve interest rate term structure modelling framework is an comparatively uncharted region in the landscape of interest rate forecast literature as most, if not all, research activity builds on the voluminous literature of single-curve modelling and interest rate forecast. It would be interesting to adapt the framework to model different segments of the yield curve using different short rate models, or a combination of different models, to investigate whether such modelling strategy may lead to improvement in short rate forecast.

Secondly, it would be an interesting research question to investigate how the implied volatilities inferred from a simple short rate model in a multi-curve framework would perform compare to the implied volatilities inferred via the Black's model from caplets and floorlets written on Libor forward rates in terms of calibration of the Libor market model and its variants designed to capture the salient features of the interest rate contingent claim implied volatility smile.

The advent of negative interest rates ushered in by the European Central Bank by cutting the deposit rate to below zero in June 2014, and the subsequent rate cut by the Bank of Japan opens up new scope of econometric research into interest rate dynamics that take into account negative interest rates. It would be interesting to apply interest rate models that allow for negative interest rates, such as the free boundary SABR model proposed by Antonov et al. (2015), in the numerical framework proposed in Chapter 4 to investigate the potential role of the multi-curve framework in short rate forecast in the context of the present day interest rate market.

Figures

Figure 1: Time series of the Libor term structure from Jan. 2nd 2007 to Dec. 31st 2009.

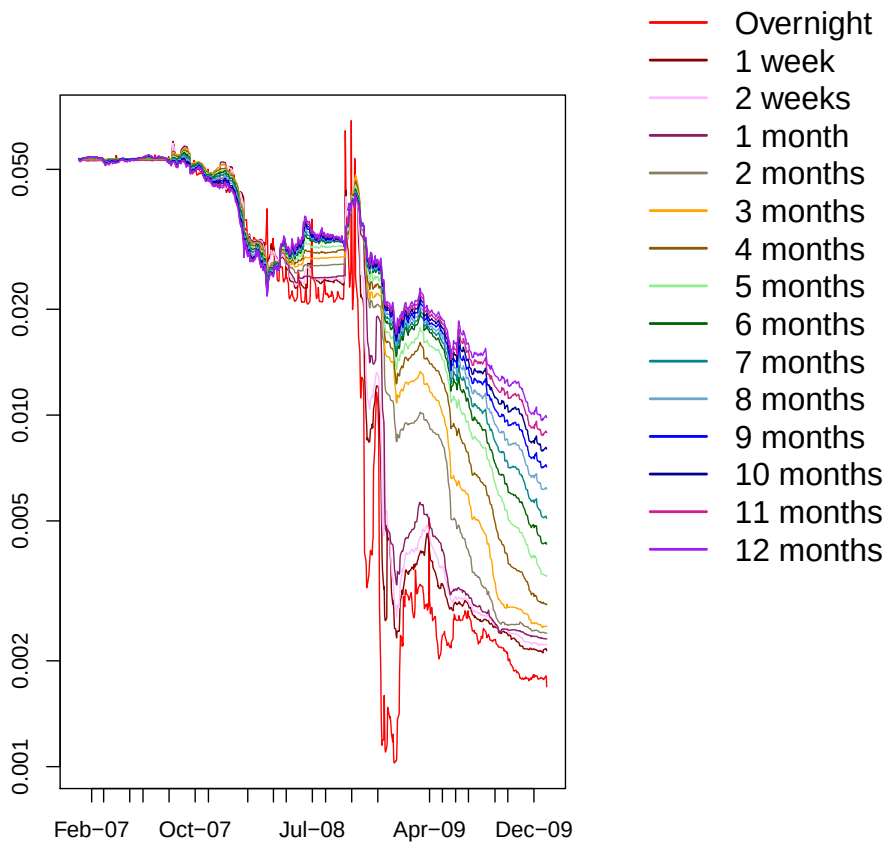

Figure 2: Time series of the Libor interest rate term structure from Jan. 4th 2010 and May 31st 2013.

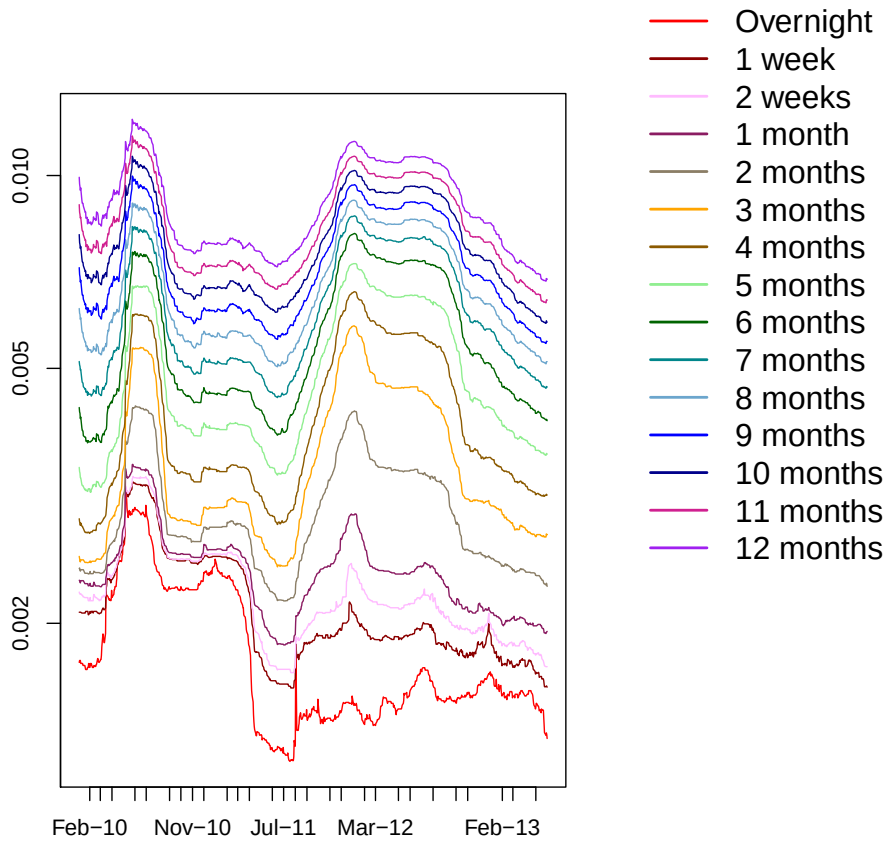

Figure 3: Time series of the range of implied volatility estimation uncertainty with respect to the range of discount rate uncertainty mimicked using Libor rates observed on May 3rd and May 31st 2011 calculated based on the prices of S&P500 index European call option contracts observed between May 3rd to May 31st 2011 inclusive. **Panel A**: Implied volatilities are estimated based on prices of the option contracts that expire on September 30th 2011. **Panel B**: Implied volatilities are estimated based on prices of the option contracts that expire on December 21st 2013.

Panel A

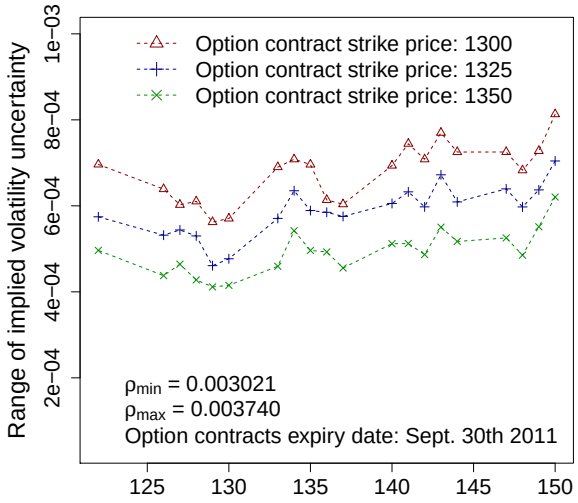

Panel B

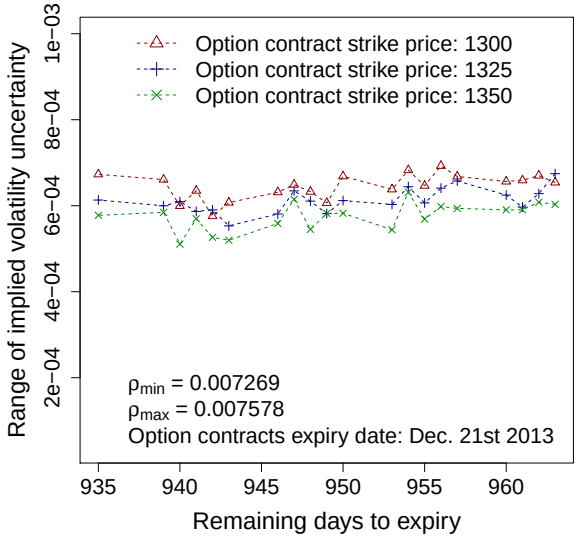

Figure 4: A graphical profile of the set of test implied volatilities, adapted from Table 1 of Andersen and Brotherton-Ratcliffe (1997), that is used to construct the test data set.

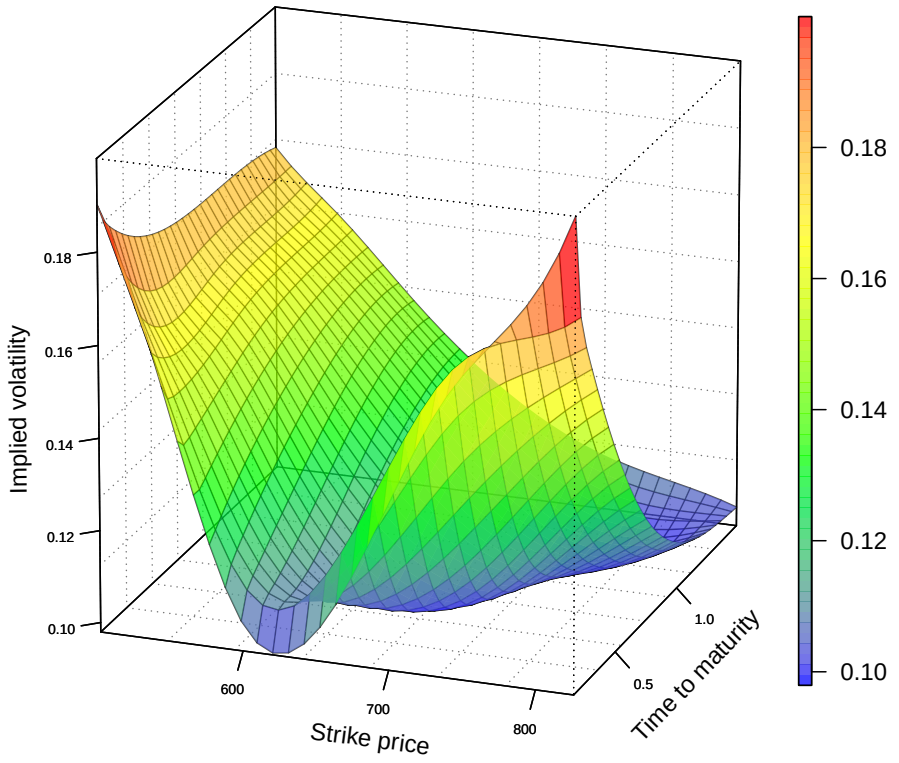

Figure 5: Convergence profile of the parameter estimation algorithm for a synthetic test data set. **Panel A**: Convergence profile for $\Psi(\boldsymbol{\theta}_{best,g})/(p \times \sum_{j=1}^{m} n_j)$, i.e., the average residual sum of squares. **Panel B**: Convergence profile for $\Psi_{L_1}(\boldsymbol{\theta}_{best,g})/(p \times \sum_{j=1}^{m} n_j)$, i.e., the mean absolute deviation. The number of iterations indexes g, where $g = 1, \ldots, 5000$. For this synthetic test data set, $p \times \sum_{j=1}^{m} n_j = 120$.

Panel A

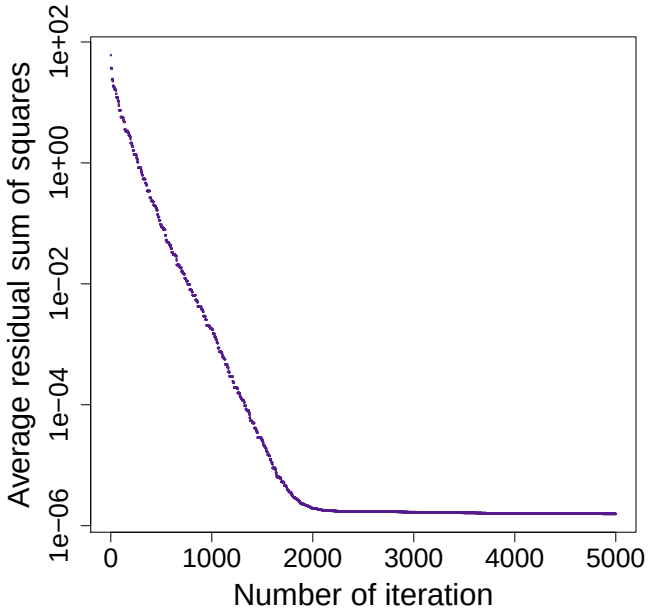

Panel B

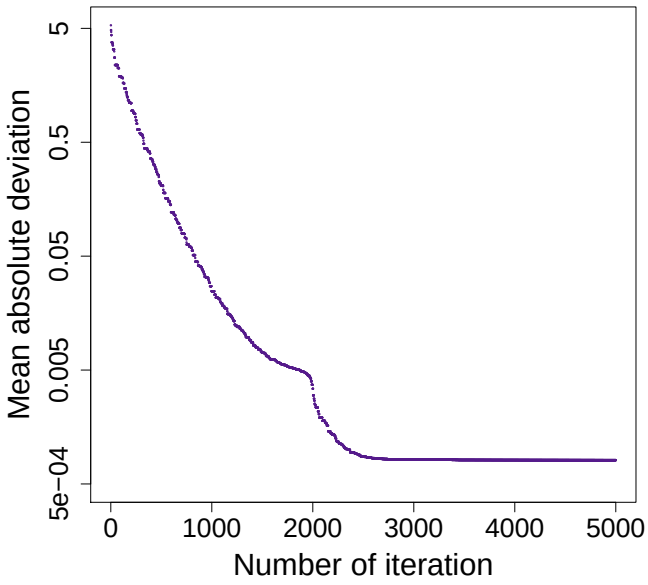

Figure 6: Convergence profiles of the parameter estimation algorithm for four different samples of S&P500 call options data. Panels A to D indicate the dates on which the prices of these samples of option contracts are observed.

Panel A: May 18th & 19th 2010

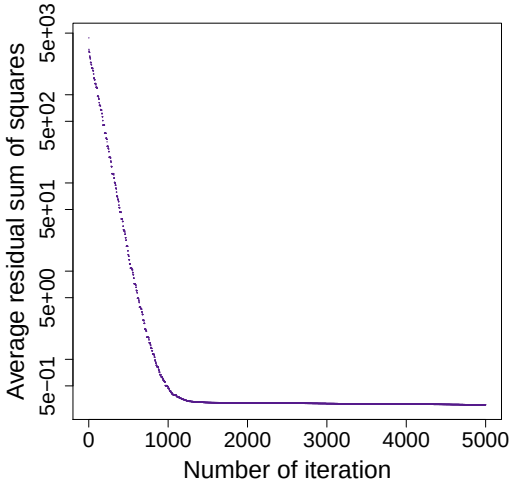

Panel B: May 18th & 19th 2011

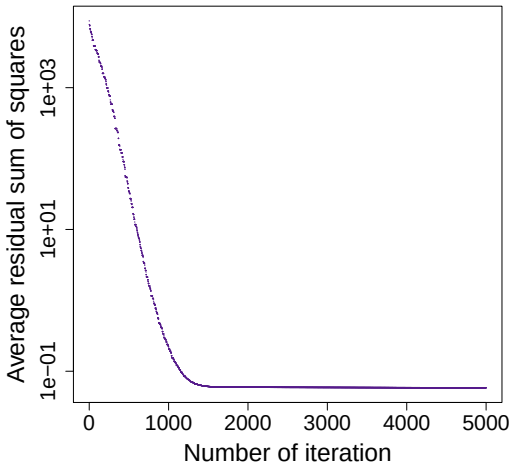

Panel A: May 23rd & 24th 2012

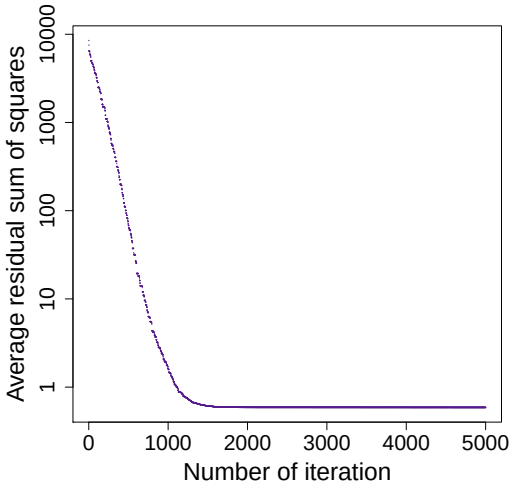

Panel B: May 22th & 23rd 2013

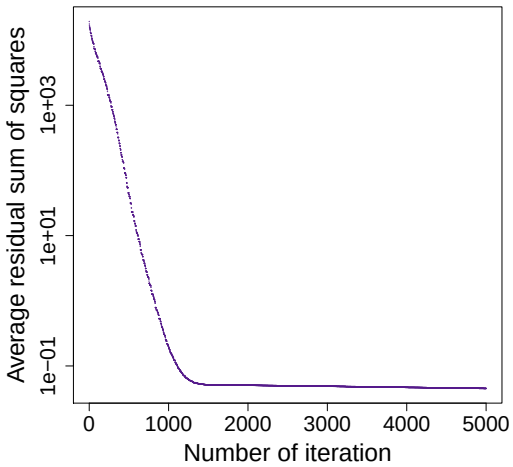

Figure 7: Each panel depicts the implied discount rate term structure estimated jointly with the implied volatilities from four different samples of S&P500 call option prices observed on different dates. The respective dates on which the option prices are observed are indicated in bold at the top of each panel. Contemporaneously quoted Libor and OIS rates are depicted alongside the implied discount rates for comparison.

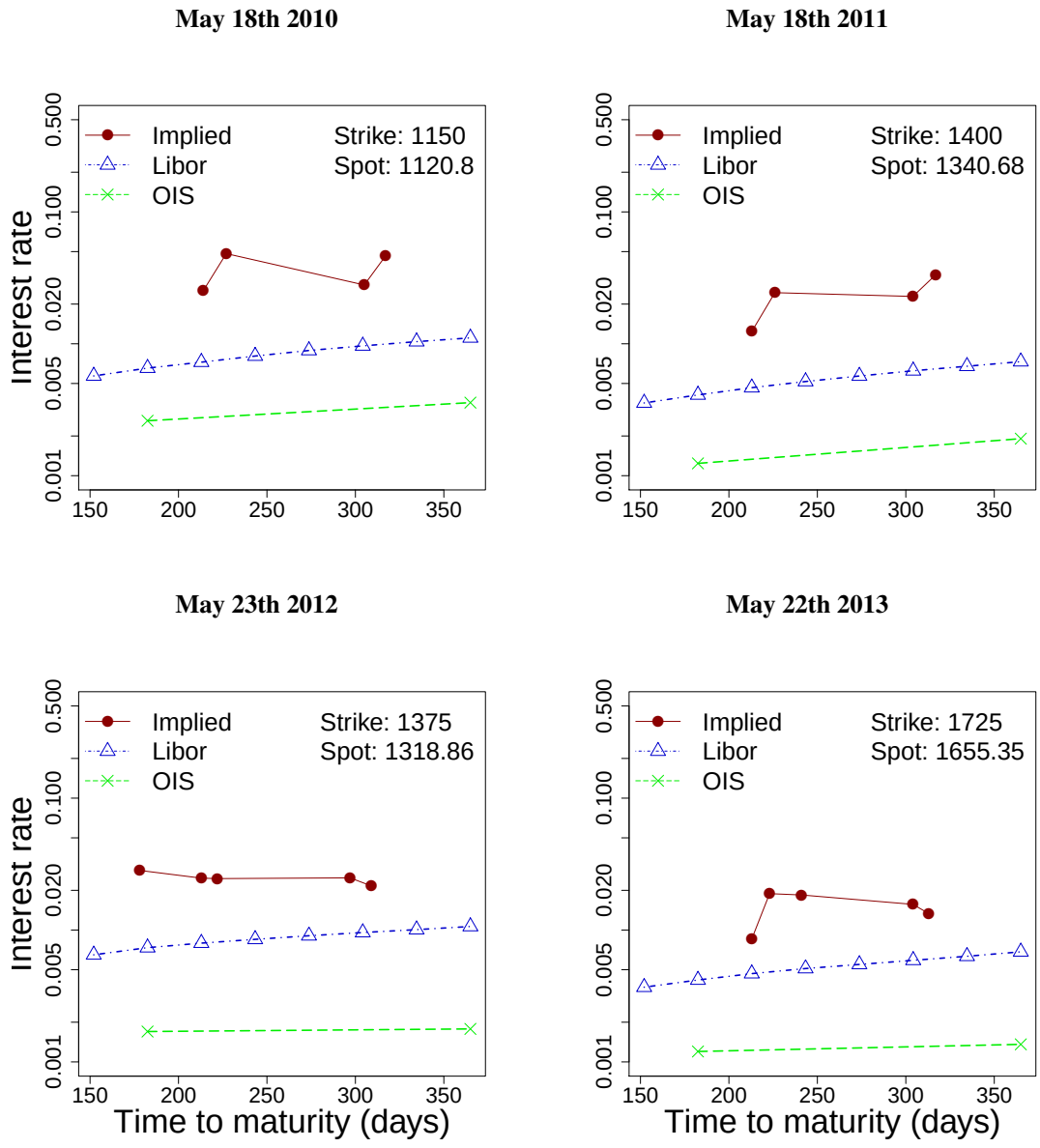

Figure 8: Each panel depicts the implied volatility term structure estimated jointly with the implied discount rates from four different samples of S&P500 call option prices observed on different dates. The respective dates on which the option prices are observed are indicated in bold at the top of each column. Term structures of implied volatility estimated based on the contemporaneously quoted Libor rates or OIS rates are depicted alongside for comparison.

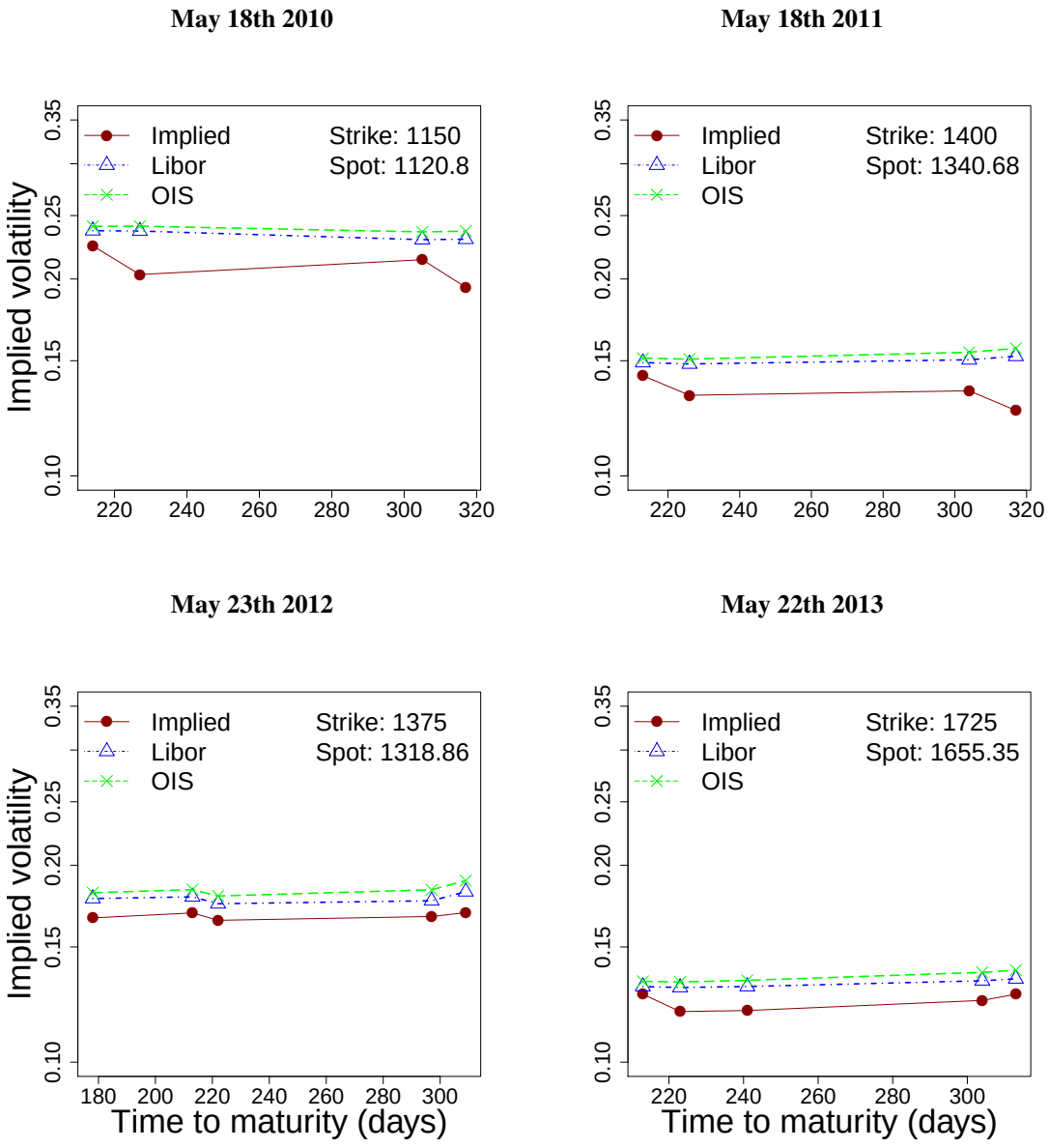

Figure 9: Term structures of the implied discount rates inferred from S&P500 options data from 2008 to 2013, and the contemporaneous Libor rates. The top of each panel shows the dates at which the option prices in each sample are observed. **Implied**: Implied discount rate. **Libor**: Contemporaneously quoted Libor rate.

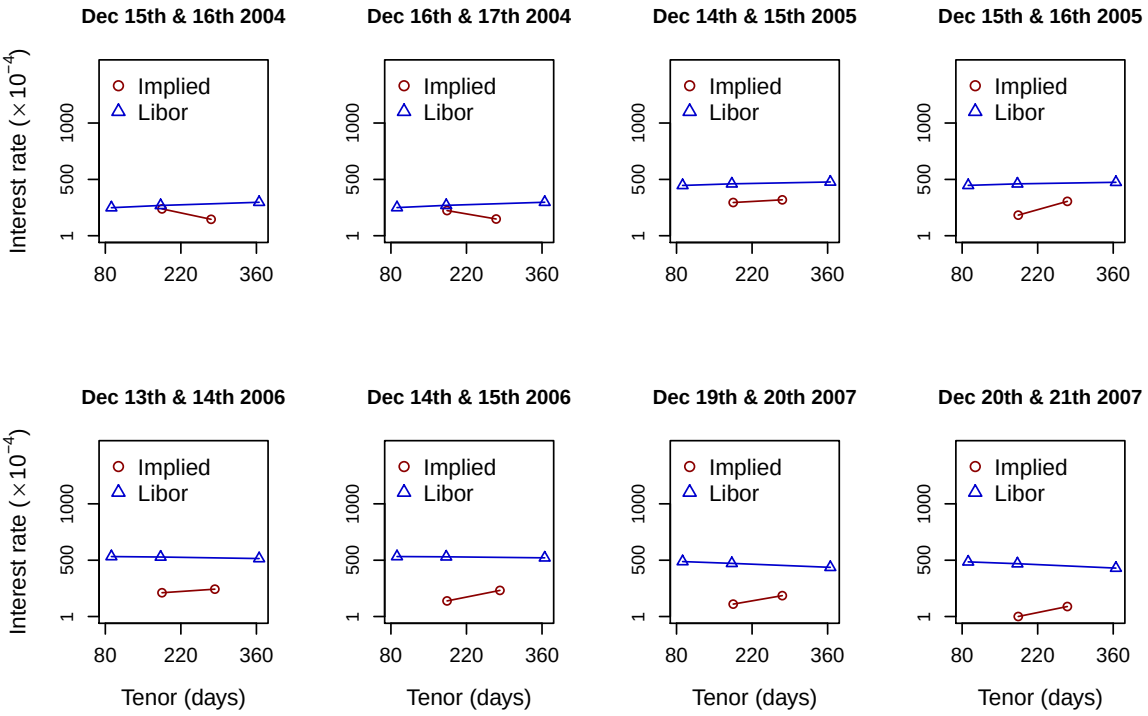

Figure 10: Term structures of the implied discount rates inferred from S&P500 options data from 2008 to 2013, and the contemporaneous Libor rates. The top of each panel shows the dates at which the option prices in each sample are observed. **Implied**: Implied discount rate. **Libor**: Contemporaneously quoted Libor rate.

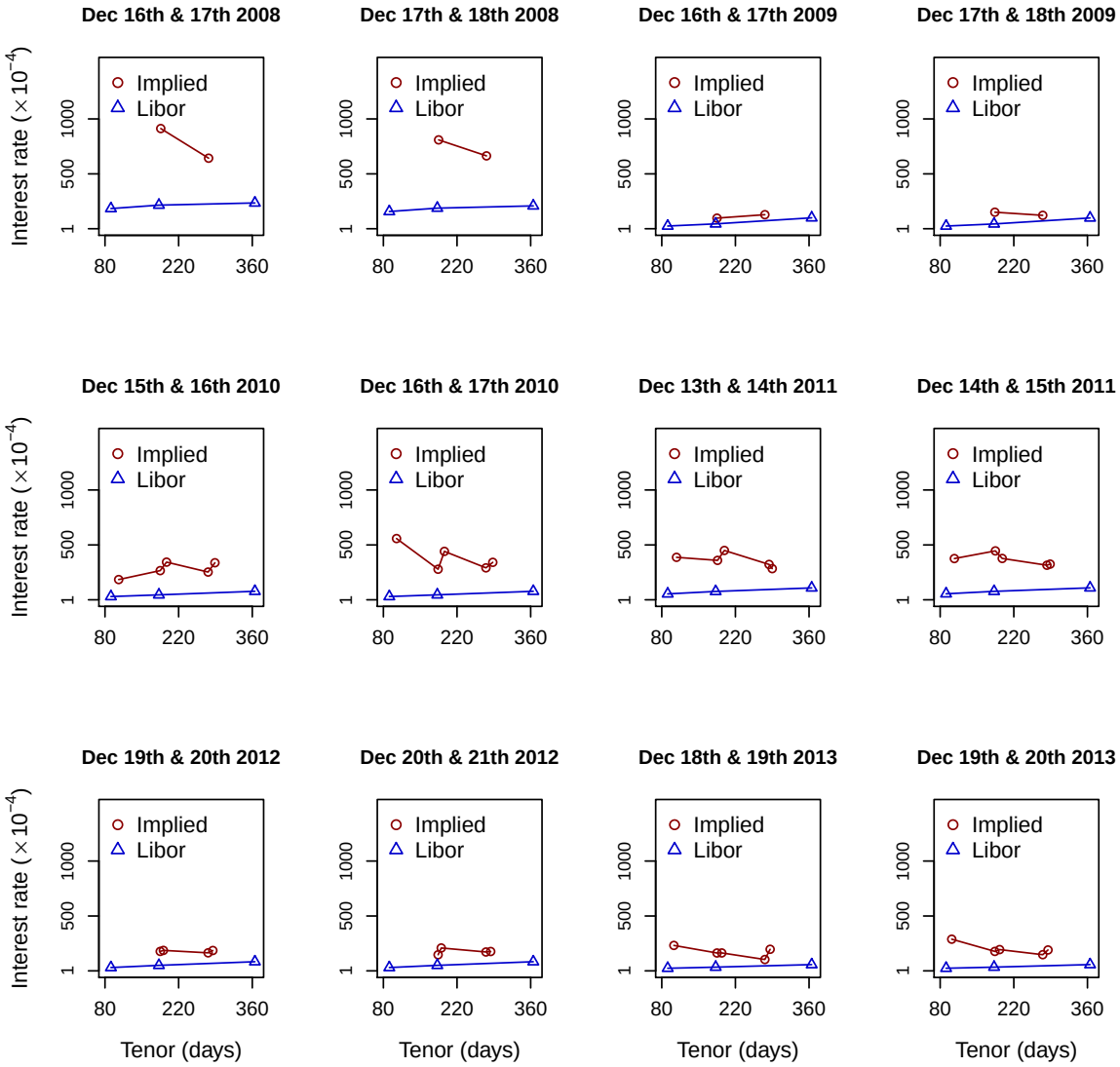

Figure 11: Tenor interval specific average of the CIR model parameters implied from 3,234 sets of US STRIPS day close prices from January 2nd 2001 to April 28th 2014 grouped into 100 intervals of tenors $(\tau_\ell, \tau_{\ell+1}]$, where τ_ℓ is the ℓ-th percentile of tenors in the data for $\ell = 0, \ldots, 99$. **Panel A**: Term structure of tenor interval specific average values of $\{\boldsymbol{\kappa}_{best,G}(t_i), i = 1, \ldots, 3234\}$, i.e., $\text{Mean}_\ell(\hat{\kappa})$. **Panel B**: Term structure of tenor interval specific average values of $\{\boldsymbol{\theta}_{best,G}(t_i), i = 1, \ldots, 3234\}$, i.e., $\text{Mean}_\ell(\hat{\theta})$. **Panel C**: Term structure of tenor interval specific average values of $\{\boldsymbol{\sigma}_{best,G}(t_i), i = 1, \ldots, 3234\}$, i.e., $\text{Mean}_\ell(\hat{\sigma})$. The solid lines indicate the trends of the tenor interval specific average values of the implied CIR parameters with respect to tenor, while the dotted lines indicate the respective inter specific standard deviation bounds.

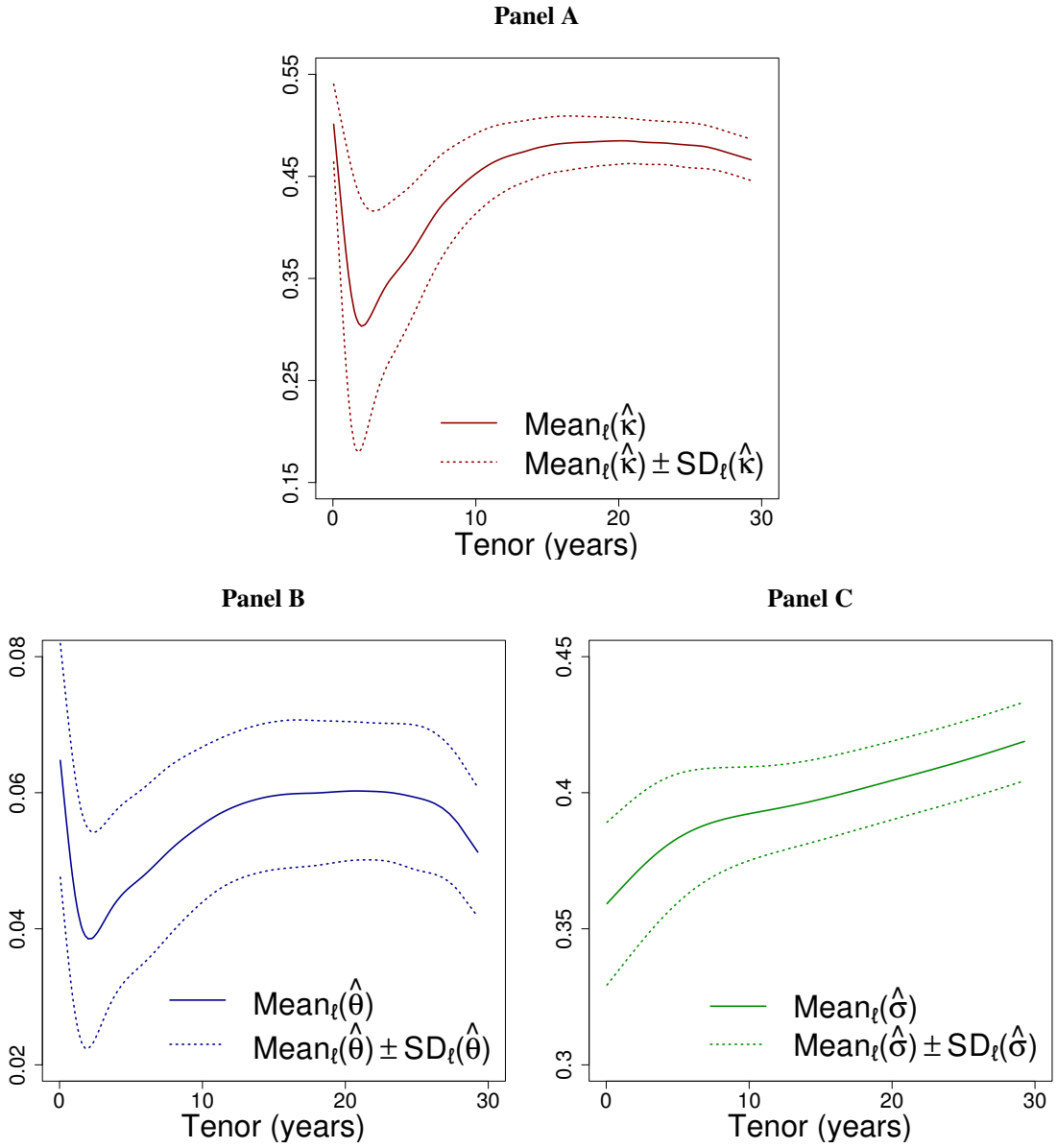

Figure 12: Prediction performance of $\hat{\rho}_{CIR}(t_i; T_{i,j,3}, T_{i,j+1,3})$, $\hat{\rho}_{CIR,1}(t_i; T_{i,j,3}, T_{i,j+1,3})$, $F(t_i; T_{i,j,3}, T_{i,j+1,3})$, and the random walk benchmark at various forecast horizons expressed in terms of forecast horizon interval specific RMSE and MAE.

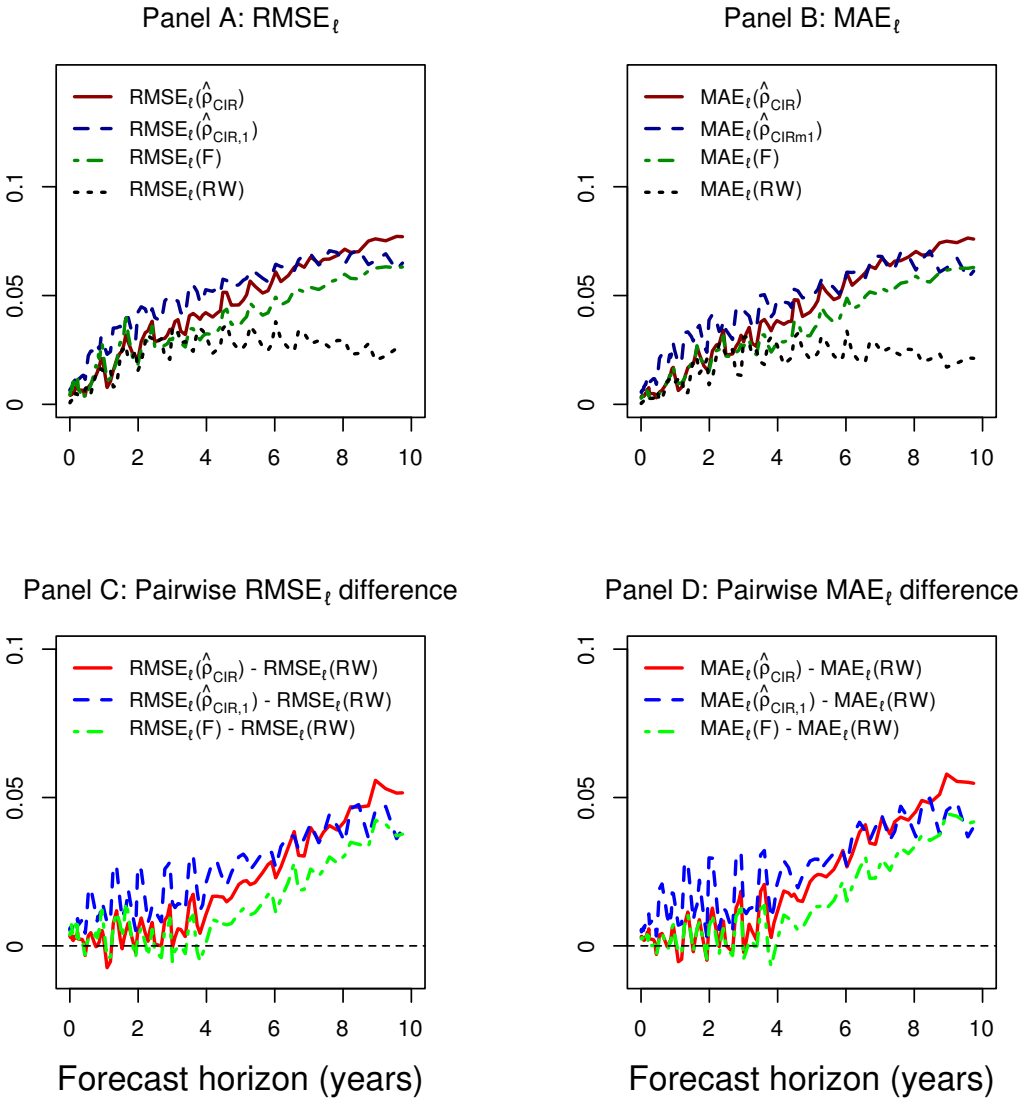

Figure 13: Theil's inequality coefficient U of $\hat{\rho}_{CIR}(t_i; T_{i,j,3}, T_{i,j+1,3})$, $\hat{\rho}_{CIR,1}(t_i; T_{i,j,3}, T_{i,j+1,3})$, $F(t_i; T_{i,j,3}, T_{i,j+1,3})$, and the random walk benchmark for different forecast horizon intervals.

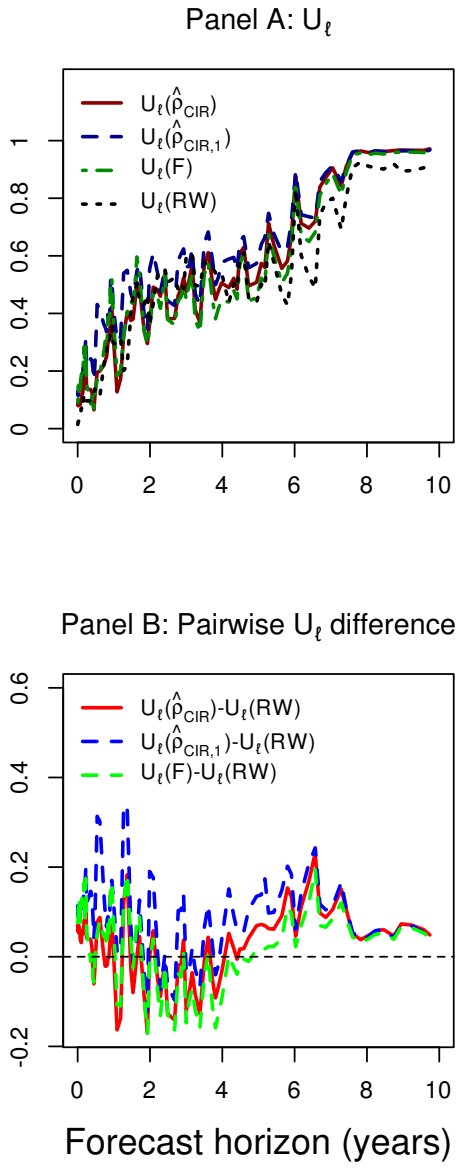

Tables

Table 1: The Libor rates corresponding to the times to maturity for the S&P500 European call option contracts with prices quoted on 5th, 13th and 27th of May 2011.

Option contracts expiry dates	Days to maturity from May 5th 2011	Libor rates (in decimal)		
		2011-05-05	2011-05-13	2011-05-27
June 18th 2011	44	0.002133	0.001967	0.001728
June 30th 2011	56	0.002295	0.002120	0.001881
July 16th 2011	72	0.002513	0.002324	0.002081
Aug. 20th 2011	107	0.003013	0.002790	0.002521
Sep. 17th 2011	135	0.003449	0.003203	0.002903
Sep. 30th 2011	148	0.003663	0.003409	0.003094
Dec. 17th 2011	226	0.005022	0.004752	0.004393
Dec. 30th 2011	239	0.005252	0.004982	0.004623
Mar. 17th 2012	317	0.006625	0.006348	0.006007
Mar. 30th 2012	330	0.006854	0.006576	0.006228

Table 2: The implied volatility estimated for near the money S&P500 European call options with prices quoted on on May 5th 2011, and maturing on either Sep. 30th 2011 or May 5th 2011. The discount rate ρ is assumed to be the Libor rates observed on May 5th, 13th or 27th 2011, which correspond to the interest rate values of 0.003663, 0.003409 & 0.003094 for options maturing on Sep. 30th 2011, and correspond to the interest rate values of 0.006854, 0.006576 & 0.006228 for options maturing on March 30th 2012. The spot price on May 5th 2011 was 1335.1.

Strike price	Strike/Spot	Implied volatilities estimated from prices observed on May 5th 2011 for option contracts expiring on Sept. 30th 2011 with discount rate proxy interpolated from Libor rates observed on		
		May 5th 2011 (ρ = 0.003663)	May 13th 2011 (ρ = 0.003409)	May 27th 2011 (ρ = 0.003094)
1000	0.7490	0.040129	0.040074	0.040474
1100	0.8239	0.209290	0.210267	0.211482
1200	0.8988	0.200491	0.200915	0.201419
1300	0.9737	0.177714	0.177956	0.178256
1400	1.0486	0.152567	0.152726	0.152886
1500	1.1235	0.132204	0.132286	0.132387

		Implied volatilities estimated from prices observed on May 5th 2011 for option contracts expiring on Mar. 30th 2012 with discount rate proxy interpolated from Libor rates observed on		
		May 5th 2011 (ρ = 0.006854)	May 13th 2011 (ρ = 0.006576)	May 27th 2011 (ρ = 0.006228)
1000	0.7490	0.108361	0.126524	0.137647
1100	0.8239	0.186538	0.187506	0.188694
1200	0.8988	0.184604	0.185138	0.185827
1300	0.9737	0.173265	0.173631	0.174092
1400	1.0486	0.158296	0.158559	0.158870
1500	1.1235	0.143280	0.143451	0.143702

Table 3: The implied volatility estimated for near the money S&P500 European call options with prices quoted on on May 5th 2011, and maturing on either Sep. 30th 2011 or May 5th 2011. The discount rate ρ is assumed to be the 90%, 100%, and 110% of the Libor rates observed on May 5th 2011, which correspond to the interest rate values of 0.003663, 0.0032967, & 0.0040293 for options maturing on Sep. 30th 2011, and correspond to the interest rate values of 0.006854, 0.0061686, & 0.0075394 for options maturing on March 30th 2012. The spot price on May 5th 2011 was 1335.1.

Strike price	Strike/Spot	Implied volatilities estimated from prices observed on May 5th 2011 for option contracts expiring on Sept. 30th 2011 with discount rate proxy interpolated from Libor rates observed on		
		May 5th 2011 (ρ = 0.003663)	May 13th 2011 (ρ = 0.003409)	May 27th 2011 (ρ = 0.003094)
1000	0.7490	0.0401293	0.04001317	0.04018039
1100	0.8239	0.2092895	0.21073115	0.20783333
1200	0.8988	0.2004906	0.20110547	0.19985694
1300	0.9737	0.1777135	0.17806266	0.17736667
1400	1.0486	0.1525666	0.15278246	0.15235801
1500	1.1235	0.1322044	0.13232187	0.13204550

		Implied volatilities estimated from prices observed on May 5th 2011 for option contracts expiring on Mar. 30th 2012 with discount rate proxy interpolated from Libor rates observed on		
		May 5th 2011 (ρ = 0.006854)	May 13th 2011 (ρ = 0.006576)	May 27th 2011 (ρ = 0.006228)
1000	0.7490	0.1083605	0.1391060	0.03851205
1100	0.8239	0.1865378	0.1889018	0.18414973
1200	0.8988	0.1846038	0.1859554	0.18324797
1300	0.9737	0.1732647	0.1741572	0.17233795
1400	1.0486	0.1582957	0.1589287	0.15762864
1500	1.1235	0.1432796	0.1437429	0.14285416

Table 4: Range of implied volatility uncertainty, $\Delta(t)$, for near the money S&P500 European call options observed for each trading day in May 2011 calculated assuming the discount rate ρ to be the Libor rates observed on May 2nd or 27th 2011, which are 0.003021 & 0.003740 for options maturing on Sept. 30th 2011, and 0.007269 & 0.007578 for options maturing on Dec. 21st 2013 respectively. K is the strike price of option contract.

Option contracts expiring on Sept. 30th 2011			Option contracts expiring on Mar. 30th 2012		
Remaining	$\Delta(t) \times 10^{-4}$		Remaining	$\Delta(t) \times 10^{-4}$	
days to expiry	$K = 1300$	$K = 1350$	days to expiry	$K = 1300$	$K = 1350$
150	8.1109	6.1961	963	15.2900	13.6729
149	7.2671	5.5069	962	14.7074	13.1785
148	6.8184	4.8442	961	14.3815	13.0682
147	7.2423	5.2465	960	14.7226	13.2310
144	7.2388	5.1645	957	14.8460	13.5592
143	7.6903	5.4952	956	15.2220	13.4902
142	7.0732	4.8597	955	14.7675	13.0340
141	7.4327	5.1182	954	14.7660	13.2549
140	6.9275	5.1113	953	14.2565	13.2757
137	6.0202	4.5480	950	14.2170	12.7400
136	6.1249	4.9204	949	14.2015	13.0187
135	6.9528	4.9476	948	14.3012	12.8745
134	7.0739	5.4153	947	14.4494	13.1024
133	6.8918	4.5891	946	14.4809	12.5228
130	5.6973	4.1463	943	14.0775	12.4794
129	5.6160	4.1096	942	13.4644	12.4921
128	6.0966	4.2712	941	14.0185	12.7519
127	6.0172	4.6379	940	14.1189	12.7614
126	6.3804	4.3716	939	14.0613	12.5497
122	6.9529	4.9584	935	14.3995	13.1295

Table 5: Range of implied volatility uncertainty, $\Delta(t)$, for near the money S&P500 European call options observed for each trading day in May 2011 calculated assuming the discount rate ρ to be 100% or 110% of the Libor rates observed on May 2nd 2011, which are 0.003021 & 0.003740 for options maturing on Sept. 30th 2011, and 0.007269 & 0.007578 for options maturing on Dec. 21st 2013 respectively. K is the strike price of option contract.

Option contracts expiring on Sept. 30th 2011			Option contracts expiring on Mar. 30th 2012		
Remaining	$\Delta(t) \times 10^{-4}$		Remaining	$\Delta(t) \times 10^{-4}$	
days to expiry	$K = 1300$	$K = 1350$	days to expiry	$K = 1300$	$K = 1350$
150	3.3341	2.6272	963	6.4497	5.8350
149	3.2847	2.3011	962	6.2659	5.3360
148	2.8563	2.1730	961	5.8354	5.4658
147	3.3050	2.3036	960	6.2761	5.4621
144	3.0765	1.7457	957	6.3193	5.5115
143	3.1160	2.2631	956	6.2865	5.5348
142	2.9744	2.1307	955	6.0264	5.5936
141	3.1810	1.9837	954	6.2720	5.5410
140	2.9244	2.3083	953	5.8849	5.7502
137	2.5776	2.1753	950	6.1962	5.2190
136	2.6620	1.9548	949	6.1785	5.4384
135	2.9530	2.2086	948	6.0110	5.6079
134	3.2369	2.2362	947	6.0415	5.5473
133	2.8327	1.8566	946	6.0354	5.1417
130	2.1873	1.7920	943	5.9616	5.3155
129	2.5275	1.6291	942	5.5683	5.3654
128	2.5380	1.9733	941	5.8539	5.4163
127	2.4360	1.7462	940	6.0597	5.4596
126	2.6972	1.9155	939	5.8618	5.3186
122	2.8647	2.3743	935	5.9159	5.7462

Table 6: Parameter estimation absolute error profiles for the implied discount rates estimated from the two synthetic test data sets, one simulating up-sloping discount rate term structure, while the other simulating an inverted discount rate term structure. The objective function used in the estimation process is the L_2-loss function.

Time to maturity at	Error $\left(\rho_{j,[t_1,t_2]}^{Test\ data}\right) \times 10^{-3}$	
first spot time (years)	Up-sloping term structure	Inverted term structure
0.17	2.942	2.990
0.42	9.047	8.902
0.69	9.350	4.650
0.94	5.900	7.182
1	6.185	7.580
1.5	2.442	8.761

Table 7: Parameter estimation absolute error profiles for the implied volatilities estimated based on the synthetic test data sets. The upper and lower panels depict results for two synthetic data sets; the upper simulating an up-sloping discount rate term structure, while the lower simulating an inverted discount rate term structure respectively. The objective function used in the estimation process is the L_2-loss function.

Time to maturity at first instance (years)	Strike/Spot									
	0.85	0.9	0.95	1	1.05	1.1	1.15	1.2	1.3	1.4
	$\text{Error}\left(\sigma^{Test\ data}_{imp,j,\ell,[t_1,t_2]}\right) \times 10^{-3}$ for synthetic test data mimicking up-sloping discount rate term structure									
0.17	42.357	9.409	3.875	1.510	0.731	0.442	0.366	0.234	2.499	102.670
0.42	57.366	24.354	12.786	7.375	4.565	3.113	2.309	2.096	1.848	1.864
0.69	40.215	23.104	14.667	9.855	6.874	4.869	3.724	3.091	2.436	2.163
0.94	21.530	14.507	10.168	7.425	5.536	4.157	3.239	2.647	1.944	1.609
1	23.104	15.746	11.096	8.190	6.158	4.672	3.643	2.963	2.136	1.899
1.5	8.694	6.592	5.115	4.037	3.228	2.607	2.150	1.792	1.338	1.042
	$\text{Error}\left(\sigma^{Test\ data}_{imp,j,\ell,[t_1,t_2]}\right) \times 10^{-3}$ for synthetic test data mimicking inverted discount rate term structure									
0.17	44.202	9.581	3.944	1.527	0.733	0.444	0.439	0.371	0.133	54.220
0.42	55.243	23.881	12.567	7.253	4.491	3.067	2.272	2.031	1.731	1.599
0.69	18.802	11.763	7.651	5.168	3.606	2.546	1.937	1.588	1.218	1.121
0.94	27.962	18.391	12.739	9.248	6.870	5.143	3.997	3.259	2.362	2.079
1	28.599	19.196	13.452	9.905	7.444	5.650	4.410	3.593	2.615	2.308
1.5	31.282	22.783	17.348	13.576	10.819	8.734	7.223	6.043	4.538	3.589

Table 8: The percentiles of the objective function values calculation based on synthetic test data sets from the entire set of population vectors. **I**: The percentile values for synthetic test data set mimicking up-sloping discount rate term structure. **II**: The percentile values for synthetic test data set mimicking inverted discount rate term structure.

	Percentile values of $\{\Psi(\boldsymbol{\theta}_{I,G}), I = 1, \ldots, 3300, G = 5000\}$ $\left(\times 10^{-4}\right)$								
Percentiles	Min	5th	10th	25th	Median	75th	90th	95th	Max
I	1.882	1.910	1.916	1.925	1.935	1.944	1.952	1.956	1.977
II	1.959	1.987	1.992	2.002	2.013	2.022	2.030	2.034	2.051

Table 9: Summary statistics for implied discount rate estimation uncertainty based on two synthetic test data sets.

Time to maturity	Up-sloping discount rate scenario				Inverted discount rate scenario			
(years)	$\rho_{best,G:j,[t_1,t_2],Test\ data}$	Min	Median	Max	$\rho_{best,G:j,[t_1,t_2],Test\ data}$	Min	Median	Max
0.17	0.00494	0.00489	0.00508	0.00518	0.00499	0.00483	0.00509	0.00519
0.42	0.01305	0.01304	0.01305	0.01305	0.01290	0.01290	0.01290	0.01290
0.69	0.01535	0.01535	0.01535	0.01535	0.02365	0.02365	0.02365	0.02365
0.94	0.01790	0.01790	0.01790	0.01790	0.02218	0.02218	0.02218	0.02218
1	0.02119	0.02118	0.02119	0.02119	0.01958	0.01958	0.01958	0.01958
1.5	0.02144	0.02144	0.02144	0.02144	0.01476	0.01476	0.01476	0.01476

Table 10: Summary statistics for implied volatility estimation uncertainty based on two synthetic test data sets.

Time to maturity (years)	Strike/Spot	Up-sloping discount rate scenario				Inverted discount rate scenario			
		$\sigma_{\text{best},G:imp,j,\ell,[t_1,t_2]}$	Min	Median	Max	$\sigma_{\text{best},G:imp,j,\ell,[t_1,t_2]}$	Min	Median	Max
0.17	0.85	0.14764	0.13655	0.14217	0.14954	0.14580	0.13567	0.14138	0.15159
0.17	0.90	0.15859	0.15777	0.15813	0.15879	0.15842	0.15773	0.15807	0.15899
0.17	0.95	0.12912	0.12880	0.12894	0.12920	0.12906	0.12878	0.12892	0.12928
0.17	1.00	0.11149	0.11138	0.11143	0.11153	0.11147	0.11137	0.11142	0.11157
0.17	1.05	0.10127	0.10121	0.10124	0.10131	0.10127	0.10121	0.10124	0.10129
0.17	1.10	0.09656	0.09647	0.09653	0.09661	0.09656	0.09646	0.09652	0.09664
0.17	1.15	0.11963	0.11945	0.11964	0.11989	0.11956	0.11938	0.11960	0.11985
0.17	1.2	0.14177	0.14110	0.14171	0.14235	0.14163	0.14094	0.14161	0.14230
0.17	1.3	0.16650	0.16287	0.16862	0.17315	0.16887	0.16309	0.16798	0.17230
0.17	1.4	0.09733	0.07323	0.13058	0.16112	0.14578	0.12220	0.15008	0.17189
0.42	0.85	0.11963	0.11956	0.11960	0.11968	0.12176	0.12173	0.12176	0.12181
0.42	0.9	0.13065	0.13063	0.13064	0.13066	0.13112	0.13111	0.13111	0.13112
0.42	0.95	0.12521	0.12521	0.12521	0.12522	0.12543	0.12543	0.12543	0.12544
0.42	1	0.11763	0.11762	0.11762	0.11763	0.11775	0.11774	0.11775	0.11775
0.42	1.05	0.10443	0.10443	0.10444	0.10444	0.10451	0.10450	0.10451	0.10451
0.42	1.1	0.09989	0.09988	0.09989	0.09989	0.09993	0.09993	0.09994	0.09994
0.42	1.15	0.09769	0.09764	0.09767	0.09770	0.09773	0.09768	0.09771	0.09774
0.42	1.2	0.11190	0.11186	0.11191	0.11194	0.11197	0.11189	0.11195	0.11198
0.42	1.3	0.12815	0.12800	0.12826	0.12868	0.12827	0.12799	0.12834	0.12864
0.42	1.4	0.14814	0.14728	0.14827	0.14920	0.14840	0.14757	0.14845	0.14918
0.69	0.85	0.13178	0.13177	0.13178	0.13179	0.15320	0.15319	0.15319	0.15320
0.69	0.9	0.13390	0.13389	0.13389	0.13390	0.14524	0.14523	0.14524	0.14524
0.69	0.95	0.12933	0.12933	0.12933	0.12934	0.13635	0.13635	0.13635	0.13635
0.69	1	0.12314	0.12314	0.12314	0.12315	0.12783	0.12783	0.12783	0.12783
0.69	1.05	0.11113	0.11112	0.11113	0.11113	0.11439	0.11439	0.11439	0.11440
0.69	1.1	0.09913	0.09913	0.09913	0.09914	0.10145	0.10145	0.10145	0.10146
0.69	1.15	0.09628	0.09627	0.09627	0.09628	0.09806	0.09805	0.09806	0.09807
0.69	1.2	0.09791	0.09789	0.09792	0.09794	0.09941	0.09939	0.09941	0.09943
0.69	1.3	0.10556	0.10541	0.10556	0.10566	0.10678	0.10668	0.10677	0.10686
0.69	1.4	0.12184	0.12137	0.12175	0.12210	0.12288	0.12261	0.12288	0.12308
0.94	0.85	0.14947	0.14947	0.14947	0.14948	0.14304	0.14303	0.14304	0.14304
0.94	0.9	0.14449	0.14449	0.14449	0.14450	0.14061	0.14060	0.14061	0.14061
0.94	0.95	0.13883	0.13883	0.13883	0.13883	0.13626	0.13626	0.13626	0.13626
0.94	1	0.12958	0.12957	0.12957	0.12958	0.12775	0.12775	0.12775	0.12775
0.94	1.05	0.12146	0.12146	0.12146	0.12147	0.12013	0.12013	0.12013	0.12013
0.94	1.1	0.10884	0.10884	0.10884	0.10885	0.10786	0.10785	0.10786	0.10786
0.94	1.15	0.10276	0.10276	0.10276	0.10276	0.10200	0.10200	0.10200	0.10201
0.94	1.2	0.10035	0.10035	0.10035	0.10036	0.09974	0.09973	0.09974	0.09975
0.94	1.3	0.09806	0.09800	0.09805	0.09809	0.09764	0.09758	0.09762	0.09766
0.94	1.4	0.10839	0.10815	0.10830	0.10848	0.10792	0.10777	0.10792	0.10806
1	0.85	0.14790	0.14789	0.14789	0.14790	0.14240	0.14240	0.14240	0.14241
1	0.9	0.14325	0.14325	0.14325	0.14326	0.13980	0.13980	0.13980	0.13981
1	0.95	0.13890	0.13890	0.13890	0.13891	0.13655	0.13655	0.13655	0.13655
1	1	0.12981	0.12981	0.12981	0.12981	0.12809	0.12809	0.12809	0.12810
1	1.05	0.12184	0.12184	0.12184	0.12184	0.12056	0.12055	0.12056	0.12056
1	1.1	0.11033	0.11033	0.11033	0.11033	0.10935	0.10935	0.10935	0.10935
1	1.15	0.10336	0.10335	0.10336	0.10336	0.10259	0.10259	0.10259	0.10259
1	1.2	0.10004	0.10003	0.10003	0.10004	0.09941	0.09940	0.09941	0.09941
1	1.3	0.09686	0.09681	0.09684	0.09687	0.09638	0.09634	0.09638	0.09642
1	1.4	0.10610	0.10602	0.10612	0.10623	0.10569	0.10559	0.10572	0.10591
1.5	0.85	0.16031	0.16030	0.16031	0.16031	0.13772	0.13771	0.13772	0.13772
1.5	0.9	0.15341	0.15341	0.15341	0.15341	0.13722	0.13721	0.13722	0.13722
1.5	0.95	0.14588	0.14588	0.14589	0.14589	0.13365	0.13365	0.13365	0.13365
1.5	1	0.13796	0.13796	0.13796	0.13796	0.12842	0.12842	0.12842	0.12843
1.5	1.05	0.12977	0.12977	0.12977	0.12977	0.12218	0.12218	0.12218	0.12218
1.5	1.1	0.12139	0.12139	0.12139	0.12139	0.11527	0.11526	0.11527	0.11527
1.5	1.15	0.11685	0.11685	0.11685	0.11685	0.11178	0.11177	0.11178	0.11178
1.5	1.2	0.11121	0.11120	0.11121	0.11121	0.10696	0.10695	0.10696	0.10696
1.5	1.3	0.10566	0.10566	0.10566	0.10567	0.10246	0.10245	0.10246	0.10247
1.5	1.4	0.10096	0.10093	0.10095	0.10097	0.09841	0.09836	0.09840	0.09845

Table 11: Error profiles for the implied discount rates estimated from the test data sets simulating up-sloping or inverted discount rate term structure for the synthetic option contracts with different times to maturity. The objective function used in the estimation process is the L_1-loss function.

Time to maturity at first spot time (years)	Error $\left(\rho^{Test\ data}_{j,[t_1,t_2]}\right) \times 10^{-3}$	
	Up-sloping term structure	Inverted term structure
0.17	3.347	2.990
0.42	8.809	8.902
0.69	10.615	4.650
0.94	7.603	7.182
1	4.765	7.580
1.5	4.139	8.761

Table 12: Parameter estimation absolute error profiles for the implied volatilities estimated from the test data sets for the synthetic option contracts with different combinations of times to maturity and strike prices. The upper and lower panels depict results for up-sloping and inverted discount rate term structures respectively. The objective function used in the estimation process is the L_1-loss function.

Time to maturity at first instance (years)	Strike/Spot									
	0.85	0.9	0.95	1	1.05	1.1	1.15	1.2	1.3	1.4
	$\text{Error}\left(\sigma^{Test\ data}_{imp,j,\ell,[t_1,t_2]}\right) \times 10^{-3}$ for synthetic test data mimicking up-sloping discount rate term structure									
0.17	63.516	10.764	4.428	1.714	0.825	0.505	0.436	0.401	0.339	0.325
0.42	53.647	23.564	12.433	7.186	4.449	3.038	2.264	2.029	1.666	1.512
0.69	48.938	26.790	16.797	11.235	7.822	5.536	4.236	3.502	2.743	2.485
0.94	29.114	19.126	13.256	9.630	7.166	5.372	4.183	3.414	2.501	2.181
1	17.171	11.908	8.464	6.271	4.728	3.593	2.805	2.284	1.662	1.437
1.5	15.250	11.410	8.783	6.902	5.503	4.436	3.651	3.042	2.266	1.781
	$\text{Error}\left(\sigma^{Test\ data}_{imp,j,\ell,[t_1,t_2]}\right) \times 10^{-3}$ for synthetic test data mimicking inverted discount rate term structure									
0.17	44.202	9.581	3.944	1.527	0.733	0.444	0.439	0.371	0.133	54.220
0.42	55.243	23.881	12.567	7.253	4.491	3.067	2.272	2.031	1.731	1.599
0.69	18.802	11.763	7.651	5.168	3.606	2.546	1.937	1.588	1.218	1.121
0.94	27.962	18.391	12.739	9.248	6.870	5.143	3.997	3.259	2.362	2.079
1	28.599	19.196	13.452	9.905	7.444	5.650	4.410	3.593	2.615	2.308
1.5	31.282	22.783	17.348	13.576	10.819	8.734	7.223	6.043	4.538	3.589

Table 13: Summary statistics for objective function values calculation based on each of the four samples of historical S&P500 options data sets, indexed by I, II, III & IV respectively, from the entire set of population vectors. **I**: May 18th & 19th 2010. **II**: May 18th & 19th 2011, **III**: May 23rd & 24th 2012. **IV**: May 22nd & 23rd 2013.

	N_p	Percentile values of $\{\Psi(\boldsymbol{\theta}_{I,G}), I = 1, \ldots, N_p\}\left(\times 10^{-4}\right)$								
Percentiles		Min	5th	10th	25th	50th (Median)	75th	90th	95th	Max
I	166	50.666	50.816	50.843	50.884	50.933	50.983	51.022	51.043	51.172
II	174	10.165	10.171	10.172	10.174	10.175	10.177	10.179	10.180	10.184
III	250	147.037	147.046	147.048	147.050	147.053	147.056	147.059	147.060	147.067
IV	262	11.834	11.879	11.888	11.901	11.916	11.930	11.942	11.949	11.981

Table 14: The implied discount rates depicted are estimated based on four samples of historical S&P500 call options prices indexed by I, II, III & IV. The two consecutive dates in each sample are indexed by (a) & (b). Tenor matching interpolated values of contemporaneously quoted Libor and OIS rates are depicted for comparison.

	I-(a). **May 18th 2010**				I-(b). **May 19th 2010**			
Times to maturity (year)	0.5863	0.6219	0.8356	0.8685	0.5836	0.6192	0.8329	0.8658
Implied discount rate	0.02525	0.04829	0.02793	0.04628	0.02525	0.04829	0.02793	0.04628
Libor	0.00730	0.00764	0.00965	0.00995	0.00746	0.00779	0.00979	0.01009
OIS rate	0.00276	0.00282	0.00323	0.00329	0.00258	0.00263	0.00301	0.00307
	II-(a). **May 18th 2011**				II-(b). **May 19th 2011**			
Times to maturity (year)	0.5836	0.6192	0.8329	0.8685	0.5808	0.6164	0.8301	0.8658
Implied discount rate	0.01244	0.02441	0.02286	0.03348	0.01244	0.02441	0.02286	0.03348
Libor	0.00463	0.00486	0.00623	0.00646	0.00459	0.00482	0.00622	0.00646
OIS rate	0.00133	0.00137	0.00165	0.00170	0.00143	0.00147	0.00178	0.00183
	III-(a). **May 23rd 2012**				III-(b). **May 24th 2012**			
Times to maturity (year)	0.5836	0.6082	0.8137	0.8466	0.5808	0.6055	0.8110	0.8438
Implied discount rate	0.02473	0.02454	0.02486	0.02160	0.02473	0.02454	0.02486	0.02160
Libor	0.00796	0.00812	0.00945	0.00965	0.00794	0.00810	0.00944	0.00964
OIS rate	0.00174	0.00174	0.00175	0.00175	0.00166	0.00167	0.00173	0.00174
	IV-(a). **May 22nd 2013**				IV-(b). **May 23rd 2013**			
Times to maturity (year)	0.6110	0.6603	0.8329	0.8575	0.6082	0.6575	0.8301	0.8548
Implied discount rate	0.01887	0.01844	0.01566	0.01333	0.01887	0.01844	0.01566	0.01333
Libor	0.00481	0.00506	0.00590	0.00602	0.00479	0.00504	0.00588	0.00601
OIS rate	0.00122	0.00123	0.00129	0.00130	0.00137	0.00138	0.00140	0.00140

Table 15: The implied volatilities estimated jointly with the implied discount rates, and the implied volatilities calculated by assuming the risk-free rate proxy to be either the contemporaneously quoted Libor or OIS rates based on four separate samples of historical S&P500 call options data indexed by I, II, III & IV. The two consecutive dates in each sample are indexed by (a) & (b) in the corresponding rows.

I. Option chain strike price: 1150	I-(a). **May 18th 2010**				I-(b). **May 19th 2010**			
Times to maturity (year)	0.5863	0.6219	0.8356	0.8685	0.5836	0.6192	0.8329	0.8658
(i) Proxy: Implied discount rate	0.22473	0.20314	0.21405	0.19427	0.22473	0.20314	0.21405	0.19427
(ii) Proxy: Libor	0.23705	0.23675	0.22968	0.23005	0.24170	0.24105	0.23511	0.23526
(iii) Proxy: OIS rate	0.24076	0.24082	0.23603	0.23670	0.24562	0.24528	0.24165	0.24219
II. Option chain strike price: 1400	II-(a). **May 18th 2011**				II-(b). **May 19th 2011**			
Times to maturity (year)	0.5836	0.6192	0.8329	0.8685	0.5808	0.6164	0.8301	0.8658
(i) Proxy: Implied discount rate	0.14229	0.13283	0.13493	0.12592	0.14229	0.13283	0.13493	0.12592
(ii) Proxy: Libor	0.14904	0.14830	0.15050	0.15236	0.14680	0.14708	0.14987	0.15152
(iii) Proxy: OIS rate	0.15135	0.15085	0.15452	0.15669	0.14906	0.14955	0.15384	0.15575
III. Option chain strike price: 1375	III-(a). **May 23rd 2012**				III-(b). **May 24th 2012**			
Times to maturity (year)	0.5836	0.6082	0.8137	0.8466	0.5808	0.6055	0.8110	0.8438
(i) Proxy: Implied discount rate	0.16908	0.16474	0.16697	0.16925	0.16908	0.16474	0.16697	0.16925
(ii) Proxy: Libor	0.17894	0.17464	0.17648	0.18219	0.18481	0.18051	0.18625	0.17913
(iii) Proxy: OIS rate	0.18353	0.17946	0.18342	0.18946	0.18950	0.18542	0.19321	0.18644
IV. Option chain strike price: 1725	IV-(a). **May 22nd 2013**				IV-(b). **May 23rd 2013**			
Times to maturity (year)	0.6110	0.6603	0.8329	0.8575	0.6082	0.6575	0.8301	0.8548
(i) Proxy: Implied discount rate	0.11950	0.11992	0.12428	0.12702	0.11950	0.11992	0.12428	0.12702
(ii) Proxy: Libor	0.13006	0.13049	0.13317	0.13409	0.12938	0.12975	0.13273	0.13307
(iii) Proxy: OIS rate	0.13258	0.13337	0.13718	0.13826	0.13176	0.13242	0.13652	0.13708

Table 16: Estimation uncertainty bounds for the implied volatilities and implied discount rates estimated jointly based on subsets of the four samples of S&P500 call options data indexed by I to IV. **I**: May 18th 2010. **II**: May 18th 2011. **III**: May 23rd 2012. **IV**: May 22nd 2013.

I. Option chain strike price: 1150	I: **Implied volatility**				I: **Implied discount rate**			
Times to maturity (year)	0.5863	0.6219	0.8356	0.8685	0.5863	0.6219	0.8356	0.8685
Lower error bound	0.22341	0.20138	0.21183	0.19207	0.02484	0.04667	0.02714	0.04557
Best estimate	0.22473	0.20314	0.21405	0.19427	0.02525	0.04829	0.02793	0.04628
Upper error bound	0.22486	0.20424	0.21519	0.19492	0.02661	0.05005	0.02992	0.04780
II. Option chain strike price: 1400	II: **Implied volatility**				II: **Implied discount rate**			
Times to maturity (year)	0.5836	0.6192	0.8329	0.8685	0.5836	0.6192	0.8329	0.8685
Lower error bound	0.14218	0.13274	0.13488	0.12582	0.01238	0.02432	0.02283	0.03339
Best estimate	0.14229	0.13283	0.13493	0.12592	0.01244	0.02441	0.02286	0.03348
Upper error bound	0.14237	0.13288	0.13499	0.12599	0.01257	0.02453	0.02293	0.03354
III. Option chain strike price: 1375	III: **Implied volatility**				III: **Implied discount rate**			
Times to maturity (year)	0.5836	0.6082	0.8137	0.8466	0.5836	0.6082	0.8137	0.8466
Lower error bound	0.16894	0.16456	0.16679	0.16922	0.02457	0.02420	0.02470	0.02157
Best estimate	0.16908	0.16474	0.16697	0.16925	0.02473	0.02454	0.02486	0.02160
Upper error bound	0.16920	0.16502	0.16711	0.16928	0.02486	0.02481	0.02500	0.02163
IV. Option chain strike price: 1725	IV: **Implied volatility**				IV: **Implied discount rate**			
Times to maturity (year)	0.6110	0.6603	0.8329	0.8575	0.6110	0.6603	0.8329	0.8575
Lower error bound	0.11947	0.11988	0.12427	0.12700	0.01882	0.01837	0.01565	0.01329
Best estimate	0.11950	0.11992	0.12428	0.12702	0.01887	0.01844	0.01566	0.01333
Upper error bound	0.11954	0.11996	0.12429	0.12704	0.01893	0.01848	0.01568	0.01336

Table 17: Forecasting performance of effective Federal Funds rate at different forecast horizons. $\text{RMSE}(\hat{\rho}_{CIR})$, $\text{RMSE}(\hat{\rho}_{CIR,1})$, $\text{RMSE}(F)$, and $\text{RMSE}(RW)$ are the forecast horizon-specific MSE for the multi-curve and single-curve CIR predictors, forward rate, and the random walk benchmark respectively, while $\text{MAE}_\ell(\hat{\rho}_{CIR})$, $\text{MAE}_\ell(\hat{\rho}_{CIR,1})$, $\text{MAE}_\ell(F)$, and $\text{MAE}_\ell(RW)$ are the forecast horizon-specific MAE for these predictors.

Forecast horizon (years)	$\text{RMSE}_\ell(\hat{\rho}_{CIR})$ $\times 10^{-3}$	$\text{RMSE}_\ell(\hat{\rho}_{CIR,1})$ $\times 10^{-3}$	$\text{RMSE}_\ell(F)$ $\times 10^{-3}$	$\text{RMSE}_\ell(RW)$ $\times 10^{-3}$	$\text{MAE}_\ell(\hat{\rho}_{CIR})$ $\times 10^{-3}$	$\text{MAE}_\ell(\hat{\rho}_{CIR,1})$ $\times 10^{-3}$	$\text{MAE}_\ell(F)$ $\times 10^{-3}$	$\text{MAE}_\ell(RW)$ $\times 10^{-3}$
0.4	6.49	13.12	4.01	4.31	4.91	11.83	2.97	2.79
0.8	13.96	23.69	17.46	14.08	10.58	20.05	10.52	10.64
1.2	7.75	22.97	10.87	15.11	6.35	18.68	9.51	11.70
1.6	24.41	34.69	28.43	25.40	18.51	29.10	18.80	20.49
1.8	28.54	39.88	31.92	20.89	23.00	36.31	22.05	14.18
2.2	28.80	44.85	25.38	19.40	24.55	41.36	22.25	11.81
2.4	36.13	40.89	31.51	30.72	30.99	34.45	28.03	25.56
2.8	30.07	38.17	26.11	30.09	23.15	29.80	21.91	25.20
3.2	38.10	48.07	33.63	35.17	32.54	41.84	29.18	30.99
3.4	33.61	42.16	28.14	28.09	28.04	35.94	24.83	23.04
3.8	40.33	51.77	31.38	33.39	36.21	45.76	26.73	28.95
4.2	42.13	52.69	32.41	31.79	38.47	48.00	28.82	27.44
4.6	51.49	57.52	42.42	34.98	48.08	52.87	37.90	30.63
5.0	45.67	54.96	35.97	24.95	42.33	49.34	31.50	20.75
5.4	56.65	61.53	46.46	36.02	55.14	57.15	44.63	31.20
5.8	51.15	57.94	40.95	26.43	48.13	53.58	37.66	22.36
6.2	60.89	64.39	49.26	37.96	60.30	60.75	48.78	33.70
6.6	59.20	63.09	47.46	25.97	57.77	61.17	45.49	19.48
7.1	62.97	68.88	51.73	32.70	62.38	68.12	50.98	28.16
7.6	66.66	65.96	54.01	28.33	65.81	62.55	53.32	23.99
8.1	68.41	69.79	57.32	29.37	67.70	68.32	56.41	25.32
8.5	69.85	69.21	57.89	22.98	68.61	66.61	56.88	19.59
9.0	75.04	64.22	61.29	27.87	74.21	60.77	60.54	23.19
9.6	75.17	69.21	63.20	22.20	74.30	67.26	62.59	18.89

Bibliography

Adams, A. and Booth, B. (1995). Sensitivity Measures for Equity Investment, *IMA Journal of Mathematics Applied in Business & Industry* **6**: 365–374.

Ahlip, R. and Rutkowski, M. (2013a). Pricing of Foreign Exchange Options under the Heston Stochastic Volatility Model and CIR Interest Rates, *Quantitative Finance* **13**(6): 955–966.

Ahlip, R. and Rutkowski, M. (2013b). Pricing of Foreign Exchange Options under the MPT Stochastic Volatility Model and CIR Interest Rates, *Quantitative Finance* **13**(6): 955–966.

Ahn, C. and Thompson, H. (1988). Jump-Diffusion Processes and the Term Structure of Interest Rates, *The Journal of Finance* **43**(1): 155–174.

Aït-Sahalia, Y. (1996a). Continuous-Time Models of the Spot Interest Rate, *The Review of Financial Studies* **9**(2): 385–426.

Aït-Sahalia, Y. (1996b). Nonparametric Pricing of Interest Rate Derivative Securities, *Econometrica* **64**(3): 527–560.

Aït-Sahalia, Y. and Duarte, J. (2003). Nonparametric option pricing under shape restrictions, *Journal of Econometrics* **116**: 9–47.

Aït-Sahalia, Y. and Lo, A. (1998). Nonparametric Estimation of State-price Densities Implicit in Financial Asset Prices, *Journal of Finance* **53**: 499–548.

Aït-Sahalia, Y., Mykland, P. and Zhang, L. (2003). How Often to Sample a Continuous-Time Process in the Presence of Market Microstructure Noise, *Review of Financial Studies* **18**: 351–416.

Akaike, H. (1973). Information theory and an extension of the maximum likelihood principle, *2nd International Symposium on Information Theory*, Akademiai Kiado, Budapest.

Albrecher, H., Mayer, P., Schoutens, W. and Tistaert, J. (2007). The Little Heston Trap, *Wilmott Magazine* **January**: 83–92.

Andersen, L. and Andreasen, J. (2000). Jump-Diffusion Processes: Volatility Smile Fitting and Numerical Methods for Option Pricing, *Review of Derivatives Research* **4**(3): 231–262.

Andersen, L. B. G. (2007). Discount Curve Construction with Tension Splines, *Review of Derivatives Research* **10**: 227–267.

Andersen, L. B. G. and Brotherton-Ratcliffe, R. (1997). The Equity Option Volatility Smile: An Implicit Finite-Difference Approach, *Journal of Computational Finance* **1**(2): 5–37.

Andersen, T. and Benzoni, L. (2010). Do Bonds Span Volatility Risk in the U.S. Treasury Market? A Specification Test for Affine Term Structure Models, *The Journal of Finance* **65**(2): 603–653.

Andersen, T., Bollerslev, T. and Diebold, F. (2007). Roughing it up: Including Jump Components in the Measurement, Modeling, and Forecasting of Return Volatility, *The Review of Economics and Statistics* **89**(4): 701–720.

Andersen, T., Fusari, N. and Todorov, V. (2015). The Risk Premia embedded in Index Options, *Journal of Financial Economics* **117**(3): 558–584.

Anderson, H. (1997). Transaction Costs and Nonlinear Adjustment Towards Equilibrium in the US Treasury Bill Market, *Oxford Bulletin of Economics and Statistics* **59**(4): 465–484.

Ang, A. and Bekaert, G. (2002). Short Rate Nonlinearities and Regime Switches, *Journal of Economic Dynamics and Control* **26**(7–8): 1243–1274.

Antonov, A., Konikov, M. and Spector, M. (2015). The Free Boundary SABR: Natural Extension to Negative Rates, *Risk* **September**. 7 pages.

Ardia, D., Boudt, K., Carl, P., Mullen, K. and Peterson, B. (2010). Differential Evolution with `DEoptim`: An Application to Non-Convex Portfolio Optimization, *The R Journal* **3**(1): 27–34.

Ardia, D., Mullen, K., Peterson, B. and Ulrich, J. (2012). *`DEoptim`: Differential Evolution in 'R'*. version 2.2-2.

Attari, M. (2004). Option Pricing Using Fourier Transforms: A Numerically Efficient Simplification. Available at SSRN: http://ssrn.com/abstract=520042 or http://dx.doi.org/10.2139/ssrn.520042.

Audrino, F., Barone-Adesi, G. and Mira, A. (2005). The Stability of Factor Models of Intrest Rates, *Journal of Financial Econometrics* **3**(3): 422–441.

Audrino, F. and Medeiros, M. (2011). Modeling and Forecasting Short-term Interest Rates: The benefits of Smooth Regimes, Macroeconomic Variables and Bagging, *Journal of Applied Econometrics* **26**(6): 999–1022.

Avellaneda, M., Friedman, C., Holmes, R. and Samperi, D. (1996). Calibrating Volatility Surfaces via Relative-Entropy Minimization. Working paper. Available at SSRN: http://ssrn.com/abstract=648 or http://dx.doi.org/10.2139/ssrn.648.

Avellaneda, M., Friedman, C., Holmes, R. and Samperi, D. (1997). Calibrating Volatility Surfaces via Relative-Entropy Minimization, *Applied Mathematical Finance* **4**(1): 37–64.

Bakshi, G., Cao, C. and Chen, Z. (1997). Empirical performance of alternative option pricing models, *Journal of Finance* **52**(5): 2003–2049.

Bakshi, G. and Kapadia, N. (2003). Delta-Hedged Gains and the Negative Market Volatility Risk Premium, *The Review of Financial Studies* **16**: 527–566.

Bakshi, G. and Madan, D. (2000). Spanning and Derivative-security Valuation, *Journal of Financial Economics* **55**(2): 205–238.

Bakshi, G. and Madan, D. (2006). A Theory of Volatility Spreads, *Management Science* **52**: 1945–1956.

Bams, D. and Schotman, P. (2003). Direct Estimation of the Risk Neutral Factor Dynamics of Gaussian Term Structure Models, *Journal of Econometrics* **117**(1): 179–206.

Bank of International Settlement (2013). Towards Better Reference Rate Practices: A Central Bank Perspective. A report by a Working Group established by the BIS Economic Consultative Committee (ECC) and chaired by Hiroshi Nakaso, Assistant Governor, Bank of Japan. Available at http://www.bis.org/publ/othp19.pdf.

Bates, D. S. (1996). Jumps and stochastic volatility: Exchange rate processes implicit in deutsche mark options, *Review of Financial Studies* **9**: 69–107.

Bates, D. S. (2000). Post-'87 crash fears in the S&P 500 futures option market, *Journal of Econometrics* **94**: 181–238.

Baviera, R. and Cassaro, A. (2015). A Note on Dual-Curve Construction: Mr. Crab's Bootstrap, *Applied Mathematical Finance* **22**(2): 105–132.

Belomestny, D. and Reiß, M. (2006). Spectral calibration of exponential Lévy models, *Finance and Stochastics* **10**(4): 449–474.

Belomestny, D. and Schoenmakers, J. (2011). A Jump-Diffusion Libor Model and its Robust Calibration, *Quantitative Finance* **11**(4): 529–546.

Ben Hamida, S. and Cont, R. (2005). Recovering Volatility from Option Prices by Evolutionary Optimization, *Journal of Computational Finance* **8**(4): 1–34.

Benko, M., Fengler, M., Härdle, W. and Kopa, M. (2007). On extracting information implied in options, *Computational Statistics* **22**(4): 543–553.

Berestycki, H., Busca, J. and Florent, I. (2002). Asymptotics and calibration of local volatility models, *Quantitative Finance* **2**: 61–69.

Berestycki, H., Busca, J. and Florent, I. (2004). Computing the Implied Volatility in Stochastic Volatility Models, *Communications on Pure and Applied Mathematics* **57**(10): 1352–1373.

Bianconi, M., MacLachlan, S. and Sammon, M. (2015). Implied volatility and the risk-free rate of return in options markets, *The North American Journal of Economics and Finance* **31**: 1–26.

Birke, M. and Pilz, K. F. (2009). Nonparametric option pricing with no-arbitrage constraints, *Journal of Financial Econometrics* **7**(2): 53–76.

Black, F., Derman, E. and Toy, W. (1990). A One-Factor Model of Interest Rates and its Application to Treasury Bond, *Financial Analysts Journal* **46**(1): 33–39.

Black, F. and Karasinski, P. (1991). Bond and Option Pricing When Short Rates are Lognormal, *Financial Analysts Journal* **47**(4): 52–59.

Black, F. and Scholes, M. (1973). The Pricing of Options and Corporate Liabilities, *Journal of Political Economy* **81**(3): 637–654.

Bliemel, F. (1973). Theil's Forecast Accuracy Coefficient: A Clarification, *Journal of Marketing Research* **10**(4): 444–446.

Bollerslev, T., Gibson, M. and Zhou, H. (2011). Dynamic Estimation of Volatility Risk Premia and Investor Risk Aversion from Option-implied and Realized Volatilities, *Journal of Econometrics* **160**: 235–245.

Bollerslev, T., Tauchen, G. and Zhou, H. (2009). Expected Stock Returns and Variance Risk Premia, *The Review of Financial Studies* **22**(11): 4463–4492.

Bollerslev, T. and Todorov, V. (2011). Tails, Fears and Risk Premia, *The Journal of Finance* **66**(6): 2165–2211.

Boyarchenko, S. and Levendorskii, S. (2014). Efficient Variations of the Fourier transform in Applications to Option Pricing, *The Journal of Computational Finance* **18**(2): 57–90.

Boyle, P. and Emanuel, D. (1980). Discretely Adjusted Option Hedges, *Journal of Financial Economics* **8**(3): 259–282.

Brace, A. (2008). *Engineering BGM*, Chapman & Hall/CRC, Boca Raton, Florida.

Brace, A., Gatarek, D. and Musiela, M. (1997). The market model of interest rate dynamics, *Mathematical Finance* **7**(2): 127–155.

Brenner, M. and Galai, D. (1986). Implied Interest Rates, *The Journal of Business* **59**(3): 493–507.

Brenner, M. and Subrahmanyam, M. (1988). A Simple Formula to Compute the Implied Standard Deviation, *Financial Analyst Journal* **44**(5): 80–83.

Brigo, D. and Mercurio, F. (2001). Displaced and mixture diffusions for analytically-tractable smile models, *in* H. German, D. B. Madan, S. R. Pliska and A. C. F. Vorst (eds), *Mathematical Finance Bachelier Congress 2000*, Springer-Verlag, Berlin, Heidelberg.

Brigo, D. and Mercurio, F. (2002a). Calibrating LIBOR, *Risk* pp. 117–121.

Brigo, D. and Mercurio, F. (2002b). Log-normal-mixture dynamics and calibration to market volatility smiles, *International Journal of Theoretical and Applied Finance* **5**(4): 427–446.

Brigo, D. and Mercurio, F. (2006). *Interest Rate Models - Theory and Practice*, Springer-Verlag, Berlin Heidelberg.

Brigo, D., Mercurio, F. and Morini, M. (2005). The LIBOR model dynamics: Approximations, calibration and diagnostics, *European Journal of Operational Research* **163**(1): 30–51.

Britten-Jones, M. and Neuberger, A. J. (2000). Option Prices, Implied Price Processes, and Stochastic Volatility, *Journal of Finance* **55**(2): 839–866.

Broadie, M. and Detemple, J. (1996). American Option Valuation: New Bounds, Approximations, and a Comparison of Existing Methods, *The Review of Financial Studies* **9**(4): 1211–1250.

Brown, S. and Dybvig, P. (1986). The Empirical Implications of the Cox, Ingersoll, Ross Theory of the Term Structure of Interest Rates, *The Journal of Finance* **51**(3): 617–630.

Busch, T., Christensen, B. and Nielsen, M, O. (2011). The Role of Implied Volatility in Forecasting Future Realized Volatility and Jumps in Foreign Exchange, Stock and Bond Markets, *Journal of Econometrics* **160**: 48–57.

Butler, J. and Schachter, B. (1996). The Statistical Properties of Parameters Inferred from the Black-Scholes Formula, *International Review of Financial Analysis* **3**: 223–235.

Cadzow, J. (2002). Minimum ℓ_1, ℓ_2, and ℓ_∞ Norm Approximate Solutions to an Overdetermined System of Linear Equations, *Digital Signal Processing* **12**(4): 524–560.

Cairns, A. (2004). *Interest Rate Models: An Introduction*, Princeton University Press, Princeton.

Câmara, A., Krehbiel, T. and Li, W. (2011). Expected Returns, Risk Premia, and Volatility Surfaces Implicit in Option Market Prices, *Journal of Banking & Finance* **35**(1): 215 – 230.

Canina, L. and Figlewski, S. (1993a). The informational content of implied volatility, *Review of Financial Studies* **6**: 659–681.

Canina, L. and Figlewski, S. (1993b). The Information Content of Implied Volatility, *Review of Financial Studies* **6**: 659–681.

Cao, C., Yu, F. and Zhong, Z. (2010). The Information Content of Option-implied Volatility for Credit Default Swap Valuation, *Journal of Financial Markets* **13**(3): 321–343.

Cao, C., Yu, F. and Zhong, Z. (2011). Pricing Credit Default Swaps with Option-Implied Volatility, *Financial Analyst Journal* **67**(4): 67–76.

Carr, P., Geman, H., Madan, D. and Yor, M. (2004). From Local Volatility to Local Lévy Models, *Quantitative Finance* **4**(5): 581–588.

Carr, P., Jarrow, R. and Myeneni, R. (1992). Alternative Characterizations of American Put Options, *Mathematical Finance* **2**(2): 87–106.

Carr, P. and Madan, D. (1999). Option Valuation Using the Fast Fourier Transform, *The Journal of Computational Finance* **2**(4): 463–520.

Carr, P. and Madan, D. B. (2005). A note on sufficient conditions for no arbitrage, *Finance Research Letters* **2**: 125–130.

Carr, P. and Mayo, A. (2007). On the Numerical Evaluation of Option Prices in Jump Diffusion Processess, *The European Journal of Finance* **13**(4): 353–372.

Carr, P. and Sun, A. (2007). A New Approach for Option Pricing Under Stochastic Volatility, *Review of Derivatives Research* **10**(2): 87–150.

Carr, P. and Wu, L. (2009). Variance Risk Premiums, *The Review of Financial Studies* **22**(3): 1311–1341.

Carr, P. and Wu, L. (2010). A New Framework for Analyzing Volatility Risk and Premium Across Option Strikes and Expiries. Available at SSRN: http://ssrn.com/abstract=1701685 or http://dx.doi.org/10.2139/ssrn.1701685.

Cassimon, D., Engelen, P., Thomassen, L. and van Wouwe, M. (2007). Closed-form valuation of American call options on stocks paying multiple dividends, *Finance research Letters* **4**(1): 33–48.

CBOE (2013). Volatility Indexes at CBOE. CBOE White Paper. Available at http://www.cboe.com/micro/VIX/pdf/CBOE30c7-VOLindex_QRG.pdf.

Chapman, D., Long, J. and Pearson, N. (1999). Using Proxies for the Short Rate: When are Three Months Like an Instant, *The Review of Financial Studies* **12**(4): 763–806.

Chapman, D. and Pearson, N. (2000). Is the Short Rate Drift Actually Nonlinear?, *The Journal of Finance* **55**(1): 355–388.

Chapman, D. and Pearson, N. (2001). Recent Advances in Estimating Term-Sructure Models, *Financial Analyst Journal* **57**(4): 77–95.

Chiu, N., Fang, S., Lavery, J., Lin, J. and Wang, Y. (2008). Approximating term structure of interest rates using cubic l_1 splines, *European Journal of Operational Research* **184**: 990–1004.

Chourdakis, K. (2005). Option Pricing Using the Fractional FFT, *Journal of Computational Finance* **8**(2): 1–18.

Christensen, B. and Prabhala, N. (1998). The Relation between Implied and Realized Volatility, *Journal of Financial Economics* **50**(2): 125–150.

Christoffersen, P., Heston, S. and Jacobs, K. (2006). Option Valuation with Conditional Skewness, *Journal of Econometrics* **131**: 253–284.

Christoffersen, P. and Jacobs, K. (2004). The Importance of the Loss Function in Option Valuation, *Journal of Financial Economics* **72**(2): 291–318.

Cochrane, J. and Piazzesi, M. (2005). Bond Risk Premia, *The American Economic Review* **95**(1): 138–160.

Collin-Dufresne, P. and Goldstein, R. (2002). Do Bonds Span the Fixed Income Markets? Theory and Evidence for Unspanned Stochastic Volatility, *The Journal of Finance* **57**(4): 1685–1730.

Collin-Dufresne, P., Goldstein, R. and Jones, C. (2008). Identification of Maximal Affine Term Structure Models, *The Journal of Finance* **63**(2): 743–795.

Collin-Dufresne, P., Goldstein, R. and Jones, C. (2009). Can Interest Rate Volatility be Extracted from the Cross Section of Bond Yields?, *Journal of Financial Economics* **94**(1): 47–66.

Constantinides, G. M., Jackwerth, J. C. and Savov, A. (2011). The puzzle of index option returns, *Technical report*, Konstanz University.

Cont, R. (2001). Empirical Properties of Asset Returns: Stylized Facts and Statistical Issues, *Quantitative Finance* **1**: 223–236.

Cont, R. (2005). Modeling Term Structure Dynamics: An Infinite Dimensional Approach, *International Journal of Theoretical and Applied Finance* **8**: 357–380.

Cont, R. and da Fonseca, J. (2002). The Dynamics of Implied Volatility Surfaces, *Quantitative Finance* **2**(1): 45–60.

Cont, R., da Fonseca, J. and Durrleman, V. (2002). Stochastic Models of Implied Volatility Surfaces, *Economic Notes* **31**(2): 361–377.

Cont, R. and Tankov, P. (2004). *Financial modelling with Jump Processes*, Chapman & Hall, CRC Press, London.

Corsi, F. (2009). A Simple Approximate Long-Memory Model of Realized Volatility, *Journal of Financial Econometrics* **7**(2): 174–196.

Cox, J., Ingersoll, J. and Ross, S. (1985). A Theory of the Term Structure of Interest Rates, *Econometrica* **53**(2): 385–407.

Cox, J., Ross, S. and Rubinstein, M. (1979). Option Pricing: A Simplified Approach, *Journal of Financial Economics* **7**(3): 229–263.

Crépey, S. (2003). Calibration of the Local Volatility in a Generalized Black-Scholes Model using Tikhonov Regularization, *SIAM Journal in Mathematical Analysis* **34**(5): 1183–1206.

Culberston, J. (1957). The Term Structure of Interest Rates, *Quarterly Journal of Economics* **71**(4): 485–517.

Da Fonseca, J., Gnoatto, A. and Grasselli, M. (2013). A Flexible Matrix Libor Model with Smiles, *Journal fo Economic Dynamics and Control* **37**(4): 774–793.

da Fonseca, J. and Grasselli, M. (2011). Riding on the Smiles, *Quantitative Finance* **11**(11): 1609–1632.

Dai, Q. and Singleton, K. (2000). Specification Analysis of Affine Term Structure Models, *Th Journal of Finance* **55**(5): 1943–1978.

Dai, Q. and Singleton, K. (2002). Expectation Puzzles, Time-varying Risk Premia, and Affine Models of the Term Structure, *Journal of Financial Economics* **63**(3): 415–441.

Das, S. (2002). The Surprise Element: Jumps in Interest Rates, *Journal of Econometrics* **106**(1): 27–65.

de Boor, C. (2001). *A practical guide to splines*, revised edn, Springer-Verlag, New York.

de Munnik, F. and Schotman, P. (1994). Cross-sectional versus Time Series Estimation of Term Structure Models: Empirical Results for the Dutch Bond Market, *Journal of Banking & Finance* **18**(5): 997–1025.

Dempster, M. and Hutton, J. (1997). Fast Numerical Valuation of American, Exotic and Complex Options, *Applied Mathematical Finance* **4**(1): 1–20.

Dempster, M. and Richards, D. (2000). Pricing American Options Fitting the Smile, *Mathematical Finance* **10**(2): 157–177.

Deng, G. (2014). Pricing American Put Option on Zero-coupon Bond in a Jump-extended CIR Model, *Commun Nonlinear Sci Numer Simulat* . http://dx.doi.org/10.1016/j.cnsns.2014.10.003.

Derman, E. and Kani, I. (1994). Riding on a Smile, *RISK* **7**(2): 32–39.

Derman, E., Kani, I. and Chriss, N. (1996). Implied trinomial trees of the volatility smile, *Journal of Derivatives* **3**(4): 7–22.

Derman, E., Kani, I. and Zou, J. Z. (1996). The local volatility surface: Unlocking the information in index option prices, *Financial Analysts Journal* **7-8**: 25–36.

Deryabin, M. (2012). On Bounds for Model Calibration Uncertainty, *The Journal of Risk Model Validation* **6**(1): 27–45.

Detlefsen, K. and Härdle, W. (2007a). Calibration Risk for Exotic Options, *Jornal of Derivatives* (Summer): 47–63.

Detlefsen, K. and Härdle, W. (2008). Calibration Design of Implied Volatility Surface, *Journal of Data Science* **6**: 303–312.

Detlefsen, K. and Härdle, W. K. (2007b). Calibration Risk for Exotic Options, *The Journal of Derivatives* **14**(4): 47–63.

Deutsche Börse (2007). Guide to the Volatility Indices of Deutsche Börse. Available at http://www.dax-indices.com/EN/MediaLibrary/Document/VDAX_L_2_4_e.pdf.

Dewachter, H., Iania, L. and Lyrio, M. (2014). Information in the Yield Curve: A Macro-finance Approach, *Journal of Applied Econometrics* **29**(1): 42–64.

d'Halluin, Y., Forsyth, P. and Vetzal, K. (2005). Robust Numerical Methods for Contingent Claims under Jump Diffusion Processes, *IMA Jounral of Numerical Analysis* **25**(1): 87–112.

Diebold, F. and Li, C. (2006). Forecasting the Term Structure of Government Bond Yields, *Journal of Econometrics* **130**(2): 337–364.

Diebold, F., Li, C. and Yue, V. (2008). Global Yield Curve Dynamics and Interactions: A Dynamic Nelson-Siegel Approach, *Journal of Econometrics* **146**(2): 351–363.

Dokuchaev, N. (2006). Two Unconditionally Implied Parameters and Volatility Smiles and Skews, *Applied Financial Economics Letters* **2**: 199–204.

Duffee, G. (2002). Term Premia and Interest Rate Forecasts in Affine Models, *The Journal of Finance* **57**(1): 405–443.

Duffee, G. (2011). Information in (and not in) the Term Structure, *The Review of Financial Studies* **24**(9): 2895–2934.

Duffie, D. and Kan, R. (1996). A Yield-Factor Model of Interest Rates, *Mathematical Finance* **6**(4): 379–406.

Duffie, D., Pan., J. and Singleton, K. (2000). Transform analysis and asset pricing for affine jump-diffusions, *Econometrica* **68**: 1343–1376.

Dumas, B., Fleming, J. and Whaley, R. E. (1998). Implied Volatility Functions: Empirical Tests, *Journal of Finance* **53**(6): 2059–2106.

Dupire, B. (1994). Pricing with a Smile, *RISK* **7**(1): 18–20.

Egger, H. and Engl, H. (2005). Tikhonov Regularization Applied to the Inverse Problem of Option Pricing: Convergence Analysis and Rates, *Inverse Problems* **21**: 1027–1045.

Ehrhardt, M. and Mickens, R. (2008). A Fast, Stable and Accurate Numerical Method for the Black-Scholes Equation of American Options, *International Journal of Theoretical & Applied Finance* **11**(5): 471–501.

Eilers, P. and Marx, B. (1996). Flexible Smoothing with B-splines and Penalties, *Statistical Science* **11**(2): 89–121.

El Karoui, N. and Karatzas, I. (1991). A New Approach to the Skorohod Problem, and its Applications, *Stochastics and Stochastic Reports* **34**(1): 57–82.

Engl, H., Kunisch, K. and Neubauer, A. (1989). Convergence Rates for Tikhonov Regularisation of Non-linear Ill-posed Problems, *Inverse Problems* **5**: 523–540.

Fabozzi, F., Leccadito, A. and Tunaru, R. (2014). Extracting market information from equity options with exponential Lévy processes, *Journal of Economic Dynamics and Control* **38**(January): 125–141.

Fama, E. (1976). Forward Rates as Predictors of Future Spot Rates, *Journal of Financial Economics* **3**(4): 361–377.

Fama, E. (1990). Term-Structure Forecasts of Interest Rates, Inflation, and real Returns, *Journal of Monetary Economics* **25**(1): 59–76.

Fama, E. and Bliss, R. (1987). The Information in Long-Maturity Forward Rates, *The American Economic Review* **77**(4): 680–692.

Farquharson, C. and Oldenburg, D. (2000). Automatic Estimation of the Trade-off Parameter in Nonlinear Inverse Problems Using the GCV And L-curve Criteria, *2000 SEG Annual Meeting, August 6 - 11, 2000, Calgary, Alberta*, Society of Exploration Geophysicists.

Feil, B., Kucherenko, S. and Shah, N. (2009). Volatility Calibration using Spline and High Dimensional Model Representation Models, *WILMOTT Journal* **1**(4): 179–385.

Feller, W. (1951). Two Singular Diffusion Problems, *Annals of Mathematics, Second Series* **54**(1): 173–182.

Fengler, M. (2012). Option Data and Modeling BSM Implied Volatility, *in* J.-C. Duan, W. Härdle and J. Gentle (eds), *Handbook of Copmputational Finance*, Springer Handbooks of Computational Statistics, Springer, Berlin Heidelberg, pp. 483–385.

Fengler, M., Härdle, W. and Mammen, E. (2007). A Semiparametric Factor Model for Implied Volatility Surface Dynamics, *Journal of Financial Econometrics* **5**(2): 189–218.

Fengler, M. R. (2005). *Semiparametric Modeling of Implied Volatility*, Lecture Notes in Finance, Springer-Verlag, Berlin, Heidelberg.

Fengler, M. R. and Hin, L.-Y. (2015a). A Simple and General Approach to Fitting the Discount Curve Under No-Arbitrage Constraints, *Finance Research Letters* . In press.

Fengler, M. R. and Hin, L.-Y. (2015b). Semi-nonparametric Estimation of the Call Price Surface under Strike and Time-to-expiry No-arbitrage Constraints, *Journal of Econometrics* **184**(2): 242–261.

Fisher, I. (1896). Appreciation and Interest, *Publications of the American Economic Association* **11**(1/3): 21–29.

Fisher, M. and Gilles, C. (1998). Around and around: The Expectations Hypothesis, *The Journal of Finance* **53**(1): 365–383.

Garfinkel, M. and Thornton, D. (1995). The Information Content of the Federal Funds Rate: Is it Unique?, *Journal of Money, Credit and Banking* **27**(3): 838–847.

Gatheral, J. (2006). *The Volatility Surface: A Practitioner's Guide*, John Wiley & Sons, Hoboken, New Jersey.

Gefang, D., Koop, G. and Potter, S. (2011). Understanding Liquidity and Credit Risks in the Financial Crisis, *Journal of Empirical Finance* **18**: 903–914.

Gil-Alana, L. and Moreno, A. (2012). Uncovering the US Term Premium: An Alternative Route, *Journal of Banking & Finance* **36**(4): 1181–1193.

Gilli, M. and Schumann, E. (2011). Calibrating Option Pricing Models with Heuristics, *in* A. Brabazon, M. O'Neill and D. Maringer (eds), *Natural Computing in Computational Finance*, Springer-Verlag, Berlin.

Gimeno, R. and Nave, J. (2009). A Genetic Algorithm Estimation of the Term Structure of Interest Rates, *Computational Statistics and Data Analysis* **53**(6): 2236–2250.

Goncalves, S. and Guidolin, M. (2004). Predictable Dynamics in the S&P500 Index Options Implied Volatility Surface. EFMA 2003 Helsinki Meetings. Available at SSRN: http://ssrn.com/abstract=406697 or http://dx.doi.org/10.2139/ssrn.406697.

Gregory, D. and Livingston, M. (1992). Development of the Market for U.S. Treasury STRIPS, *Financial Analyst Journal* **48**(2): 68–74.

Grinblatt, M. and Longstaff, F. (2000). Financial Innovation and the Role of Derivative Securities: An Empirical Analysis of the Treasury STRIPS Program, *The Journal of Finance* **55**(3): 1415–1436.

Guidolin, M. and Timmermann, A. (2009). Forecasts of US Short-term Interest Rates: A Flexible Forecast Combination Approach, *Journal of Econometrics* **150**(2): 297–311.

Guo, Z. (2008). A Note on the CIR Process and the Existence of Equivalent Martingale Measures, *Statistics & Probability Letters* **78**(5): 481–487.

Hagan, P., Kumar, D., Lesniewski, A. and Woodward, D. (2002). Managing smile risk, *Wilmott Magazine* **1**: 84–108.

Hagan, P., Kumar, D. and Lesniewski, A. Woodward, D. (2014). Arbitrage-Free SABR, *Wilmott* **69**(January): 60–75.

Hagan, P. and West, G. (2006). Interpolation Methods for Curve Construction, *Applied Mathematical Finance* **13**(2): 89–129.

Hall, A., Anderson, H. and Granger, C. (1992). A Cointegration Analysis of Treasury Bill Yields, *The Review of Economics and Statistics* **74**(1): 116–126.

Hansen, P. C. (2000). The L-Curve and its Use in the Numerical Treatment of Inverse Problems, *in Computational Inverse Problems in Electrocardiology, Ed. P. Johnston, Advances in Computational Bioengineering*, WIT Press, pp. 119–142.

Hansen, P. and O'Leary, D. (1993). The Use of the L-curve in the Regularization of Discrete Ill-posed Problems, *SIAM Journal of Scientific Computing* **14**: 1487–1503.

Hardouvelis, G. (1988). The Predictive Power of the Term Structure During Recent Monetary Regimes, *The Journal of Finance* **43**(2): 339–356.

Haug, E. (2006). *The Complete Guide to Option Pricing Formulas (2nd ed.)*, McGraw-Hill, New York.

Hayashi, T. and Mykland, P. (2005). Evaluating Hedging Errors: An Asymptotic Approach, *Mathematical Finance* **15**(2): 309–343.

Heath, D., Jarrow, R. A. and Morton, A. (1992). Bond pricing and the term structure of interest rates: A new methodology for contingent claims valuation, *Econometrica* **60**: 77–105.

Hein, S. and Spudeck, R. (1988). Forecasting the Daily Federal Funds Rate, *International Journal of Forecasting* **4**(4): 581–591.

Hein, T. (2005). Some Analysis of Tikhonov Regularization for the Inverse Problem of Option Pricing in the Price-Dependent Case, *Journal of Analysis and its Applications* **24**(3): 593–609.

Henrard, M. (2010). Swaptions in Libor Market Model with Local Volatility, *Wilmott Journal* **2**(3): 135–154.

Hensen, E. and Walster, G. (1993). Nonlinear Equations and Optimization, *Computer & Mathematics with Applications* **25**(10-11): 125–145.

Heston, S. (1993). A closed-form solution for options with stochastic volatility with applications to bond and currency options, *Review of Financial Studies* **6**: 327–343.

Heston, S. and Nandi, S. (2000). A closed-form garch option valuation model, *Review of Financial Studies* **13**: 585–625.

Hin, L.-Y. and Dokuchaev, N. (2015a). Computation of the Implied Discount Rate and Volatility for an Overdefined System using Stochastic Optimization, *IMA Journal of Management Mathematics* . DOI:10.1093/imaman/dpv007
http://imaman.oxfordjournals.org/cgi/content/abstract/dpv007?ijkey=qMTk0IzgOY6vikX&keytype=ref .

Hin, L.-Y. and Dokuchaev, N. (2015b). Short rate forecasting based on the inference from the cir model for multiple yield curve dynamics, *Annals of Financial Economics* . In press.

Ho, T. and Lee, S.-B. (1986). Term structure Movements and Pricing Interest Rate COntingent Claims, *The Journal of Finance* **41**(5): 1011–1029.

Homescu, C. (2011). Implied Volatility Surface: Construction Methodologies and Characteristics. Available at SSRN: http://ssrn.com/abstract=1882567 or http://dx.doi.org/10.2139/ssrn.1882567.

Hu, Z., Xiong, S., Su, Q. and Zhang, X. (2013). Sufficient Conditions for Global Convergence of Differential Evolution Algorithm, *Journal of Applied Mathematics* **2013**(Article ID 193196): 1–14.

Huang, R. and Lin, C. (1996). An Analysis of Nonlinearities in Term Premiums and Forward Rates, *Journal of Empirical Finance* **3**(4): 347–368.

Hull, J. and White, A. (1987). The Pricing of Options on Assets with Stochastic Volatilities, *Journal of Finance* **42**: 281–300.

Hull, J. and White, A. (1990). Pricing Interest-Rate-Derivative Securities, *The Review of Financial Studies* **3**(4): 573–592.

Hull, J. and White, A. (1994a). Numerical Procedures for Implementing Term Structure Models I: Single-factor models, *Journal of Derivatives* **2**: 7–16.

Hull, J. and White, A. (1994b). Numerical Procedures for Implementing Term Structure Models I: Single-factor models, *Journal of Derivatives* **2**: 37–48.

Hurn, A., Lindsay, K. and McClelland, A. (2015). Estimating the Parameters of Stochastic Volatility Models using Option Price Data, *Journal of Business & Economic Statistics* **33**(4): 579–594.

Hurvich, C., Simonoff, J. and Tsai, C.-L. (1998). Smoothing parameter selection in nonparametric regression using an improved Akaike information criterion, *Journal of the Royal Statistical Society B* **60**(2): 271–293.

Itkin, A. and Carr, P. (2012). Using Pseudo-Parabolic and Fractional Equations for Option Pricing in JUmp Diffusion Models, *Computational Economics* **40**(1): 63–104.

Jacka, S. (1991). Optimal Stopping and the American Put, *Mathematical Finance* **1**(2): 1–14.

Jackwerth, J. C. (1999). Option-implied risk-neutral distributions and implied binomial trees: A literature review, *Journal of Derivatives* **7**(2): 66–82.

Jackwerth, J. C. and Rubinstein, M. (1996). Recovering probability distributions from contemporaneous security prices, *Journal of Finance* **51**: 1611–1631.

Jamshidian, F. (1995). A Simple Class of Square-root Interest-rate Models, *Applied Mathematical Finance* **2**(1): 61–72.

Jamshidian, F. (1997). Libor and swap market models and measures, *Finance and Stochastics* **1**: 291–328.

Jamshidian, F. and Zhu, Y. (1997). Scenario Simulation: Theory and Methodology, *Finance and Stochastics* **1**: 43–67.

Jarrow, R., Li, H. and Zhao, F. (2007). Interest Rate Caps "Smile" Too! But can the LIBOR Market Models Capture the Smile?, *The Journal of Finance* **62**(1): 345–382.

Jiang, G. J. and Tian, Y. S. (2005). The Model-Free Implied Volatility and Its Information Content, *The Review of Financial Studies* **18**(4): 1305–1342.

Jiang, G. J. and Tian, Y. S. (2007). Extracting Model-Free Volatility from Option Prices: An Examination of the VIX Index, *Journal of Derivatives* (Spring): 1–26.

Jiang, G. and Van Der Sluis, P. (1999). Index Option Pricing Models with Stochastic Volatility and Stochastic Interest Rates, *European Finance Review* **3**(3): 273–310.

Jones, C. (2003). Nonlinear Mean Reversion in the Short-Term Interest Rate, *The Review of Financial Studies* **16**(3): 793–843.

Jungbacker, B., Koopman, S. and van der Wel, M. (2014). Smooth Dynamic Factor Analysis with Application to the US Term Structure of Interest Rates, *Journal of Applied Econometrics* **29**(1): 65–90.

Kahl, C. and Jäckel, P. (2005). Not-so-complex Logarithms in the Heston Model, *WIlmott Magazine* **September**(2005): 94–103.

Kamara, A. and Miller, T. (1995). Daily and Intradaily Tests of European Put-Call Parity, *The Journal of Financial and Quantitative Analysis* **30**(4): 519–539.

Kanevski, M., Maignan, M., Pozdnoukhov, A. and Timonin, V. (2008). Interest Rates Mapping, *Physica A* **387**: 3897–3903.

Karatzas, I. and Shreve, S. (2005). *Brownian Motion and Stochastic Calculus*, Springer-Verlag, Berlin, Heidelberg.

Karr, C., Weck, B. and Freeman, L. (1998). Solution to Systems of Nonlinear Equations via a Genetic Algorithm, *Engineering Applications of Artificial Intelligence* **11**(3): 369–375.

Kim, D. (2007). The Bond Market Term Premium: What is it, and How can We Measure It? BIS Quarterly Review. Available at http://www.bis.org/publ/qtrpdf/r_qt0706e.pdf.

Kim, I. (1990). The Analytic Valuation of American Options, *The Review of Financial Studies* **3**(4): 547–572.

Klebaner, F., Le, T. and Lipster, R. (2006). On Estimation of Volatility Surface and Prediction of Future Spot Volatility, *Applied Mathematical Finance* **13**(3): 245–263.

Kohn, R., Ansley, C. and Tharm, D. (1991). The Performance of Cross-Validation and Maximum Likelihood estimators of Spline Smoothing Parameters, *Journal of the American Statistical Association* **86**(416): 1042–1050.

Kou, S. G. (2002). A jump-diffusion model for option pricing, *Management Science* **48**: 1086–1101.

Lagnado, R. and Osher, S. (1997). A Technique for Calibrating Derivative Security Pricing Models: Numerical Solution of an Inverse Problem, *The Journal of Computational Finance* **1**(1): 13–25.

Latané, H. and Rendleman, J. (1976a). Author's Correction: Standard Deviations of Stock Price Ratios Implied in Option Prices, *Journal of Finance* **34**(4): 1083.

Latané, H. and Rendleman, J. (1976b). Standard Deviations of Stock Price Ratios Implied in Option Prices, *Journal of Finance* **31**(2): 369–381.

Laurini, M. and Moura, M. (2010). Constrained Smoothing B-splines for the Term Structure of Interest Rates, *Insurance: Mathematics and Economics* **46**: 339–350.

Lee, R. (2004). Option Pricing by Transform Methods: Extensions, Unifications, and Error Control, *Journal of Computational Finance* **7**(3): 51–86.

Leibowitz, M., Sorensen, E., Arnott, R. and Hanson, H. (1989). A Total Differential Approach to Equity Duration, *Financial Analysts Journal* **45**(5): 30–37.

Leippold, M. and Stromberg, J. (2014). Time-changed Lévy LIBOR market model: Pricing and joint estimation of the cap surface and swaption cube, *Journal of Financial Economics* **111**(1): 224–250.

Levendorskii, S. and Xie, J. (2012). Fast Pricing and Calculation of Sensitivities of out-of-the-money European Options under Lévy Processes, *The Journal of Computational Finance* **15**(3): 71–VI.

Lewis, A. (2000). *Option Valuation Under Stochastic Volatility: With Mathematica Code*, Finance Press, New Port Beach, California, USA.

Lewis, A. (2001). A Simple Option Formula for General Jump-Diffusion and Other Exponential Levy Processes. Available at www.optioncity.net.

Li, S. (2005). A New Formula for Computing Implied Volatility, *Applied Mathematics and Computation* **170**(1): 611–625.

Litterman, R. and Scheinkman, J. (1991). Common Factors Affecting Bond Returns, *Journal of Fixed Income* **1**(June): 54–61.

Longstaff, F. (2000). The Term Structure of Very Short-term Rates: New Evidence for the Expectations Hypothesis, *Journal of Financial Economics* **58**(3): 397–415.

Longstaff, F., Mithal, S. and Neis, E. (2005). Corporate Yield Spreads: Default Risk or Liquidity? New Evidence from the Credit Default Swap Market, *The Journal of Finance* **60**(5): 2213–2253.

Lord, R. and Kahl, C. (2007). Optimal Fourier Inversion in Semi-analytic Option Pricing, *Journal of Computational Finance* **10**(4): 1–30.

Madan, D. (2015). Recovering Statistical Theory in the Context of Model Calibrations, *Journal of Financial Econometrics* **13**(2): 260–292.

Madan, D. and Schoutens, W. (2012). Tenor Specific Pricing, *International Journal of Theoretical and Applied Finance* **15**(6): 1–21.

Madan, D. and Seneta, E. (1990). The Variance Gamma (V.G.) Model for Share Market Returns, *The Journal of Business* **63**(4): 511–524.

Maghsoodi, Y. (1996). Solution of the Extended CIR Term Structure and Bond Option Valuation, *Mathematical Finance* **6**(1): 89–109.

Marangio, L., Bernaschi, M. and Ramponi, A. (2002). A Review of Techniques for the Estimation of the Term Structure, *International Journal of Theoretical and Applied Finance* **5**: 189–221.

McAleer, M. and Medeiros, M. (2008). A Multiple Regime Smooth Transition Heterogeneous Autoregressive Model for Long Memory and Asymmetries, *Journal of Econometrics* **147**(1): 104–119.

Medvedev, A. and Scaillet, O. (2007). Approximation and Calibration of Short-Term Implied Volatilities Under Jump-Diffusion Stochastic Volatility, *The Review of Financial Studies* **20**(2): 427–459.

Mercurio, F. (2009). Interest Rates and The Credit Crunch: New Formulas and Market Models. Bloomberg Portfolio Research Paper No. 2010-01-FRONTIERS. Available at SSRN: http://ssrn.com/abstract=1332205.

Mercurio, F. (2010). Modern Libor Market Models: Using Different Curves for Projecting Rates and for Discounting, *International Journal of Theoretical and Applied Finance* **13**(1): 113–137.

Merton, R. C. (1973). Theory of rational option pricing, *Bell Journal of Economics and Management Science* **4**(Spring): 141–183.

Merton, R. C. (1976). Option pricing when underlying stock returns are discontinuous, *Journal of Financial Economics* **3**: 125–144.

Meyer, P. (1976). *Un cours sur les intégrales stochastiques*, *Lecture Notes in Mathematics*, number 511, Springer-Verlag, Berlin, Heidelberg.

Mikhailov, S. and Nögel, U. (2003). Heston's Stochastic Volatility Model Implementation, Calibration and Some Extensions, *WILMOTT magazine* **July**: 74–79.

Miltersen, K., Sandmann, K. and Sondermann, D. (1997). Closed form solutions for term structure derivatives with log-normal interest rates, *Journal of Finance* **1**(52): 409–430.

Mincer, J. and Zarnowitz, V. (1969). The Evaluation of Economic Forecasts, *in* J. Mincer (ed.), *Economic Forecasts and Expectations*, NBER, New York, pp. 3–46.

Modigliani, F. and Sutch, R. (1966). Innovations in Interest Rate Policy, *The American Economic Review* **56**(1): 178–197.

Moench, E. (2008). Forecasting the Yield Curve in a Data-rich Environment: A No-arbitrage Factor-augmented VAR Approach, *Journal of Econometrics* **146**(1): 26–43.

Moreni, N. and Pallavicini, A. (2014). Parsimonious HJM Modelling for Multiple Yield Curve Dynamics, *Quantitative Finance* **14**(2): 199–210.

Morini, M. and Webber, N. (2006). An EZI Method to Reduce the Rank of a Correlation Matrix in Financial Modelling, *Applied Mathematical Fiannce* **13**(4): 309–331.

Nelson, A. and Arthur, R. (2013). Fast trees for Options wth Discrete Dividends, *Journal of Derivatives* **21**(1): 49–63.

Nelson, C. R. and Siegel, A. F. (1987). Parsimonious Modeling of Yield Curves, *Journal of Business* **60**: 473–489.

Neubauer, A. (1989). Tikhonov Regularization for Non-linear Ill-posed Iroblems: Optimal Convergence Rates and Finite-dimensional Approximation, *Inverse Problems* **5**: 541–557.

Nowak, P. and Romaniuk, M. (2010). Computing Option Price for Levy process with fuzzy parameters, *European Journal of Operational Research* **201**(1): 206–210.

Pak, Y. and Kim, T. (2012). The Information Content of OTC Individual Put Option Implied Volatility for Credit Default Swap Spreads, *Asia-Pacific Journal of Financial Studies* **41**: 491–516.

Palandri, A. (2014). Risk-free Rate Effects on Conditional Variances and Conditional Correlations of Stock Returns, *Journal of Empirical Finance* **25**: 95–111.

Panigirtzoglou, N. and Skiadopoulos, G. (2004). A New Approach to Modeling the Dynamics of Implied Distributions: Theory and Evidence from the S&P500 options, *Journal of Banking and Finance* **28**: 1499–1520.

Perignon, C. and Villa, C. (2003). Extracting Information from Options Markets: Smiles, State-Price Densities and Risk Aversion, *European Financial Management* **8**(4): 495–513.

Piazzesi, M. (2005). Bond Yields and the Federal Reserve, *Journal of Political Economy* **113**(2): 311–344.

Poon, S.-H. and Granger, C. W. J. (2003a). Forecasting volatility in financial markets: A review, *Journal of Economic Literature* **41**: 478–539.

Poon, S.-H. and Granger, W. (2003b). Forecasting Volatility in Financial Markets: A Review, *Journal of Economic Literature* **41**(2): 478–539.

Portnoy, S. and Koenker, R. (1997). The Gaussian Hare and the Laplacian Tortoise: Computability of Squared-error versus Absolute-error Estimators, *Statistical Science* **12**(4): 279–300.

Price, K., Storn, R. and Lampinen, J. (2005). *Differential Evolution: A Practical Approach to Global Optimization*, Springer-Verlag, Berlin Heidelberg.

R Core Team (2012). *R: A Language and Environment for Statistical Computing*, R Foundation for Statistical Computing, Vienna, Austria. ISBN 3-900051-07-0.
URL: *http://www.R-project.org/*

Ramponi, A. (2002). Adaptive and Monotone Spline Estimation of the Cross-Sectional Term Structure, *International Journal of Theoretical and Applied Finance* **6**: 195–212.

Randow, J. and Kennedy, S. (2016). Negative Interest Rates: Less Than Zero. Available at http://www.bloomberg.com/quicktake/negative-interest-rates.

Rebonato, R. (1999). On the Simultaneous Calibration of Multifactor Lognormal Interest Rate Models to Black Volatilities and to the Correlation Matrix, *The Journal of Computational Finance* **2**: 5–27.

Rebonato, R. (2004). *Volatility and Correlation*, Wiley Series in Financial Engineering, 2nd. edn, John Wiley & Son Ltd.

Rindell, K. (1995). Pricing of Index Options when Interest Rates are Stochastic: An Empirical Test, *Journal of Banking & Finance* **19**(5): 785–802.

Rindell, K. (2005). On Multigrid for Anisotropic Equations and Variational Inequalities: Pricing multi-dimensional European and American Options, *Computing and Visualization in Science* **7**(3): 189–197.

Roberds, W., Runkle, D. and Whiteman, C. (1996). A Daily View of Yield Spreads and Short-Term Interest Rate Movements, *Journal of Money, Credit and Banking* **28**(1): 34–53.

Rodrigo, M. and Mamon, R. (2008a). A New Representation of the Local Volatility Surface, *International Journal of Theoretical and Applied Finance* **11**(7): 691–703.

Rodrigo, M. and Mamon, R. (2008b). Recovery of Time-Dependent Parameters of a Black-Scholes-Type Equation: An Inverse Stieltjes Moment Approach, *Journal of Applied Mathematics* . Article ID 62098.

Rodrigo, M. and Mamon, R. (2014). An Alternative Approach to the Calibration of the Vasicek and CIR Interest Rate Models via Generating Functions, *Quantitative Finance* **14**(11): 1961–1970.

Rubenthaler, S. and Wiktorsson, M. (2003a). Improved Convergence Rate for the Simulation of Stochastic Differential Equations driven by Subordinated Lévy Processes, *Stochastic Processes and their Applications* **108**(1): 1–26.

Rubenthaler, S. and Wiktorsson, M. (2003b). Numerical Simulation of the solution of a Stochastic Differential Equations driven by a Lévy Processes, *Stochastic Processes and their Applications* **103**(2): 311–349.

Rubinstein, M. (1983). Displaced Diffusion Option Pricing, *The Journal of Finance* **38**(1): 213–217.

Rubinstein, M. (1994). Implied Binomial Trees, *Journal of Finance* **49**(3): 771–818.

Rudebusch, G. (1995). Federal Reserve Interest Rate Targeting, Rational Expectations, and the Term Structure, *Journal of Monetary Economics* **35**(2): 245–274.

Rudebusch, G. (2012). The Bond Premium in a DSGE Model with Long-Run Real and Nominal Risks, *American Economic Journal: Macroeconomics* **4**(1): 105–143.

Samperi, D. (2002). Calibrating a Diffusion Pricing Model with Uncertain Volatility: Regularization and Stability, *Mathematical Finance* **12**(1): 71–87.

Sarno, L. and Thornton, D. (2003). The Dynamic Relationship between the Federal Funds Rate and the Treasury Bill Rate: An Empirical Investigation, *Journal of Banking & Finance* **27**(6): 1079–1110.

Schlögl, E. and Schlögl, L. (2000). A Square Root Interest Rate Model Fitting Discrete Initial Term Structure Data, *Applied Mathematical Finance* **7**(3): 183–209.

Schoutens, W. and Simons, E. andTistaert, J. (2004). A Perfect Calibration! Now what?, *Wilmott Magazine* **March**: 66–78.

Schwarz, G. (1978). Estimating the dimension of a model, *Annals of Statistics* **6**: 461–464.

Scott, L. (1987). Option Pricing when the Variance Changes Randomly: Theory, Estimation, and an APplication, *The Journal of Financial and Quantitative Analysis* **22**(4): 419–438.

Scott, L. (1997). Pricing Stock Options in a Jump-Diffusion Model with Stochastic Volatility and Interest Rates: Applications of Fourier Inversion Methods, *Mathematical Finance* **7**(4): 413–424.

SenGupta, I. (2013). Option Pricing with Transaction Costs and Stochastic Interest Rate, *Applied Mathematical Finance* **21**(5): 399–416.

Simon, D. (1990). Expectations and the Treasury Bill-Federal Funds Rate Spread over Recent Monetary Policy Regimes, *The Journal of Finance* **45**(2): 567–577.

Skindilias, K. and Lo, C. (2015). Local Volatility Calibration during Turbulent Periods, *Review of Quantitative Finance and Accounting* **44**(3): 425–444.

Smith, R. and Bowers, K. (1993). Sinc-Galerkin Estimation of Diffusivity in Parabolic Problems, *Inverse Problems* **9**: 113–135.

Söhl, J. and Trabs, M. (2012). Option Calibration of Exponential Lévy Models: Confidence Intervals and Empirical Results, *Journal fo Computational Finance* **18**(2): 91–119.

S&P Dow Jones Indices (2013). S&P/ASX 200 VIX Methodology, *Technical report*, McGraw Hill Financial.
URL: *http://us.spindices.com/documents/methodologies/methodology-sp-asx-200-vix.pdf*

Stanton, R. (1997). A Nonparametric Model of Term Structure Dynamics and the Market Price of Interest Rate Risk, *The Journal of Finance* **52**(5): 1973–2002.

Stein, E. and Stein, J. (1991). Stock Price Distributions with Stochastic Volatility: An Analytic Approach, *The Review of Financial Studies* **4**(4): 727–752.

Stoll, H. (1969). The Relationship Between Put and Call Option Prices, *The Journal of Finance* **24**(5): 801–824.

Storn, R. and Price, K. (1997). Differential Evolution - A Simple and Efficient Heuristic for Global Optimization over Continuous Spaces, *Journal of Global Optimization* **11**: 341–359.

Tanaka, H. (1963). Note on Continuous Additive Functionals of the 1-dimensional Brownian Path, *Zeitschrift für Wahrscheinlichkeitstheorie* **1**: 251–257.

Taylor, S., Yadav, P. and Zhang, Y. (2010). The Information Content of Implied Volatilities and Model-free Volatility Expectations: Evidence from Options written on Individual Stocks, *Journal of Banking & Finance* **34**(4): 871–881.

Theil, H. (1966). *Applied Economic Forecasts*, North Holland, Amsterdam.

Tikhonov, A. N. (1943). On the stability of inverse problems, *Doklady Akademii Nauk SSSR* **39**(5): 195–198.

Todorov, V. (2010). Variance Risk-remium Dynamics: The Role of Jumps, *The Review of Financial Studies* **23**(1): 345–383.

Trolle, A. and Schwartz, E. (2009). A General Stochastic Volatility Model for the Pricing of Interest Rate Derivatives, *The Review of Financial Studies* **22**(5): 2007–2057.

Turinici, G. (2014). Calibration of local volatility using the Local and Implied Instanteous variance, *The Journal of Computational Finance* **13**(2): 1–18.

Tzavalis, E. (2004). The Term Premium and the Puzzles of the Expectations Hypothesis of the Term Structure, *Economic Modelling* **21**(1): 73–93.

Van Horne, J. (1980). The Term Structure: A Test of the Segmented Market Hypothesis, *Southern Economic Journal* **46**(4): 1129–1140.

Vasicek, O. (1977). An Equilibrium Characterization of the Term Structure, *Journal of Financial Econometrics* **5**(2): 177–188.

Vollrath, I. and Wendland, J. (2009). Calibration of Interest Rate and Option Models using Differential Evolution. Available at SSRN: http://ssrn.com/abstract=1367502 or http://dx.doi.org/10.2139/ssrn.1367502.

Wang, H., Zhou, H. and Zhou, Y. (2013). Credit Default Swap Spreads and Variance Risk Premia, *Journal of Banking & Finance* **37**: 3733–3746.

Wright, J. and Zhou, H. (2009). Bond Risk Premia and Realized Jump Risk, *Journal of Banking & Finance* **33**(12): 2333–2345.

Xi, X., Rodrigo, M. and Mamon, R. (2011). Parameter estimation of a regime-switching model using an inverse stieltjes moment approach, *in* S. Cohen, D. Madan, T. Siu and H. Yang (eds), *Stochastic processes, finance and control: a Festschrift in honor of Robert J. Elliott*, World Scientific, Singapore.

Yamamura, K. and Suda, K. (2007). An Efficient Algorithm for FInding All SOlutions of Separable Systems of Nonlinear EQuations, *BIT Numerical Mathematics* **47**(3): 681–691.

Yin, Q., Qi, Y. and Xiao, J. (2010). Detecting roots of nonlinear equations through a novel differential evolution algorithm, *Information Engineering and Computer Science (ICIECS), 2010 2nd International Conference on*, pp. 1–4.

Zhang, J. and Sanderson, A. (2009). JADE: Adaptive Differential Evolution with Optional External Archive, *IEEE Transactions on Evolutionary Computation* **13**(5): 945–958.

Zhang, S. and Wang, L. (2013). Fast Fourier Transform Option Pricing with Stochastic Interest Rate, Stochastic Volatility and Double Jumps, *Applied Mathematics and Computation* **219**(23): 10928–10933.

Zhou, N. and Mamon, R. (2012). An Accessible Implementation of Interest Rate Models with Markov-Switching, *Expert Systems with Applications* **39**(5): 4679–4689.

Zhu, D. and Qu, D. (2016). Libor Local Volatility Model: A New Interest Rate Smile Model, *Wilmott* **82**(March): 78–87.

Every reasonable effort has been made to acknowledge the owners of copyright material. I would be pleased to hear from any copyright owner who has been omitted or incorrectly acknowledged.

Written statements on co-authored peer reviewed papers

To Whom It May Concern

I, Lin Yee HIN, contributed

1. majority of theoretical conception.
2. majority of mathematical framework construction.
3. vast majority of literature review and connecting the current work to extant literature.
4. vast majority of numerical algorithm development.
5. vast majority of programming implementation of the mathematical framework,
6. vast majority of historical data set selection, collection, processing, and empirical analysis,
7. vast majority of interpretation of results and connection of results to extant literature, and
8. vast majority writing and editing of manuscript to be submitted for the peer reviewed publications, and preparation of responses to the panel of referee,

to the paper entitled Hin, L.-Y. and Dokuchaev, N. (2014) "On the Implied Volatility Layers Under the Future Risk-Free Rate Uncertainty," *International Journal of Financial Markets and Derivatives*, 3(4), 392–408.

5/11/2015

I, as a Co-Author, endorse that this level of contribution by the candidate indicated above is appropriate.

Nikolai Dokuchaev 5/11/2015

To Whom It May Concern

I, Lin Yee HIN, contributed

1. majority of theoretical conception,
2. majority of mathematical framework construction.
3. vast majority of literature review and connecting the current work to extant literature,
4. vast majority of numerical algorithm development,
5. vast majority of programming implementation of the mathematical framework,
6. vast majority of synthetic test data construction, and numerical testing,
7. vast majority of historical data set selection, collection, processing, and its empirical analysis,
8. vast majority of interpretation of results and connection of results to extant literature, and
9. vast majority of writing and editing of manuscript to be submitted for the peer reviewed publications, and preparation of responses to the panel of referee,

to the paper entitled Hin, L.-Y. and Dokuchaev, N. (2015) "Computation of the Implied Discount Rate and Volatility for an over-defined System using Stochastic Optimization," *IMA Journal Of Management Mathematics*, in press. DOI:10.1093/imaman/dpv007 .

5/11/2015

I, as a Co-Author, endorse that this level of contribution by the candidate indicated above is appropriate.

Nikolai Dokuchaev 5/11/2015

To Whom It May Concern

I, Lin Yee HIN, contributed

1. majority of theoretical conception,
2. majority of mathematical framework construction,
3. vast majority of literature review and connecting the current work to extant literature,
4. vast majority of numerical algorithm development,
5. vast majority of programming implementation of the mathematical framework,
6. vast majority of historical data set selection, collection, processing, and empirical analysis,
7. vast majority of interpretation of results and connection of results to extant literature, and
8. vast majority of writing and editing of manuscript to be submitted for the peer reviewed publications, and preparation of responses to the panel of referee,

to the paper entitled Hin, L.-Y. and Dokuchaev, N. (2015) "Short Rate Forecasting based on the Inference from the CIR Model for Multiple Yield Curve Dynamics," *Annals of Financial Economics*, accepted.

— 5/11/2015

I, as a Co-Author, endorse that this level of contribution by the candidate indicated above is appropriate.

Nikolai Dokuchaev 5/11/2015